Republic of Iraq
Ministry of Higher
Education and Scientific Research
University of Babylon
College of Engineering
Civil Engineering Department

Computational Fluid Dynamic Based Simulation of Flow Over a Mildly Sloped Pool -Riffle Sequence

A Thesis

Submitted to the College of Engineering at University of Babylon in Partial Fulfillment of the Requirements for the Master Degree in Engineering \Civil Engineering\Water Resources

By

Saja Ali Obeid Wawi

Supervised By

Prof. Dr.
Thair Jabbar Mizhir Alfatlawi

Lect. Dr.
Faiz Hussein Al-Merib

2022AD **1444AH**

بسم الله الرحمن الرحيم

وَمَآ أُوتِيتُم مِّنَ ٱلْعِلْمِ إِلَّا قَلِيلًا ﴿٨٥﴾

صدق الله العلي العظيم

سورة الاسراء - 85

Supervisor Certification

We certify that this thesis entitled " **Computational Fluid Dynamic Based Simulation of Flow Over a Mildly Sloped Pool -Riffle Sequence"** is prepared by "**Saja Ali Obeid**" under our supervision at University of Babylon as a partial fulfillment of requirements for the degree of Master of Science in Engineering/Civil Engineering /Water Resources Engineering.

Signature:
*Name:***. *Prof. Dr. Thair Jabbar Mizhir Alfatlawi***
Date: / / 2022

Signature:
Name: ***Lect. Dr. Faiz Hussein Al-Merib***
Date: / / 2022

Certificate of the Examining Committee

We certify that we have read this thesis entitled ***"Computational Fluid Dynamic Based Simulation of Flow Over a Mildly Sloped Pool -Riffle Sequence"*** presented by ***"Saja Ali Obeid"*** and as an examining committee, we examined the student in its content and in what is connected with it, and that in our opinion it meets standard of a thesis for the degree of Master of Science in Engineering/Civil Engineering / Water Resources Engineering.

Signature:

Name: **Prof.Dr. Mahmoud Saleh Mahdi**
(Chairman)
Date: / / 2022

Signature:

Name: **Asst.Prof.Dr.Atheer Zaki Al-Qaisi**
(Member)
Date: / / 2022

Signature:

Name: **Asst. Prof.Mohammed Abid Almajeed Abid Alabas**
(Member)

Date: / / 2022

Signature:

Name: **Prof. Dr. *Thair Jabbar Mizhir Alfatlawi***
(Member and Supervisor)
Date: / / 2022

Signature:

Name: **Lect. Dr. Faiz Hussein Al-Merib**
(Member and Supervisor)
Date: / / 2022

Approved by the Head of the Civil Engineering Department

Signature:

*Name: **Prof. Dr. Thair Jabbar Mizhir Alfatlawi***
(The Head of the Civil Engineering Department)
Date: / / 2022

Approved by the Dean of the College of the Engineering

Signature:

*Name: **Prof. Dr. Hatem Hadi Obeid***
(The Dean of College of Engineering)
Date: / /2022

ACKNOWLEDGEMENTS

First of all, I would like to thank "**Allah**", Who guide and aide me to come out this work, with His might assistance; I was able to be here today.

I would like to express my deepest thanks and appreciation to my supervisors **Prof. Dr. Thair Jabbar Mizhir Alfatlawi and Lect. Dr. Faiz Hussein Al-Merib,** for guidance, suggestion, support and encouragement during the whole duration of this research.

Also, I would like to express my deepest gratitude to all professors and the staff members of the Department of Civil Engineering and Laboratories of Civil Engineering in the College of Engineering at University of Babylon, Iraq.

Finally, I wish to express my heartfelt thanks to my family and my friends for encouragement and moral support, they play an important role in all my life, so I dedicate this work to them.

Abstract

The problem of erosion and sedimentation that affects the bottom of open channels and their sides are among the problems that have attracted the attention of researchers and workers in the hydraulic field, as these channels, especially their sides, are exposed to sedimentation and erosion factors, as a result of the high velocity of flow that the channels are exposed to great damage. In this field, several techniques are used to protect hydraulic structures and open channels from erosion and sedimentation problems and to obtain high-stability protection that is resistant to external forces affecting and among the techniques of this protection are used Riprap, Concrete blocks and Gabions. A new technique called pool riffle sequences was used in this study, pool-riffle bedforms are fundamental units of many gravel bed rivers have been shown to be crucial to ecosystem health and channel stability.

Increasing the riverbed's roughness will lower flow velocity, which will also lower erosion. This concept was used in this investigation. To get the best river erosion solution at the lowest cost and with the least amount of bed scouring. A number of investigations were carried out to investigate velocity distributions and turbulence intensity along the flume for various bed roughness heights.

Computational Fluid Dynamics (CFD)was used to simulate the flow in an open channel with a rough bed. With bed roughness heights of 1, 2, and 4 cm, two applied discharges of 15L/s and 21L/s with two water depths upstream and downstream of the flume are used, which consider some of the variables that affect the design of the runs.

As a whole, riffle and pool length have a significant impact on flow and turbulence distribution within a channel. Turbulence and the redistribution of the flow to uniform flow conditions both lose energy in the pool. As the flow velocity rises in the riffle, kinetic energy increases, and as the length grows, the flow tends towards a new uniform flow condition.

The results show that increasing water flow discharge increases the effect of roughness bedforms on velocity distribution.

The thesis concluded that the CFD technique is efficient in simulating this phenomenon and obtaining good results, and that this phenomenon is useful in controlling the environment of rivers and maintaining stable levels and sections for them, as the velocity of water flow decreases in rivers, which leads to achieving the required aims. When the effect of bed roughness on turbulence intensity was also investigated, a significant impact in reducing flow turbulence intensity was discovered.

Table of Contents

List of Symbols

Symbol	Description	Dimensions
d_{50}	Median grain size of sediment	L
D_{84}	Sediment size for which 84%of the particles are finer	L
g	Acceleration due to the gravity	LT^{-2}
k	Turbulent kinetic energy	$L^3 T^{-2}$
ks	Equivalent Nikuradse grain roughness	L
t	Time	T
ui	i-th component of the Reynolds averaged velocity	LT^{-1}
v	kinematic viscosity	L^2T^{-1}
ε	Specific dissipation	$L^2 T^{-3}$
ω	Specific dissipation rate	T^{-1}
p	Reynolds averaged pressure	ML^{-2}
xi	i-th axis	L
ρ	water density	ML^{-3}

List of Abbreviations

Abbreviation	Description
CFD	Computational Fluid Dynamics
VOF	Volume of Fluid
PISO	Pressure Implicit with Splitting of Operators
SST	Shear Stress Transport
R.H	Roughness Height
PRS	Pool Riffle Sequence
CDF	Convective Deceleration Flow
CAF	Convective Acceleration Flow

List of Figures

List of Tables

Chapter One

Introduction

1.1 General

Flow characteristics and their interaction with channel geometry and plan shape are essential to all river engineering concerns. The characteristics vary, however, with the type of channel bed (sand-bed, gravel-bed, boulder-bed, steep pool / fall and vegetated). Therefore, the differences among channel beds need to be recognized and to ensure that calculation techniques are appropriate for the form under consideration. Flow characteristics are important not only to understand better flow-sediment interaction, but also to solve hydraulic engineering problems, particularly channel erosion and deposition issues, such as the distribution of time-average velocities, turbulence intensities, bed and Reynolds shear stress in the open-channel. In recent decades, numerous systematic research studies have been carried out. Rivers are self-organizing systems. Patterns will be developed from the interactions within the system between specific elements or sections as a result of sediment and water inputs. From development of ripples on sand bed to the structuring of watershed river networks, these patterns may be found on a wide range of sizes. Fluvial geomorphology is all about understanding how these patterns evolve and how they affect the system's characteristics and behavior. This thesis concentrates on a certain pattern that is important in gravel beds river a riffle-pool sequence. In a wide range of rivers with gravel bottoms, riffle-pools describe the structure of macro scales (Grant et al. 1990 and Montgomery and Buffington 1997) . This bed form aids in stream bed stabilization (Madej, 1999; Eaton and Lapointe, 2001) as well as energy dissipation (Thompson, 2002; Walker et al., 2004).

A deeper knowledge of features and management of pool-riffle dynamics is crucial in planning of water resources, ecological, and river management challenges.

Instead of undertaking time-consuming and costly field or laboratory experiments, Computational Fluid Dynamics, (CFD), has become a useful tool for studying the hydrodynamics of open channel under various conditions in great detail. CFD may be used to model and study flow in an open channel with roughness components. The research is carried out using the ANSYS Fluent CFD program.

The general aim of this study is to describe hydrodynamic of pool-riffle sequences at various bedforms length and roughness. This entails determining how flow and turbulence in a channel, especially along bed, vary as the size of bedform varies.

1.2 Aim of Thesis

In general, the objectives of this thesis are to:

- Investigate how the bedform roughness has an impact on hydrodynamic of pool-riffle sequences .
- Determine how length and spacing of simplified bedforms impact flow and turbulence distribution in channels, especially along the bed of channel, where sediment transfer may be critical.
- Apply ANSYS CFD software to create a two-dimensional model to simulate flow in an open channel with roughness features.

1.3 Limitations and Assumptions

1. Stable bedform, no sediment moving.
2. Steady non uniform flow.

3. The effects of viscosity and surface tension were ignored due to the free surface, open channel flow condition.

1.4 Thesis layout

The following are the five chapters that forms this thesis:

1. Chapter 1 (Introduction) discusses general concepts for flow characteristics in pool riffle sequences and the aims of this study.
2. Chapter 2 (Theoretical Background and Literature Review) Highlight pervious research on the subject of pool riffle sequnces
3. Chapter 3 (Numerical Work) contains the following information: Creating CFD models to mimic the channel's velocity patterns.
4. Chapter 4 (Results and Discussion): demonstrates the investigation of the effects of combining roughness height with the effects of changing the geometry, on flow dynamics in an open channel and discusses and explains them.
5. Chapter 5 (Conclusions and Suggestions): summarizes the findings and makes recommendations based on them.

1.5 Methodology

1. Reviewing previous literature.
2. Using ANSYS Fluent CFD to simulate waterflow across the open channel while creating 2D models of the channel.
3. Conducting research into how the use of roughness height with various pool and riffle geometry, and configurations affects the hydrodynamics of the flow in open channels.
4. Investigating the findings to determine the velocity distribution and turbulent intensity.
5. Documentation.

Chapter Two

Theoretical Background and Literature Review

The pool-riffle sequence is defined in this portion of the study, as well as the size at which it occurs naturally in open channels. Pool-riffle sequences are noted for their importance in channel stability and ecology. The results of both experimental and numerical research are discussed.

2.1 **Bedform Classification**

Bed material in natural streams is usually made up of a variety of sizes and shapes, all of which are formed at various threshold that is influenced by the threshold of neighboring particle (Komar, 1996).

Every reach of channel in variable systems of drainage will have variable features, slope, grain size, and roughness are all factors to consider. In Sedimentary systems are a type of system with non-consolidated material that could be degraded and carried away in a flow (Keller and Melhorn ,1978). On the basis of varied components of these features, there are five unique range bedform types that can exist. These types are a cascade, a step pool, a plane bed, a pool-riffle, and dune ripple (Montgomery and Buffington, 1997).

The difference between five morphologies of the bedform, and the main element that manages each kind are highlighted in (Table 2.1) and (Figure 2.1).

The formation of riffles and pools in river systems is a method of self-adjustment that reduces their time rate of potential energy expenditure for each unit of water mass in accordance with the law of the least degree of energy expenditure. The actual creation of pools and riffles is a combined dispersion and sorting process (Montgomery and Buffington, 1997).

Table 2.1. Diagnostic features of different alluvial bedforms (Montgomery and Buffington, 1997)

	Dune Ripple	Pool-Riffle	Plane Bed	Step Pool	Cascade
Type of bed material	Sand	Gravel	Gravel-cobble	Cobble-boulder	Boulder
Bedform pattern	Multilayered	oscillatory Laterally	Featureless	oscillatory Vertically	Random
Dominant roughness elements	Sinuosity, bedforms (dunes, ripples, bars), grains, banks	Bedforms (bars, pools), grains, sinuosity, banks	Grains, banks	Bedforms (steps, pools), grains, banks	Grains, banks
Pool spacing (channel widths)	5 to 7	5 to 7	None	1 to 4	<1

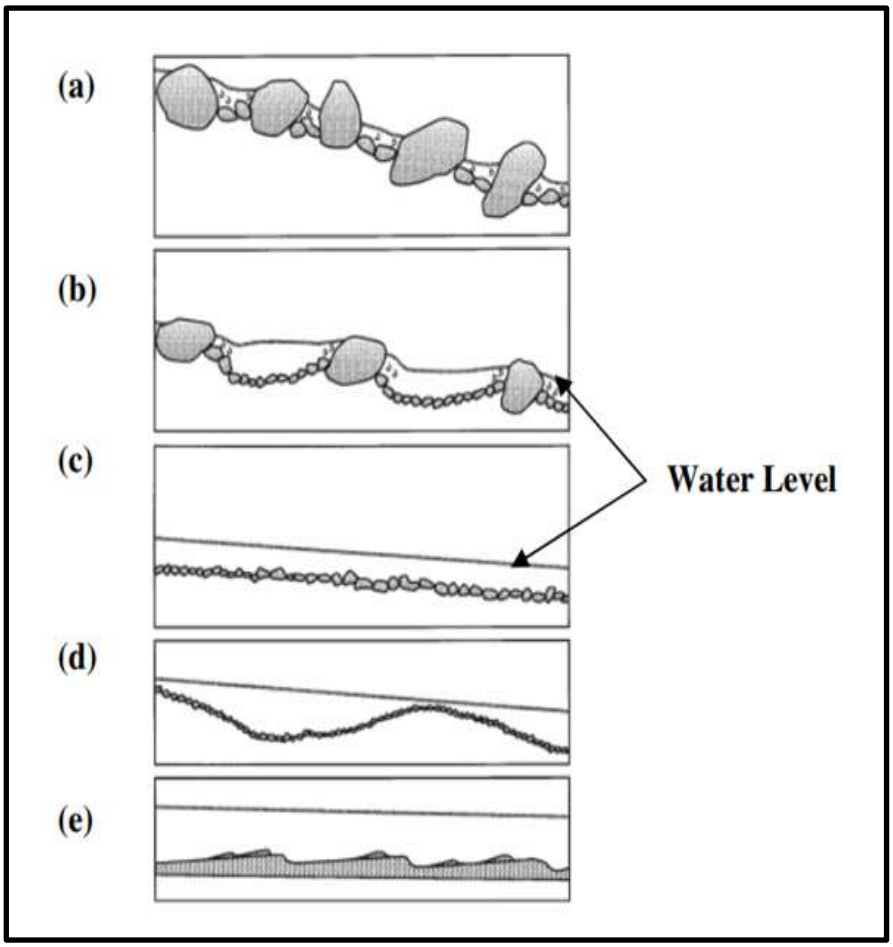

Figure 2.1. Side view sketch of different bedform classifications including (a) cascade, (b) step pool, (c) plane bed, (d) pool-riffle, and (e) dune ripple (Montgomery and Buffington, 1997).

Any degree of bed material Size heterogeneity tends to be one of the conditions for the presence of pool and riffles in non-meandering streams. It appears the channels holding uniform sand or uniform silt they had little tendency for pools and riffles to form. Pools and riffles are less well formed in braided than in straight (Leopold et al., 1964).

2.2 Pool-Riffle Morphology

Pool and riffle are topographically low and high portions of the channel bed that are created in relation to one another (Wohl, et al., 1993; O'Neill and Abrahams, 1984), and as comparable to meandering in vertical path (Keller and Melhorn, 1978). In terms of depth and water-surface gradient, runs are transitional between pools and riffles and it can include isolated elements of boulder roughness (Wohl et al., 1993 ;Lisle, 1982).

A neighboring pool and riffle are defined as a pool-riffle sequence Instead of migrating downstream like sand bars, the characteristics appear to stay in a relatively fixed location longitudinally (Leopold et al., 1964). They may be located in both alluvial and bedrocks channels, although gravel-bed channels are the more prevalent (Leopold et al., 1964). They occur at transition ranges with respect to transport ability and supply of sediments, occur someplace between a limited supply of sediments and a roughly equivalent quantity of transport capability.

The precise transport-supply correlation depends on degree of armouring of the bed material and occurrence of mobility of the bed-surface (Montgomery and Buffington, 1997). The slope of the water surface larger over riffle than pool at low flows, but the differences decrease as discharge rises until nearly straight water surface obtained (Leopold et al., 1964). The friction slope rises over the pools and decreases over the riffles under high flow conditions leading to excavation of pools and the building of riffles.

In together straight and meandering channel, pool riffle sequences are found (Leopold et al., 1964). Pools are repeatedly correlated with curvatures in meandering channels and often are followed via adjacent point bar, resulting in asymmetric cross sectional profile, while riffles appear to have more symmetric cross-sectional profiles (Lofthouse and Robert,2008; Keller and Melhorn, 1978).

There is no minimum size requirement for a riffle-pool (Buffington et al., 2002). During low flow, (Lisle and Hilton 1992) wanted the pool's residual depth to be at least twice the flow depth at the riffle crest.

Pools had to possess residual depths of at least 25% of the bankfull depth, according to Montgomery et al. (1995).

In forested mountain drainage basins, forced pool-riffle morphologies are common. They occur when obstructions like large woody debris, boulders, and bedrock outcrops force pools. From the standard 5-7 channel widths, bedform spacing can be decreased (Montgomery and Buffington, 1997). Obstructions frequently applied to channel to force creation of features throughout reconstruction efforts that target to build pool-riffle sequences (Newbury and Gabourey, 1993). For equivalent grain sizes, PRS is normally broader and deeper than other morphologies, with sediment sorting of distinct trends, shear stress and roughness variance (Montgomery and Buffington, 1997). In both alluvial and bedrock channels, pool and riffle occur, but are better created in gravelly-bed substrates or meandering channels. In moderate gradient channels, pools and riffles happen, typically less than 2% slope (Leopold et al., 1964; Sear, 1996; Wohl, 2000). In almost all constant channels wherein the bed content larger than coarse sand, the pool-riffle sequence is present, but seems to just be most common of stream with gravel bed (Leopold et al., 1964; Montgomery and Buffington, 1997)

2.3 Formation and Maintenance of the Pool-Riffle

Maintenance of pool-riffle states to the mechanisms that maintain pool-riffle relieved. Processes of maintenance cause fine sediment accumulated during small flows in pools and during strong flows, removed from pools. By same manner, maintenance processes in riffles allow sediment to scoured apart and deposited respectively at high and low flow (Milan, 2013). The creation of bedforms, especially those relating to scouring and deposition, can also be explained by certain maintenance processes, but others just clarify the self-maintenance of present features**.** Cherkauer (1973) and Yang (1971, 1987) suggested that rivers change to reduce their dissipation of energy rate or power of stream's unit. This general trend was also used by Wohl et al. (1993) to describe differences in pool properties with channels slope in California.

Thompson (2002) indicated that, in relation to higher initial stream power, the propensity of pools to elongate is mechanism leading to stream power minimization. Then, Wohl (2007) proposed that as the level rises, the shape drag from the pool restricts the rate of increase in velocity. Buffington et al. (2002) proposed that lesser relative velocity upstream of pool restrict the provide of sediment to pools at high flow. Therefore, a decreased supply of local sediment will facilitate net transport out of high-flow pools**.**

The seminal theory, the concept of velocity reversal (Keller, 1971), has been discussed for years and alternative hypotheses have been presented, but there is no scientific consensus.

2.3.1 Velocity Reversal Hypothesis

Gilbert (1914) was first to argue that varying the bed velocity causes scouring pools at high flows and filling pools at low flows, but he was incapable to obtain measurement to quantify his theory. On this definition,

Keller (1971) expanded and was the first to show a systematic hypothesis for methods of sorting fine materials in deep pools and coarse materials into shallow riffle. Keller suggested that the bottom velocity is lower in the pool than in the adjacent riffles at low flow the bottom velocity in pools increases faster than in riffles with increased discharge.

Caamano et al. (2009) presented a theoretic evaluation of theory of velocity-reversals and found where pool is slimmer than riffle, reversal is variable of pools' residual depth, in deeper pool, it is fewer probable.

Wilkinson et al. (2004) claimed opposing reversal owing to change in channel width with grade, but recommended that site of shear stresses maximize transition from a high to a low flow position in relation to the bed pattern.

2.3.2 Sediment Routing

Group of different hypotheses explore the spatial and temporal dissimilarities in channel bed sediment as well as their maximum effect on shear stresses distributions besides the suggested of sequence of pool-riffle generation and models of maintenance that concentrate on hydraulic factors (Lisle, 1979; Clifforrd, 1993).

when sediments of bed in riffles are coarser than sediments in pools that increase regional bed resistance, bed-shear stress in pools surpass riffle values as (Carling and Wood, 1994; Milan et al., 2001) pointed.

Booker et a l., (2001) suggest that the protection of the morphology of pool-riffle may be attributed to absence of sediment being transported to pools instead of an improved tendency to disintegrate based on flow convergence into pool.

At the riffle's head, the flow moves away, resulting in riffle sedimentation and the preservation of a topographical high at the pool's end (Macwilliams et al., 2006).

As an alternate to velocity reversal hypothesis, Milan (2013) proposed a sediment routing hypothesis. The study proposed that clast is effectively routed round pools at bankfull flow with riffles serving as pools in the conventional model and bar as riffles, as the bar at this point have the greatest height and tractive force. Using field of sediment tracer analysis and computational fluid dynamics , these results have been obtained.

De Almeida and Rodríguez (2011) proposed that combining flow and sediment dynamics could solve the information gap about pool-riffle maintenance and morphodynamics. They discovered that sediment transport reversals were more common than shear stress or velocity reversals.

2.4 Sediment Transport in Pool Riffle Sequences

The word "sediment transport" refers to the movement of material (such as silt, sand, gravel, and boulders) through rivers and streams. Bed material in natural streams is often made up of a variety of size and shape, all of which are trapped at different threshold that are influenced by the threshold of adjacent particles (Komar, 1996). The problem of sediment transfer in gravel-bed rivers is well-known (Henderson, 1966). Solid material can be moved by rolling or sliding on the bed, making short jumps known as saltations, or suspending in the flow (Chanson,2004). Gravelly streams have been observed to armor their bed, i.e., bed surface is usually coarser than subsurface material, and to transfer sediment in a size selected manner, i.e., bigger size is under-represented in bed load when contrasted to their occurring in substrate (Andrews, 1994; Church and Hassan, 2002).

The amount of sediment transport can be accelerated by turbulent fluctuations (Nelson et al., 1995; Sumer et al., 2003), and sediment transport can even occur while group of mean average critically shears stress is not reached (Sumer et al., 2003; Hassan and Woodsmith 2004).

2.5 Geometry of Pool and Riffle

It is possible to break the geometric characteristics of pools and riffles based on inter features that comprise width, depth, in addition to length of the characteristics and based on cross settings that involve the total number and spacing along a specific river range of pool-riffle couplets. Those characteristics together offer details on number of characteristics also percentage of the channels region which is forecasted to fall within the pool, the riffle, or the run feature across a specified range. The repeated longitudinal and lateral pattern of alternating cross-section symmetry is the most distinctive characteristic of the riffle-pool sequence. The channel cross-section alternates between symmetric (riffle) and asymmetric (pool) in the longitudinal direction, while the form of the asymmetric cross-section alternates between being left-skewed and right skewed in the lateral direction.

Although the riffle size problem is not thoroughly studied, (Lisle, 1986; Carling and Orr, 2000; Lofthouse and Robert, 2008) recorded that the average riffle length is between 1.31 and 4.5 width of channel, and (Carling and Orr, 2000) stated the values recorded were shorter in river with greater bankfull depth.

(Wohl et al., 1993; Carling and Orr, 2000) recorded length of riffle as a pool length ratio, pools-to-riffles length ratio vary from 1:0.8 to 1:1.9 in channels with gradient less than or equals to 2%, and riffle tend to become shorter in channels with a steeper gradient (Wohl et al., 1993).

The lengths are measured from one pool to the next or from one riffle to the next,based on which method is used, the inter-features distance measurement along pool-riffle system is pointed to as pool or riffle spaces(figure 2.2). Researchers frequently standardize the values of spacing of specific reach by dividing distance by mean bankfull distance, after then, it acts like a self-

scaling ruler. There is no universally accepted hypothesis to explain pool-riffle spacing, despite the recognition of associations between spacing and channel features (Carling and Orr, 2000).

In a number of gravel-bed and bedrock-influenced channels, researchers recorded mean pool to pool space is between 5 and 7 width of channel (Leopold et al.,1964; Keller and Melhorn, 1978; Gregory et al., 1994; Sear,1996). Based on random forcing element distribution, there is no typical spacing in forced pool-riffles (Madej,1999). (Montgomery et al., 1995) it can occur in space value of lower than predicted range for freely shaped pools-riffles channel.

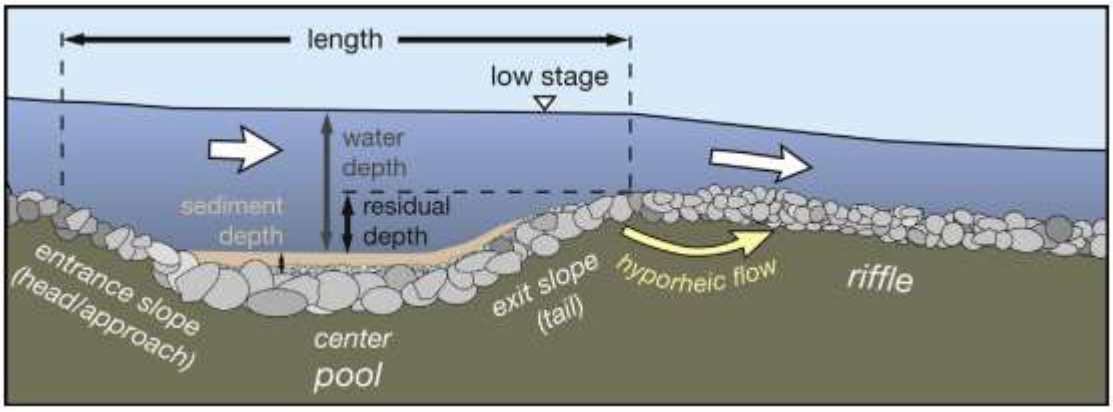

Figure 2.2: Pool and riffle features and definitions (Thompson ,2018)

Researches indicate that increases in numbers of the channel obstacles contributes to increase in numbers of pool and decrease in the space of pools riffle sequence(Montgomery et al., 1995; Wood-Smith and Buffingten,1996; Thompson, 2001; Keeton et al., 2007). (Lisl (1986), Montgomery et al. (1995)) detected interference between obstructions that are adjacent spaced, which results in just a single pool being created.

2.6 Pool-Riffle Advantage

In a channel, a pool-riffle sequences have two primary roles, a physical function, as well as an environmental function. Physically, by reducing the

possible loss of energy per unit mass of water, channel's stability is provided by the pool-riffle. (Yeng, 1971; Keller and Molhorn, 1978; Wohl et al., 1993).

Riffles serves as hydraulics flow regulation across upstream pools at low flows (Richard, 1978). Riffles are immersed at high flows and acts as large-scale feature of roughness to help stabilize the channel (Caamaño et al., 2009).

It was found in research by Walker et al. (2004) in southwestern British Columbia of riffle systems in four gravel-cobble bed rivers showed that 50 to 100 percent of total energies were missing at high flows over a riffle and its downstream pools, confirming its value as a structure of stabilization **.**

The pool-riffle sequence acts an essential purpose in ecology of the rivers, fish ecosystem protection because they offer feeding, breeding, and covering regions (Keller, 1978).

2.7 Bed Roughness

Roughness is utilized in fluid mechanics to calculate the momentums and energy loss that aren't clearly calculated for in simple or discontinuous equation utilized in numerical science and engineering (Morvan et. al 2008). The link between particle sizes and also the roughness was previously studied in reasonably smooth test channel to determine the height of roughness, ks, on assumption that widely visible shape of roughness was that caused via grain imperfections at wall. As described by Clifford et al., (1992) other formulations have been presented, such as $k_s = 3.5\ D_{84}$ or $k_s = 6.8\ D_{50}$. But other like Afzalimehr and Anctil (2000) used equivalent Nikuradse grain roughness k_s as D_{50}.

Bed roughness can be directly or indirectly defined (particle size) or (flow resistance coefficient). The particle size distribution is always lognormal (Kellerhals and Bray 1971). Gilbert (1987) stated that the median particle

size, d_{50}, and the standard deviation ((d_{50}/d_{16} + d_{84}/d_{50})/2) are two metrics widely used to characterize cumulative frequency distribution. The range used by Rosgen (1994) to describe gravel-bed streams is described as gravel material with a particle size between 2 and 64 mm.

2.8 Experimental and Field Studies

Thompson et al. (1998) In order to determine interactions between pool geometry and hydraulics, an experimental and numerical research approach were used. In 20m long, 1.8m wide and 0.6 m depth flume, carried out their experimental work to analyze the influence of four different geometric aspects of pool form on flow velocity. In four-way factorial analyses, an empirical evaluation of the function of the four geometric elements on the pool flow patterns and therefore the stability of the pool was developed using the resulting 16 runs geometries with calculated pool velocities. A two-dimensional computational flow model was used to investigate the relationships over a larger range of conditions between pool geometry and flow patterns, in order to complement the conclusions of these analyses.

The study found that in the jet portion of the pool, experimental and computational findings indicate that constriction and depth effects dominate and that pool length exhibits a growing effect within the recirculating-eddy framework. Strong backwater effects and local water-surface slopes created by constriction that are 4-6 times higher than the average water-surface slopes along the model reach. In the pool center, flow pushed through the constriction and appears to create a narrow zone of high-velocity flow called a vena contracta. The exit slope of the pool tends to force flow reattachment and accelerates flow spreading and dissipation of the strong jet produced by the constriction. The length of the pool regulates recirculating-eddy length and intensity of the vena contracta.

In turn, the recirculating eddy and vena contracta control velocities in pool center and exit slop of pool and downstream riffle. They also observed that the formation of a vena contracta in the pool center is essential to the maintenance of such pool systems. The length of the pool appears to influence vena contracta and recirculating-eddy characteristics due to variations in water-surface elevation with pool elongation.

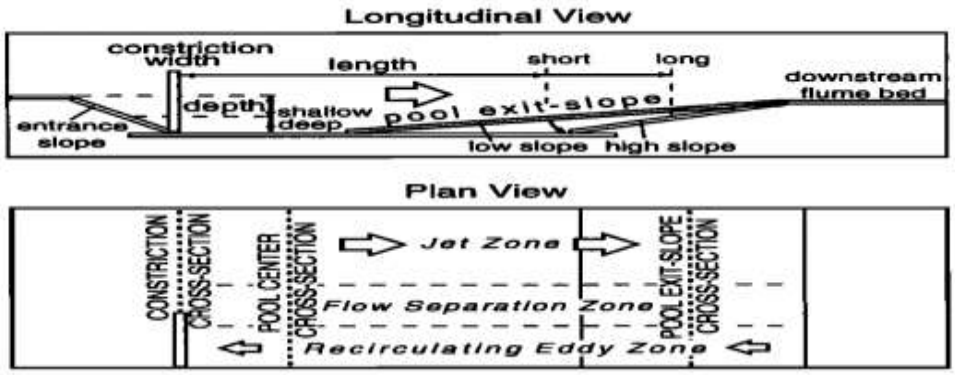

Figure 2.3. Measurement section in flume experiment. (Thompson et al., 1998)

Thompson (2004) carried out experimental study to see how the length of the pool affected the turbulence strength of produced by vortex shedding. Eight experimental pool geometries in a 6 m length recirculated flume were created as shown in figure 2.4.

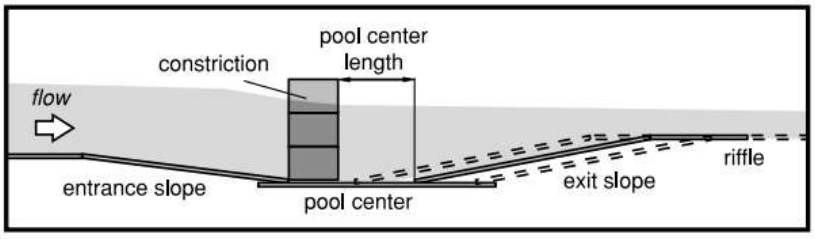

Figure 2.4. Longitudinal view of experimental channel morphology used in the flume experiments. (Thompson ,2004)

For the flume, the average channel-bed slope was 0·007 and the depth of water was regulated by the use of a tailgate to produce a maximum pool depth of 17 cm. The discharge was 31·6 l/s in the flume.

Study found that Pool elongation results in a non-linear change in turbulence strength and average velocity in many places. The greatest turbulence occurs in the middle of the pool between the jet and the recirculating eddy along the shear zone, based on the overall flow pattern. The lateral location of this shear zone is susceptible to pool length changes. Because of a combination of greater pool length and shorter pools result in more head loss, energy slope was also susceptible to pool length.

A study showed that the flow on the pool exit slope exhibits a wide range of responses to pool elongation in the various areas tested. One of the most important responses to pool elongation occurs at the base of exit slope near the flume wall, where velocities appear maximum values should be achieved at a pool length of around 40 cm. Head loss and energy slope, with pool elongation, both show a logarithmic decrease. Loss head is over six times greater in the shortest pool than in the longest pool tested. Likewise, over the shortest pools, the energy slope is more than 10 times greater than over the longest pool. According to these findings, pool elongation will lead to a minimization of unit stream power and the rate of dissipation of energy.

Lofthouse and Robert (2008) in order to evaluate the dynamic adaptation of the sequence of riffle–pool in regard to enlarged expenditure of energy in meander channel, field study was carried out. They chose five gravel-bed channels where six longitudinally profiles were evaluated in six of the examined reaches, for a total length of 5.7 kilometers. Statistical relationships were used, both the differentiation and regression techniques between parameters describing the morphology of the riffle pool (The sequence's length and amplitude) and curvature of planform. In addition to

field work they examined supplementary data, to demonstrate possible effect of sediment ability on the morphology of bedform the database contained longitudinal profiles of 161 ranges, size dimensions of bed materials and other important morphological features.

Investigation showed that the increased sequence length, which can be seen in combination riffle-riffle and pool-riffle unit sequences, is due to the rise in sequence length, suggesting an increase in overall curvature. Pool length increased instead of a rise in the length of riffle. This pattern is especially significant in showing significance of pool in the growth of meanders. Conclusion from this study is, the degree of curvature, the amount of platform migration, and the scale of the bed materials all influence the length of the sequence. The results confirmed the most repeated relationship between pool–riffle sequence length and channel width that is between 5 and 6 channel widths

Thompson and McCarrick (2010) performed in 6m long, 0.5m wide recirculating flume using a bed gradient 0.8 percent, a sequence of 18 flume runs to decide the effect of obstacle form on forced pool formation and properties. The flume bed was packed with unvarying gravel comprising d_{16}, d_{50} and d_{84}, 4.1 mm, 5.4 mm and 7.0 mm, respectively. Six different shaped obstructions with the extreme width of obstacle kept fixed at 20 cm have been added to the flume, which a 40% flow constriction was equal. Analysis of Variance (ANOVA) test results showed the depth of the pool, position of the pool, and the distance between the middle of the pool and the riffle crest all differ with the form of the obstruction. Deeper pools, more total scouring and longer pool-riffle sequence lengths were created by obstructions with a more sharp upstream face than pools created by barriers with a more gradual narrowing of flow. The increased scour volume correlated with obstructions that quickly narrow flow often produces larger volume riffles that cover the channel bed to a greater extent.

MacVicar and Rennie (2012) worked on an experimental study to decide if flow phenomena like velocity reversal, merging of lateral flow, and bigger turbulence occurred in a simplify pool morphology and to evaluate whether they are applicable to the definition of spatial variations in shear stress of the near-bed and to establish a conceptual model for a simplified pool of three-dimensional flow and turbulence distribution. In a straight pool, a proposed model of flow and turbulence redistribution is presented in figure 2.6. Experiments were done in a flume 1.5 m wide ,30m long and 0.7 m depth, with a straight pool 7.3 m long and 0.5 depth, entrance and exit slope with 5°, walls of vertical side, and gravel sediments (D_{50} = 9.9 mm). During the tests, the standard flow depth in the channel was 0.25 m as well as corresponding ratio of width-depth was 6.0.

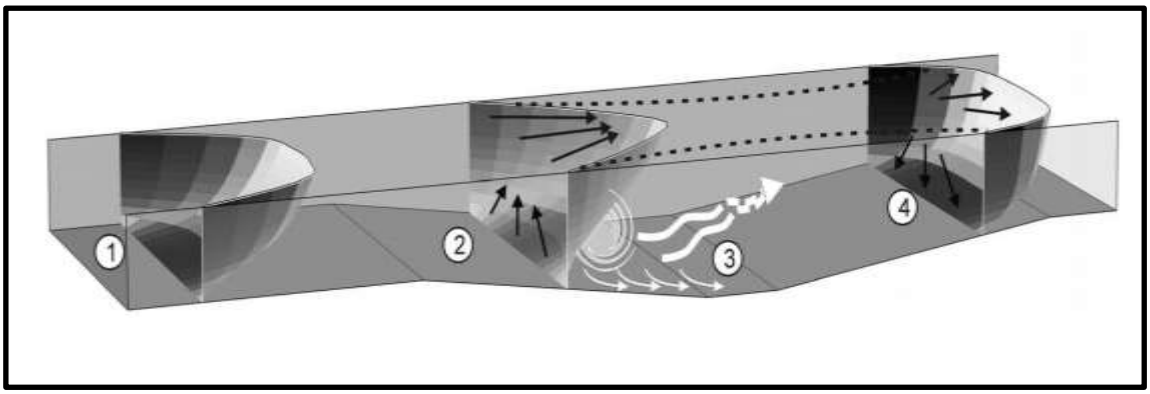

Figure 2.5. Proposed model of flow and turbulence redistribution in a straight pool. (MacVicar and Rennie, 2012)

Research indicated that the velocity distribution in the created pool varies as a result of convective acceleration and deceleration. During convective deceleration (CDF), the near-bed velocity decreased as depth increased, but flow increased. During convective acceleration (CAF), near-bed velocity was pretty high as depth decreased. Convergence of lateral flow took place where depths increase, which during flow deceleration, convergence is shown to be induced and there was no need for lateral flow restriction.

Throughout deceleration, turbulence was defined by sweeps oriented toward the channel's sidewalls, an influence that could contribute to the creation of non-uniform pool depth in deposition of mobile sediments through lateral gradients.

Caamano et al. (2012) examined three-dimensional of hydraulic simulations in addition to field observations on portion of Red River, Idaho, for two pool-riffle sequences that self-formed. The study area was a gravel-bed meandering channel that flowing across 4.5-kilometer-long green meadow at elevation of 1280 meters, surrounded by wooded mountains up to 2134 meters. Three different discharges were used in this study, 0.38,5.67 and 9.23 m^3/s. For comprehensive three-dimensional modeling, a calibrated one-dimensional hydraulic model (MIKE 3 Flexible Mesh) was utilized to represent flow conditions over the whole meadow under which a 150 m river reach was defined, with pool-riffle sequence of concern. Within this section, a 45-meter-long channel was covered.

The results indicated that there are changes in the upstream PRS. Flow structure, but very little change in the downstream sequence, implying that downstream riffle works as hydraulic control. With increasing discharge, deeper pools demonstrate shorter, broader and stronger jets. Little depth pools created jets that are comparatively longer and have a slower rate of width increase than similar pools using a greater residual depth. During comprehensive inspection of flow structures, they noticed a link between the jet also macroscale turbulence properties.

Macvicar and Best (2013) conducted a laboratory test to examine the influence of channel width on flow disturbance and restoration in straight pool and riffle and to describe the mean flow response and Reynolds stresses to convective accelerations and decelerations . The application of this analysis restricted to simplified types of two-dimensional smooth beds

without moveable sediments. In a 17m length, 0.6m wide flume, experiments were performed. Slope of the channel was set at 0.001m/m. Flume experiments using two-dimensional bed shapes that have been simplified and an internal mobile wall to segregate effect of the width of the channel. In the current case, four channel widths were investigated. In order to explain the influence of CDF and CAF on streamwise velocity profiles, shear velocity (u*) and Coles wake parameter (𝕀𝕀) were calculated . The results of the study indicated that the shear velocity recovery (u*) and Coles wake parameter are guided by a simple effect reaction to uniform flow environments which are unresponsive to the width of the channel, whereas lateral flow concentration (Ψ) as well as main stress of Reynolds (u'w') happen as two-phase spreading in addition to relaxation reactions that adopted a scaling relationship on order of 3-4 times width of a channel, or around half usual distance among pools. During CDF, the u'w' increased, in the position where the mean bed velocity was at lowest. Therefore, hydrodynamic recovery from disruption thus tends to help clarify the sensitivity of size of macro bed forms to channel width in rivers.

Rodrıguez et al. (2013) concentrated on assessment of 3-D flow structure and the measurement of hydrodynamic variety of this unique pool-riffle configuration, in their laboratory study. The experiments used a sloping flume 12.20 m length, 0.91m wide, and 0.6m height. Employing commercial 3/8 in. crumpled stone chips (D_{90} =1 cm, D_m =0.57 cm, channel slope S_0 of 0.25 %), immovable, hydraulically rough, irregular bed was constructed includes 3 riffles and 3 pools as pointed in figure 2.7. Two flow situations were examined, with 0.03 and 0.11 m^3/s discharges.

Figure 2.6. The experiments tilting flume (Rodrıguez et al., 2013)

A study observed that lower discharge showed a strong topography influence, at the riffle, high-velocity cores were formed by the alternation of lateral convergence and divergence. For the two discharges tested, they were discovered that reversal condition did not happen shear stresses in the bed at the pool and riffle portions, just a convergence of values as discharge rises. While local values were assessed rather than cross-sectional values, the convergence level did not increase. Maximum velocities and bed shear stresses were measured and compared to a flat-bed reference circumstance; spatial flow variability was evaluated. The low discharge showed greater variance than the flatbed case, however, the larger discharge resulted in a low amount of fluctuation, similar to that computed on a flat bed.

Obach (2015) performed a series of laboratory study to investigate Shear stress and hydrodynamic recovery in a straight Channel over fixed bedforms of different lengths, they carried out nine runs were investigated on seven bedform configurations. In the first four tests, the shallow uniform riffle's length was measured and in the fourth through seventh runs, the deep uniform pool's length was put to the test. The last bed configuration was used to test the effect of a rough bed which covered with TrueGrip Traction Tape. Experiments were performed at slope of 0.001 in a 17 m length, 0.6 m width

recirculated flume. Flow velocities was measured by (UDVPs) across the half-width of the channel 4 to 7 profiles were measured, and in the streamwise direction, cross section was separated at 0.15 m intervals. Results showed that as flow accelerate and decelerate over the bedform, the velocity profiles have a tendency to fluctuate in gradient. Velocity profiles, for example, are flatter in CAF than in upstream uniform flow and riffles, resulting in a higher near-beds velocity. In comparison, as a result of CDF, in the outer zone, velocity profiles are steeper, resulting in a lower near-bed velocity.

In uniform flow in the pool, the velocity profile has a tendency to recover towards that detected. In their only one rough bed run found that roughness appeared to impact magnitude instead of the spatial Flow patterns and measures of turbulence. For this run, the estimate for shear velocity was less than for the other runs. At longitudinal scale of small numerous widths of channel, the results of thesis found that in any case of the length of the created bedform, in pool and riffle, hydrodynamic recovering of shear stress and velocity defects happens, and Skin friction, turbulent stress, and total stresses vary from macro-scaling bedform in order for total and turbulent stress in head as well as through the center of a pool surpass skin friction. A study concluded that long bedforms may fail due to flow recovery because boundary layer expansion, rising turbulences, as well as concentration of lateral flow induced erosion in riffle while dissipation of turbulent induced sedimentation in pool, also short bedforms may fail because the limited area

Fazlollahi et al., (2015) performed an experimental investigation to explain how an artificial pool's entrance and exit slopes influence the mean velocity of Reynold shear stress and intensity of turbulence distribution for various slopes.

Based on field data and previous studies two-dimensional pools were chosen for experiments, to be conducted in an 8-meter-long, 0.4-meter-wide, and 0.6-meter-deep flume. The flow depth and aspect ratio, respectively, were 0.2 m and 2, for the uniform section. The angles of 5, 10, 15, 20 picked for entry and exit slopes, based upon field investigations on the Zayandeh-rud river in central Iran and for each experiment, the wavelength of the two-dimensional bed shape was 1.5 m and discharge of flow 18.5 L/s kept constant during all experiments.

The researchers pointed out that in deceleration flow, near bed velocity is less than free surface for all four slope angles, and this variation increases in the direction of the stream. With increase in angle of slope, overall normalized shear stress increased. The form of the stress distribution of Reynolds was normally depending on the angle of slope and flow deceleration or acceleration, and small angle (5°) made major difference in the values of velocity and shear stresses, and influence of the pool on characteristics of flow cannot be ignored. Secondary current was easily noticed when the slope angle rose, particularly for slope of 20.

Bayat et al., (2017) through their field studies in a reach of Bear Creek in Arkansas in United States for the purpose of examining the degree to which all of these mechanisms contribute to overall self-maintenances of PRS (multidimensional flow and multifractional sediment transport) and to identify whether different methods may be prevalent in a real stream under different conditions. With PRS that is well-defined and stable, a gravel bed river. The reach possesses 0.2 percent longitudinal slope, 30 to 40 m width, 5 to 7 m a bankfull depth as well as a bed sediment (D_{50}= 29.5 mm and D_{90} = 50 mm) consisting mainly of gravel but also of some sand and also cobble. Investigation demonstrated that the combined influence of 3-D flow and sediments motion in the analysis of reversal situations revealed that self-

maintenance circumstances occurred much more frequently (2 to 4 times) than before assumed, constructed on the expectations of conventional hypothesis of velocity reversal. Approach estimation indicated that for discharges significantly smaller than bankfull discharge, self-maintenance conditions can occur, and hydrographs using discharge as less as 1/7 of bankfull discharge could show reversal of local sediment transport condition due to finer concentration of sediments and flow velocity in pool.

Their observations led to a better understanding of the complex interacting processes that influence natural PR sequences' self-maintenance. The findings can be used to choose procedures for the creation of manufactured PRS or to protect those that already existed.

Najafabadi et.al., (2017) performed an experimental study for the purpose of comparison between two-dimensional and three-dimensional flow structure over manufactured sequences of pool-riffles in a rectangular flume 16 m length, 0.9 m width in addition to 0.6 m depth, depth of flow was 0.26 m in channel, d_{50} was 10mm.The length of the artificial bed shape series was 2 m. Together entrance and exit slope of pools were established in the stream-wise direction with a slope of 15°.Three discharges used in their experiments as following, 21.4L/s, 25L/s and 30L/s.

The study found that for 2D PRS, velocities along the center line at the channel bed were greater in all sections than those for the 3D PRS. Also, for 2D PRS, as with the 3D PRS, near-bed velocities were reduced along the decelerating flow segment. By observing the separation of the flow, they found that the longest flow separation distance was located 30 cm far from the wall of canal along longitudinal axis and then declined towards the center line of channel. Also observed that in 3D PRS near the channel wall flow separation not occurred, while in 2D PRS along the central line, there was a

short separating zone that begins around the end of the entry slope and disappeared in deepest section of pool's center.

From analysis on shear stress profiles, shear stress at bed of channel was discovered to have the greatest value for normal flow in both 2D and 3D PRS and has decreased linearly to zero at the water level.

2.9 Numerical Studies

Booker et al. (2001) carried out a 3D CFD model in order to better understand how pool-riffle morphology is maintained in a natural pool-riffle sequence, researchers studied hydraulic patterns. From field measurements in 70 m reach in meandering channel with prevailing geomorphological characteristics, including pools, riffles and point-bars, of the Highlands Water in New Forest, Hampshire, UK, model data were gained. Two measured discharges were used for model simulation. High flow discharge was 1.88 m^3/s, and an intermediate flow 0.91m^3/s was observed. Table 2.2 shows the channel characteristics.

Table (2.2): channel characteristics (Booker et al., 2001)

Catchment area	12·7 km^2
Drainage density	2·18
Channel width	2·8 m
Bankfull depth	0·94 m
Bed slope	0·0085
$Q_{bankfull}$	2·2 $m^3 s^{-1}$
Maximum mean boundary shear stress (DuBoys method)	29·1 N m^{-2}
Maximum stream power	24·2 W m^{-2}
D_{16}	8·5 mm
D_{50}	18·6 mm
D_{84}	36·9 mm
Corey shape factor	0·52

SSIIM was the CFD code used in this investigation. For 3D simulations within SSIIM, to calculate turbulent shear stress, $k - \varepsilon$ model was employed. The eddy-viscosity conception with $k - \varepsilon$ model was utilized to simulate

Reynolds stress expression. In the simulation, a boundary condition that is resistant to flow in the form of boundary roughness was used. Roughness of bed on every pool, riffle or bar for this research was considered to be constant. The parameters of roughness height were entered into model built on 3.5 D_{84}. When the modeling estimates were compared to field measurements, inconsistencies of the size comparable to the estimation errors for water surface heights were discovered. The simulation findings showed that as discharge increases, cross-sectional pool velocity rises but cross-sectional riffle velocity decreases. With rising discharge, the bed shear stresses decreased in all cross-sections of the mid-riffles. These reductions were spread through the cross-sections in a relatively uniform manner. Unlike in the pools, wherein bed shear stress grew with outflow grew. Highest rises were in deepest areas of pools. The results also showed that by recirculating eddies, high velocity at pool-head maybe induced.

Researchers showed that in Spatial hydraulic pattern analysis that general explanations of patterns of pool-riffle hydraulic, such as reversal of velocity, are too simple to describe the repair of all pool-riffle sequences. Near-bed velocity trends indicates that a strong effect on pool-riffle maintenance is the direction of sediment routing. Patterns of velocity near the bed confirmed by findings from tracing tests indicated that the direction of flow near to the bed may cause sediment must be diverted away from the pool's deepest parts.

Stoesser et al. (2010) studied the flow statistics, second order turbulence statistic, and characteristic of flow over mildly slope pools-riffle series of longitudinal and near bed turbulence. High resolutions Large-Eddy simulation were carried out and compared with experimental data acquired in laboratory. Simulations were done using the HYDRO3D-GT code. Utilizing a cell-centered Finite-Volume approach with collocate storing of Cartesians velocity elements, the code solves the filtered incompressible

Navier-Stokes equations on block-structured curvilinear grids. The Smagorinsky dynamic model were used. Setup and boundary conditions were chosen in relation to laboratory experimentations that carried out in a 60cm wide, 30m long rectangular smooth surface bed flume, bulk velocity in the pool was 0.22m/s, and the flow depth in the pool, H=0.115m, Re=20,000. Primary and secondary flow velocity components were measured over cross sections throughout the flow using vectrino ADVs.

At top of the pool-riffle sequence, a separate shear layer arises and expand above the decelerating section. This causes Kelvin-Helmholtz instability above the boundary layer on the downslope, resulting in turbulence structures. Coherent structures exist along the upslope in the shape of near wall stripes, and the shallow portion of series, flow deceleration and formation of shear layer on downslope tends to result in a break-up of those stripes, and incoherence of flow in pool near the bed.

Dashtpeyma and MacVicar, (2018) did a numerical study in an isolation pool-riffle with distinct riffle height, they used large eddy simulation (LES) of the turbulence flow to show how vortice were formed, dissipated, and interacted with one another to shape the total flow patterns and turbulences that detected. The program used is version 16.2 of ANSYS CFX. The model is three-dimensional and has a structured mesh. They simulated a simplified model with a single pool and riffle unit geometry. In a numerical simulation, the simulated flume was 6 m length with riffles and pool length of 0.4 m and 2.4 m, respectively. Froude number was 0.2 in the pool. The flow depth was 0.12 m at the center of the pool and inlet, and the velocity of the inlet was 0.21 m/s. results validation made with experimental data.

A new theory was proposed named vortex-resistances, which indicated that structures of turbulent behave as an obstruction that steers the flow by

changing pressure domain and increasing eddy viscosity. Four different vortex forms have been described and called as follows, surface rollers (SR), corner rollers (CR), ramp rollers (RR) and axial tails (AT) . The simulations showed that as they move downstream, all four forms of vortices interacted with one another, merge, reinforce or cancel each other out. The power and interaction of vortices result in various forms of patterns of flow. The flow pattern is called skimming flow, if vortices near the pool's bed force the flow up and make it skimming the top surface nearby. In addition, if the vortices are formed near the surface, resisting the flow and plunging flow into pool. The name of this form of flow is plunging flow. The third pattern was named flow rifting, which formed when vortex near bed and free-surface apply equal resistive to flow. Flow would have highest velocity about middle of channel depth in balanced conditions.

Chapter Three

Numerical Simulation Model and Studied Cases

The shapes, roughness heights, and configurations of the elements placed in the bed of the flume were included in the parameters that were used to investigate flowing water in open channels with roughness bedforms using CFD software. The CFD program was then used to create research runs. The geometry with roughness components, their settings, and the design of the CFD program runs are covered in detail in this chapter. This chapter also includes general information about the CFD program that was utilized as well as specifics the input settings.

3.1 Bedform Discerption

This study used simplified two-dimensional bedforms, which assumed no lateral variability. Various bedform geometries were evaluated by placing bedforms on the bottom of the flume, the simulated region consists of a straight channel with a rectangular cross section with constant slope equal 0. 001.Numerical simulation were carried out in a 10-meter-long, 0.45-meter-depth, and 0.3-meter-width molded flume (Figure 3.1). Bedform were set as a succession of shallow and deep parts with gentle transitions in between. By varying the lengths of the shallow and deep parts, the hydrodynamics of three distinct bedform lengths were investigated (Table 3.1 and Figure 3.1).

The number of bedforms used for the simulations was changed depending on the longitudinal dimension of the bedforms, while the length of the modeled domain was held constant at 10 m. Length of Riffle as a pool length ratio, pools-to-riffles length ratio vary from 1:0.8 to 1:1.9 in channels with gradient less than or equals to 2%, as recorded in previous studies (Wohl et al., 1993; Carling and Orr, 2000).

Table (3.1) Lengths of three distinct bedform used in numerical simulation

Geometry	Riffle Length(R.L)	Pool length(P.L)
G1	0.4	0.4
G2	0.4	0.7
G3	0.4	1.6

And also, researchers recorded mean pool to pool space is between 5 and 7 width of channel, relying on these facts, the dimensions in the table(3.1) were extracted. Over streamwise length of 0.50-meter, transition portions were inclined at 7.2° from horizontal, resulting in a 0.06 m variation in height and a 0.51 m bed slope length. That slope prevents separation of flow (Simpsons, 1989) and is within the zone of normal macrobedform leeside angle (Carling et al, 2000). For all runs, the measurements were performed over the second bedform in the sequence.

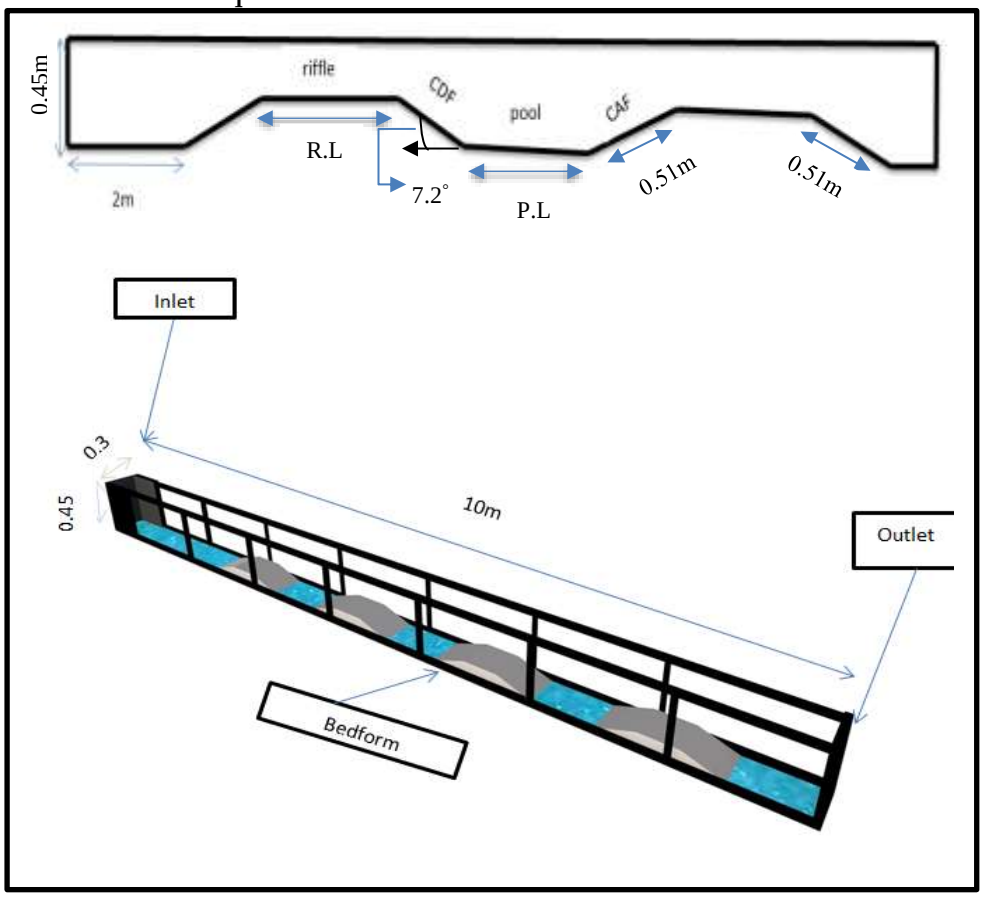

Figure 3.1. A schematic drawing shows the bedform test section within the flume.

3.2Numerical Model Runs Design

It is necessary to create the runs of this mathematical model in order to examine the flow in a flume with roughness components using ANSYS FLUENT. The tested discharge and the water depth at the downstream end are other characteristics that were introduced to perform the hydraulic calculations, in additional to the shape, height, and setup of the roughness components. In the thesis, two discharges were used. These discharge rates were 15 l/s, which have Froude number indicated subcritical flow, which occurs when Fr < 1 and 21 l/s, which have Froude number indicated critical flow. At downstream end of flume, equivalent water depths were 0.12 and 0.08 meters, respectively. Two runs were done within the flume without any roughness components for comparing purposes.

Pre-processing simulations, setting up parameters, and postprocessing are all steps in the ANSYS CFD process.

3.3 Pre-processing

Simulation is a vast topic area that is now utilized to assess a design products and processes. Within simulations, numerous factors such as structural, thermal, and fluid flow can be investigated; nevertheless, the mesh, often known as the "grid" is the foundation for all simulation software and research. Pre-processing refers to the requirement to process a CAD model before going on to the solver in order to integrate into the solver or supply the solver with the necessary information. Geometry is produced during pre-processing, as well as clean-up, to ensure that any unnecessary portions are removed or changed. Additionally, the mesh may be generated and boundary conditions can be specified. To achieve any result, the initial step was to create a mesh or a CFD CAD model before starting any simulation. Meshing is a key factor of the CFD process, and without it, the problem can't solve or

even hope to get any useful results. Also, meshing has a direct relationship with the accuracy of CFD simulation results: the higher the mesh quality, the more accurate the results may be predicted. Basically, a mesh is necessary because the variables such as flow and heat transport, as well as any other variable, are solved by physics or mathematical theory at these cell centers or nodes. Furthermore, theoretical methods such as the fine difference technique, finite element method, and finite volume method are utilized to solve the variable at these discrete cells/nodes in any CFD research.

3.4 Mesh Generation

Triangles, quadrilaterals, tetrahedrals, and hexahedrals are examples of grid forms; a mesh is a collection of these components. The following mesh types are often used in commercial software for academic or industrial uses: 1. Cartesian; 2. Structured; 3. Unstructured; 4. Hybrid.

Structured mesh is a single block covers the whole geometry and was also used for single forms where a single block was adequate to cover the CAD model. The components of a structured mesh were oriented in a certain way or follow a structured pattern. Unstructured mesh, on the other hand, was created when the components were randomly placed.

The meshing size was quite small near the boundaries, sides and bed, so a reasonable estimate of the gradients was achieved. Near the roughness bed, the meshing should be dense, but not overly so in other places. To achieve a more precise outcome, a finer mesh was employed. The accuracy of a coarse mesh was poorer. The finer mesh, on the other hand, was utilized more time and with more elements. The skewness and orthogonal factors were used to assess the mesh's quality. The range of skewness and orthogonal quality in our research is 0 to 1.

The computational domain was meshed using the face sizing and inflation technique within the workbench, and the resulting two-dimensional mesh system was then exported to the solver (FLUENT). As illustrated in figure (3.2), an unstructured mesh comprises quadrilaterals on 2D faces of 0.005 m element size and the grids ranged in size from 1-4cm, with a total number of nodes and elements arrange in Table (3.2) for each run.

Lastly, the mesh quality was within acceptable bounds, with an orthogonal quality in range of 0.83 and a skewness in range of 0.55.

Table (3.2): Number of nodes and elements used for meshing

Geometry	Nodes	Elements
1	95870	46906
2	370484	183188
3	399072	197471

Define every part in the geometry as a name selection throughout the model's development. This was done in order to move forward with the research and to establish boundary conditions for a certain domain. Inlet, outlet, Bed, free surface and fluid domain are among the listed options.

3.5 Governing Equations

The Navier-Stokes and continuity equations were numerically solved in ANSYS CFD. The Navier Stokes equation were nonlinear partial differential equations of second order and unsteady. Built on Newton's Second Law and mass conservation concepts in physics. For simple turbulent and laminar flow, it can be solved immediately. Eqs. (3- 1) and (3- 2), respectively, explain these equations (ANSYS FLUENT Theory Guide, version 16.1, Fluent Inc.):

$$\frac{\partial u_i}{\partial t} + \frac{\partial u_i\,\partial u_j}{\partial x_j} - v\frac{\partial^2 u_i}{\partial x_i\,\partial x_j} - v\frac{\partial^2 u_j}{\partial x_i\,\partial x_j} + \frac{1}{\rho}\frac{\partial \tau_{ij}}{\partial x_j} + \frac{1}{\rho}\frac{\partial p}{\partial x_i} + \frac{1}{\rho}\frac{\partial p}{\partial x_j} + g\delta_{ij}$$

$$= 0 \qquad (3.1)$$

$$\frac{\partial u_i}{\partial x_j} = 0 \qquad (3.2)$$

Where:

ui = i-th Reynolds averaged velocity component, L/T

x_i = i-th axis, L

t = time, T

ρ = density of water, M/L^3

p = Reynolds averaged pressure, M/L^2

g = acceleration due to the gravity, L/T^2

v = kinematic viscosity, L^2/T

δij = Kronecker delta, and

τij = Reynolds stresses, M/L^2

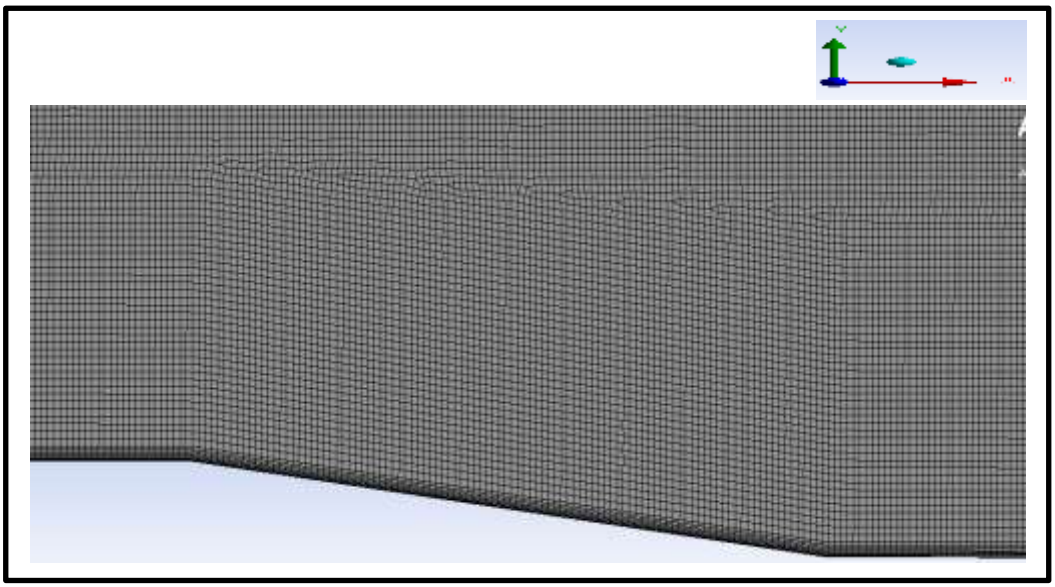

Figure 3.2. Quadrilaterals mesh Cells in 2D faces for section of channel

Using a mixing function, the SST (Shear Stress Transport) approach integrates the k- ε and k- ω models. In the zone near to the wall, SST model turn on the k- ω model, while the remainder of flow was handled by the model of k- ε. This method makes use of the k- ω model's near-wall performance while avoiding the possible mistakes caused by the model's free stream sensitivity. This can be represented by the equations (3-3) and (3-4)

$$\frac{\partial}{\partial t}(\rho k) + \frac{\partial}{\partial x_i}(\rho k u_i) = \frac{\partial}{\partial x_j}\left(\Gamma_{\mathrm{k}} \frac{\partial k}{\partial x_j}\right) + G_{\mathrm{k}} - Y_{\mathrm{k}} + S_{\mathrm{k}} \qquad (3-3)$$

$$\frac{\partial}{\partial t}(\rho \omega) + \frac{\partial}{\partial x_j}\left(\rho \omega u_j\right) = \frac{\partial}{\partial x_j}\left(\Gamma_{\omega} \frac{\partial \omega}{\partial x_j}\right) + G\omega - Y_{\omega} + D_{\omega} + S_{\omega} \qquad (3-4)$$

Where

G_k : symbolizes the turbulent kinetic energy generated as outcome of mean velocity gradient.

G_ω : refers for the ω generation .

Γ_k and Γ_ω : The efficient diffusivity of k and ω , respectively

The effective dissipation of k and ω owing to turbulence is represented by Y_k and $Y\omega$.

S_k and $S\omega$:are source terms that have been defined by the user.

The effective diffusivities for the k and ω model are calculated as follows:

$$\Gamma_{\mathrm{k}} = \mu + \frac{\mu_{\mathrm{t}}}{\sigma_{\mathrm{k}}} \qquad (3-7)$$

$$\Gamma_{\omega} = \mu + \frac{\mu_{\mathrm{t}}}{\sigma_{\omega}} \qquad (3-8)$$

Where

σ_k and σ_ω are turbulence Prandtl numbers for k and ω correspondingly.

3.6 Volume of Fluid (VOF)

The Volume of Fluid (VOF) technique was most popular finite volume method approach utilized in CFD systems. The air and water free surface development in ANSYS FLUENT is governed by the volume of fluid technique. The VOF formula was based on the non-interpenetrating nature of two or more fluids (or phases). A variable was provided for each successive phase add to model: phase's volume fractions in computational cells. All of the phases' volume fractions in each control volume add up to one. So long as the volume fraction of each phase is specified at each region, the fields including all characteristics and attributes are maintained throughout phases and reflect volume-averaged values. Depending on volume fraction values, factors and characteristics in every particular cell are each entirely indicative of 1 phase or representational of a combination of phases. At each discretization cell in this approach, a passive scalar called volume fraction is allocated, representing the percentage of each phase in that cell.

i.e. if volume of fractions of q^{th} fluid in cell is indicated as α_q the following three criteria can be met:

$\alpha_q = 0$: The cell (of the q^{th} fluid) is empty.

$\alpha_q = 1$: The cell (of the q^{th} fluid) is full.

$0 < \alpha_q < 1$: The connection between the q^{th} fluid and one or further additional fluids is contained in this cell. (ANSYS FLUENT theory guide version16.1, Fluent Inc.)

3.7 Defining Materials

The key stage in the model setup is the definition of materials and their characteristics. Solids, fluids, mixes, inert particles, droplet particles, and combusting particles are the six kinds of materials defined. The name of the

substance that is connected with its characteristics and is used as a boundary condition.

Fluid materials (including air and water) were employed in the current investigation. The physical characteristics of water (density and viscosity), as well as the surface tension strength of materials, were significantly altered.

3.8 Setting Up a Numerical Model

Modeling is the process of creating a simpler mathematical reality from a more complicated physical reality. It was able to create the shape of the channel with rough bed as well as the boundary conditions using ANSYS FLUENT software to design of runs presented above. In this simulation, various options are used, including transient flow, fluid volume, multiphase flow (air and water), K-ω –SST , and the PISO process (Pressure-Implicit Splitting of Operators). A double-precision method was required to solve the pressure differences in order to extract the flow. The choice of defined operating density in operating conditions should be turned on for the volume of fluid measurement, and the air phase in operating density should be set. The main phase of the process is defined as air, while the secondary phase is characterized as water. The normalize residual should equal 0.001 as a convergence condition.

3.9 Conditions of Flow

Conditions on the problem domain boundaries were defined in order to finish the mathematical model. Initial conditions are those that are connected to the start time, whereas boundary conditions are those that are related to space.

3.9.1 Initial conditions

The number of iterations necessary to achieve a solution can be reduced by specifying beginning circumstances that are close to the desired answer. The

starting conditions can be established similarly to the fluid domain's inlet conditions. Initial conditions are given on a continuous level; if no initial conditions are specified, Fluent will initialize the solution with default values. The following are the starting conditions: velocity, pressure, turbulence, and volume fraction.

Table (3-3) Initial Conditions

Items	Value
VELOCITY	**(0.0,0.0) m/s**
PRESSURE	**0.0Pa**
TURBULENCEINTENSITY	**0.01**
TURBULENTVISCOSITYRATIO	**10.0**
VOLUME FRACTION	**CONSTANT**
WATER	**0**
AIR	**1**

3.9.2 Boundary Conditions

The surfaces that surrounding the solution domain are known as boundaries. The discretized Navier-Stokes equations are used to create a closed system of equations that can be solved. some boundary conditions must be set. Inflow boundaries, outflow boundaries, and wall boundaries are the most common types of boundaries utilized in free-surface calculations.

The simulated domain's boundaries are divided into four categories: inlet, outlet, top, and walls, as shown below:

1. **Inlet Boundary**: Massflow-inlet was chosen as the upstream inlet boundary. Two water massflow are applied to the study 15 kg/s (equal to 0.015 m^3/s) and 21 kg/s (equal to 0.021 m^3/s) while the air massflow was set to zero (initial condition).
2. **Outlet Boundary**: The boundary type was set to Pressure-outlet. The gradients for all variables were set to zero at the downstream output.

Water depths at downstream end of flume were put equal to 0.12 and 0.08m.

3. **Top Boundary**: The free, surface was considered as plane of symmetry and was configured as a frictionless rigid lid.
4. **Wall Boundary**: Wall boundary criteria were applied on the surfaces of bed. The boundary condition of no slip was used to make the velocity at the rigid boundary zero. The roughness height at the bed was utilized as the d_{50}. Roughness height was set to (0.01,0.02 and 0.04 m) for the whole domain according to the research scenarios.

3.10 Criteria for Stopping

Stopping criteria were enabled to specify how long the solution run and when it finished iterating or moving in time. At the end of each simulation step, each given stopping criterion was assessed, and a logical rule was employed to decide if the interaction of all of the criteria stops the solver.

When the implicit unstable model was selected, the node of this criteria emerged and has its own features. This criteria can also control the amount of inner iterations to be executed at each physical time-step if the implicit unstable solver was employed. The time-step feature of the implicit unstable node in the solvers node was connected to the maximum physical time stopping criterion. Because it was wanted to watch the running day by day and pause it in various conditions, the maximum physical duration in this simulation was set to 150 seconds and the maximum steps to 15.000 steps.

3.11 Post-Processing

When the solution is obtained, post-processing software can help to view and analysis the obtained results. Depending on what the user wants to study and observe, a number of flow characteristics might be considered. The velocity field and the turbulence intensity distribution have been the focus of this

study. The data was examined using a variety of colors, contour plots, lines, vectors plots, and graphs, among other things. The ANSYS CFD-Post post-processor, which was used by all ANSYS fluid dynamics products, gives clients everything they need to present and assess their results. The first stage was to validate the model once it had completed the simulation and met all of the stopping conditions.

Figures (A-1) to (A-14) presented in Appendix A, shows the simulation setting and boundary conditions for case study.

Chapter Four

Results and Discussion

In this chapter, the results of the investigations the effects of adding roughness bedform configurations in a flume are presented, which is divided into two sections. The first section includes a comparison of two discharges with the control case and a variation of velocity profiles represented by contours inside the flow domain in the flume for varied configurations and roughness heights. The second section compares the change of velocity with water depth for varied roughness heights, forms, roughness element combinations, and two discharges with the control case.

4.1 Model Validation

The model is validated by comparing numerical simulations to the results of the experiment of (Obach,2011). In xy-plane, the mean streamwise velocity (u) was compared along the simulated domain's centerline. The numerical simulation's findings were compared to the experimental plots as pointed in figures (4.1 and 4.2). An observed and simulated data are taken and illustrated at sections apart at 10% ,50% and 80% from pool length as in (Obach,2011) work to compare the strength of the numerical model with the experimental data. Root Mean Squared Error (RMSE) and Nash-Sutcliffe efficiency (E) are estimated.

1. **Root Mean Squared Error or Root Mean Squared Deviation** is a metric for the disparities between the values predicted by a model or estimator and the actual values observed. When the computations are conducted across the data sample that is used for estimate, these individual differences are referred to as residuals, and when they are computed outside of the sample, they

are referred to as estimation errors. The RMSE is defined as (Dawson et al.,2007),

$$\text{RMSE} = \sqrt{\frac{\sum_{i=1}^{n} (P_i - O_i)^2}{n}}$$

where n signifies the number of observations, i the series' ith term, Pi the simulated value, and Oi the observation value

2. Nash-Sutcliffe Efficiency (E) are expected to offer further information on the model simulation's systematic and dynamic mistakes. Nash and Sutcliffe (1970) developed the efficiency E, which is defined as

$$E = 1 - \frac{\sum_{i}^{n} (O_i - P_i)^2}{\sum_{i}^{i} (O_i - \bar{O})^2}$$

where O is the observed data's mean. E has a range of values ranging from 1.0 (perfect match) to $-\infty$.

Table (4.1): Statistical coefficients to investigate model accuracy.

Coefficient	Obtained value		
	10%	50%	80%
RMSE	0.022	0.011	0.01
NSH	0.771	0.502	0.552

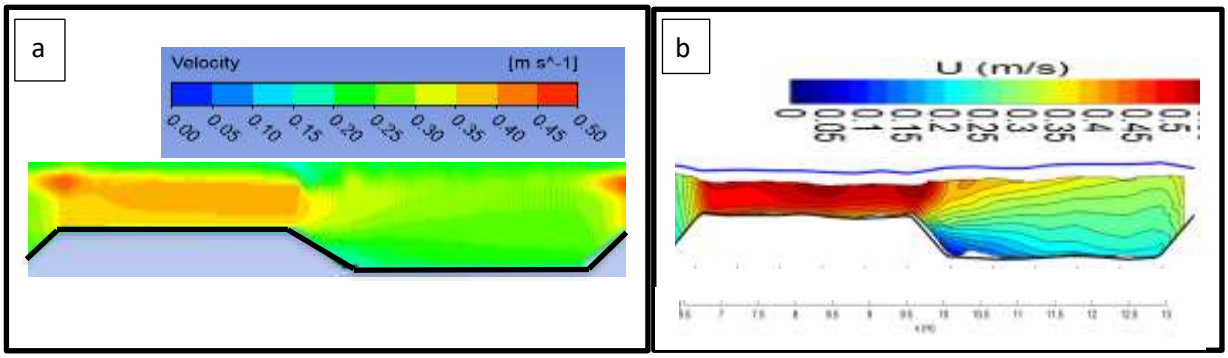

Figure 4.1. Velocity contour in flume (a)Numerical simulation results,(b) physical experimental results.

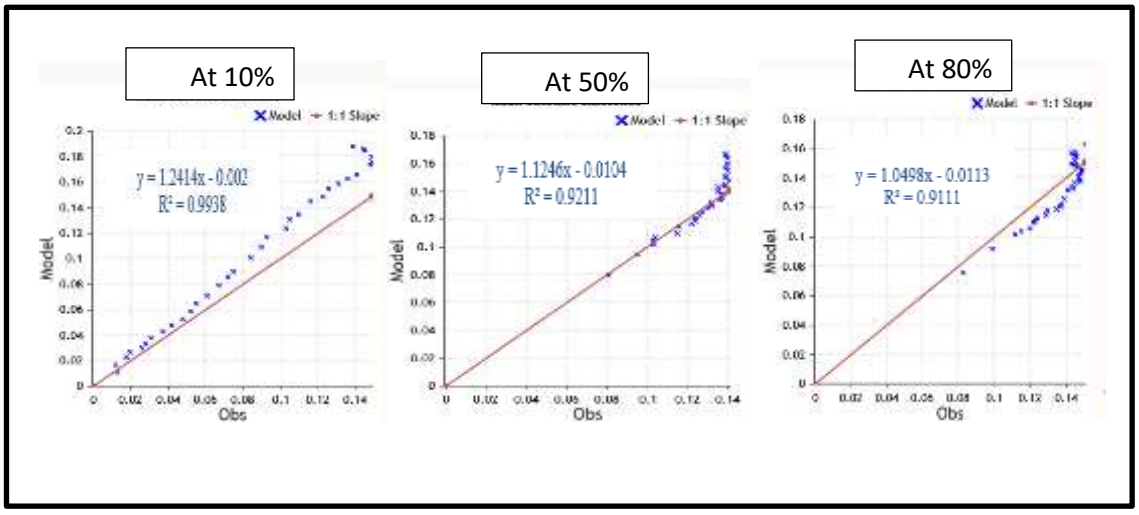

Figure 4.2. Observed versus simulated velocity at sections apart 10%,50% and 80% from pool length.

4.2Using the Straight Channel Case as a comparison

This section compares the velocity profiles, which are shown as contours in the flume, for all instances to the straight channel case.

Figures 4.3 and 4.4 show the directions and values of flow velocity as contours within the flume flow under the control case flow circumstances, without bedform components.

Because the cross section of the flume did not vary, the velocity profiles along the flow domain were generally unaffected. In the situation of a discharge of 15 L/s, sections of the velocity were taken in the same places in which the velocity was taken at the channel containing the bedform (center of pool region) and found to be equivalent to 0.12 m/s, and have maximum velocity at surface of water of about 0.15 m/s. In situation of a discharge equal to 21 L/s, it is about 0.25 m/s, and have maximum velocity magnitude at water surface equal 0.30 m/s.

Results summarized in tables (4-2) and (4-3), which show the change in the velocity as a result of the change in the roughness height (R.H) for two discharges 15L/s and 21L/s, as a percentage of the increase (+) and decrease

(-) in the value of the velocity compared to the straight channel in each of (Riffle, CDF, Pool and CAF) regions for each of the three geometries.

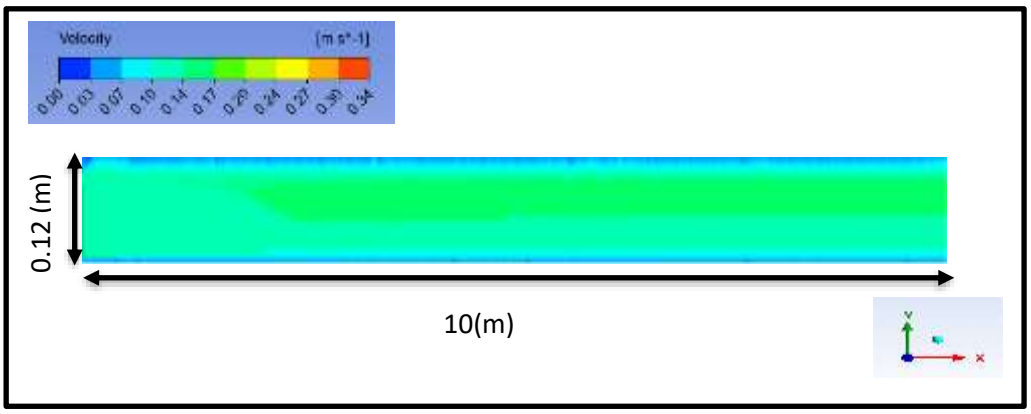

Figure 4.3. Velocity contour in flume without bedform at discharge 15 L/s.

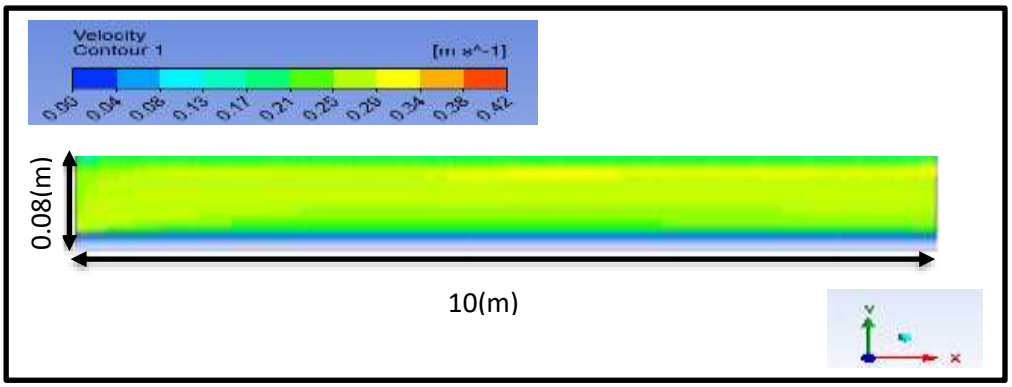

Figure 4.4 Velocity contour in flume without bedform at discharge 21 L/s

4.2.1 For Discharge Equal 15 L/s

Table (4.2): Indication of velocity along the channel geometries and roughness height for Q=15L/s

R.H	1cm				2cm				4cm			
Geometry	Riffle	CDF	Pool	CAF	Riffle	CDF	Pool	CAF	Riffle	CDF	Pool	CAF
G1	+52	+25	0	+14	+50	+20	-4	+12	+45	+17	-9	+13
G2	+50	+25	-9	+25	+47	+23	-6	+20	+48	+20	-14	+18
G3	+50	+27	-9	+20	+49	+25	-5	+18	+48	+20	-14	+14

Figure 4.5 shows the velocity contours within the flow in flume for run of first geometry.

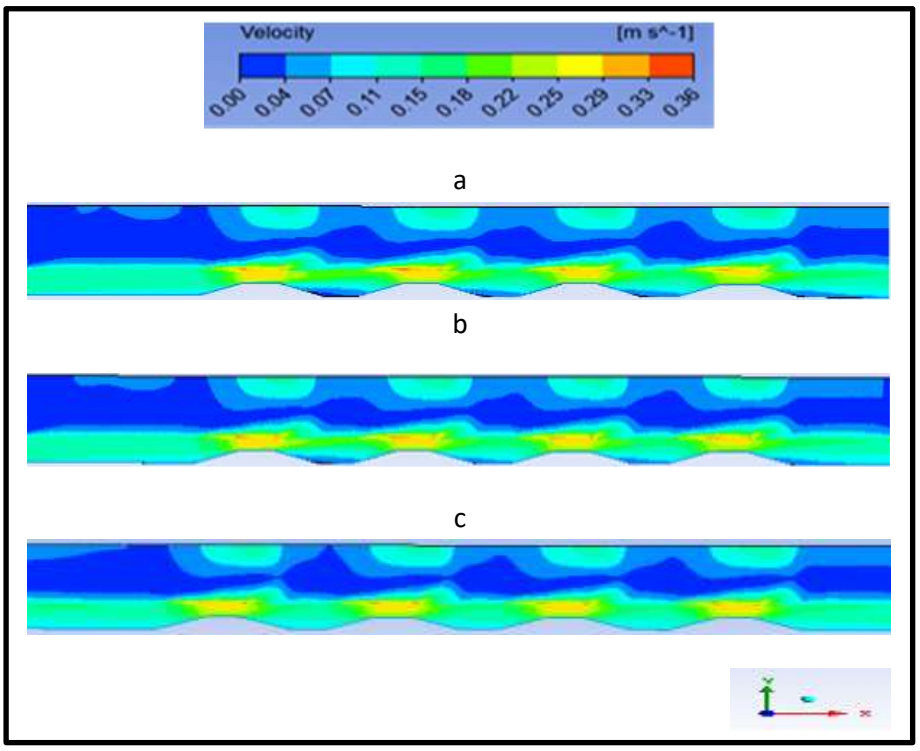

Figure 4.5 Velocity distribution along the channel for G1 for (a) 1cm R.H (b) 2cm R.H (c) 4cm R.H

Figure 4.6 shows the velocity contours within the flow in flume for run of second geometry.

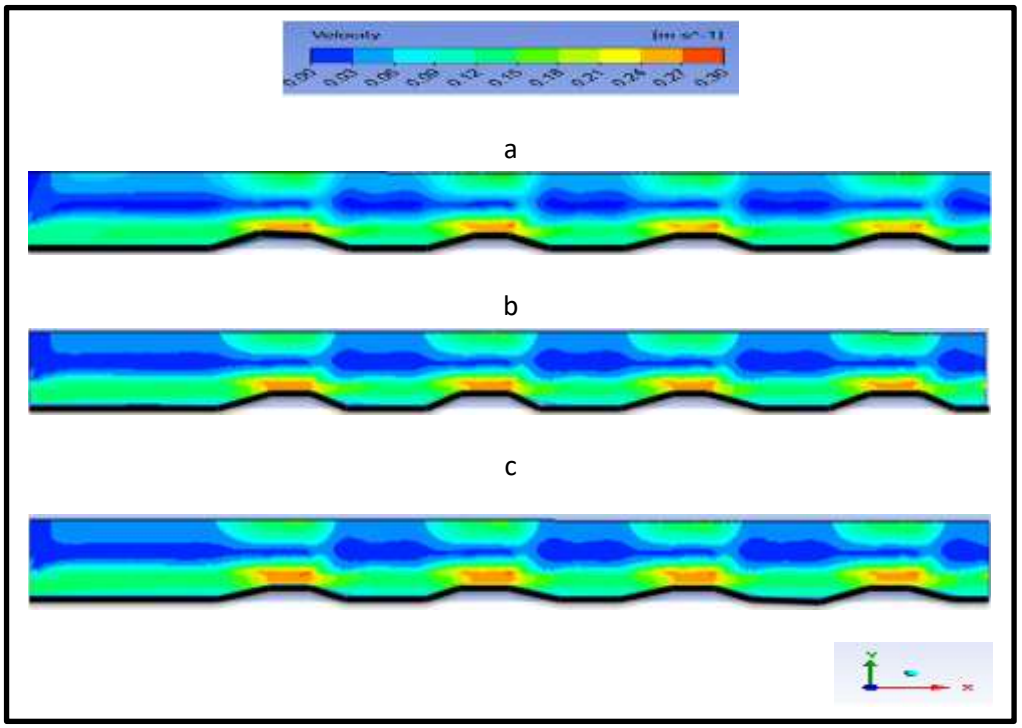

Figure 4.6 Velocity distribution along the channel for G2 for (a) 1cm R.H (b) 2cm R.H (c) 4cm R.H

Figure 4.7 shows the velocity contours within the flow in flume for run of third geometry.

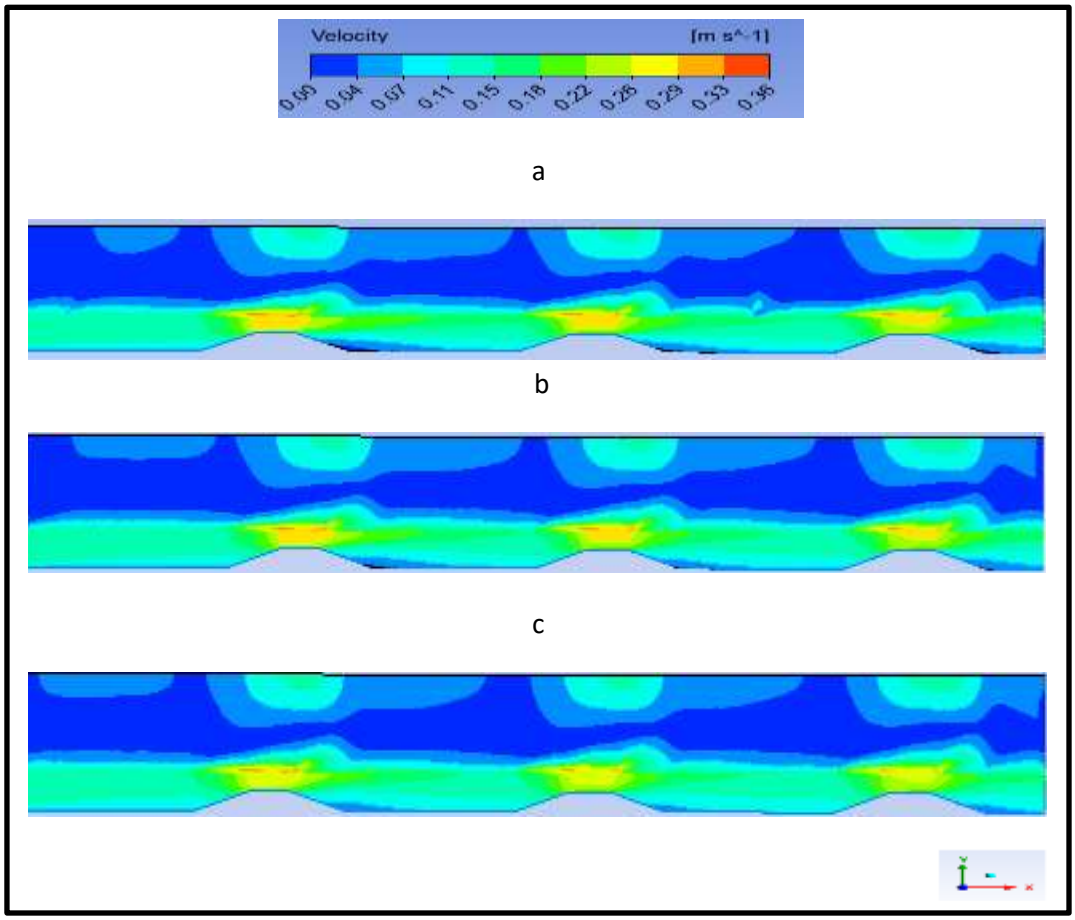

Figure 4.7 Velocity distribution along the channel for G3 for (a) 1cm R.H (b) 2cm R.H (c) 4cm R.H

4.2.2 For Discharge Equal 21L/s

Table (4.3): Indication of velocity along the channel geometries and roughness height for Q=21L/s

R.H	1cm				2cm				4cm			
Geometry	Riffle	CDF	Pool	CAF	Riffle	CDF	Pool	CAF	Riffle	CDF	Pool	CAF
G1	+40	-9	-47	-19	+38	-10	-47	-14	+20	-19	-56	-25
G2	+39	-2	-32	-4	+38	-3	-47	-9	+36	-8	-56	-14
G3	+44	+4	-44	-10	+43	+3	-45	-9	+35	-4	-61	-20

Figure 4.8 shows the velocity contours within the flow in flume for run of G1.

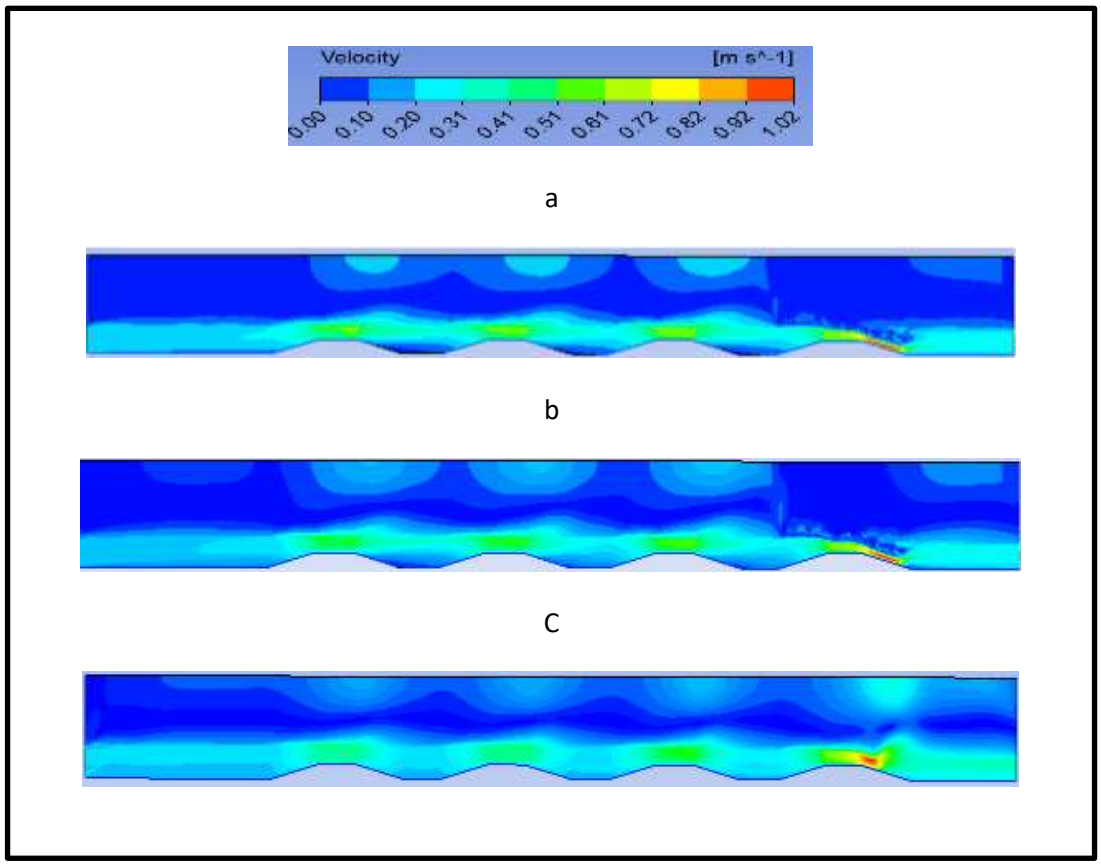

Figure 4.8 Velocity distribution along the channel for G1 for (a) 1cm R.H (b) 2cm R.H (c) 4cm R.H

Figure 4.9 shows the velocity contours within the flow in flume for run of G2.

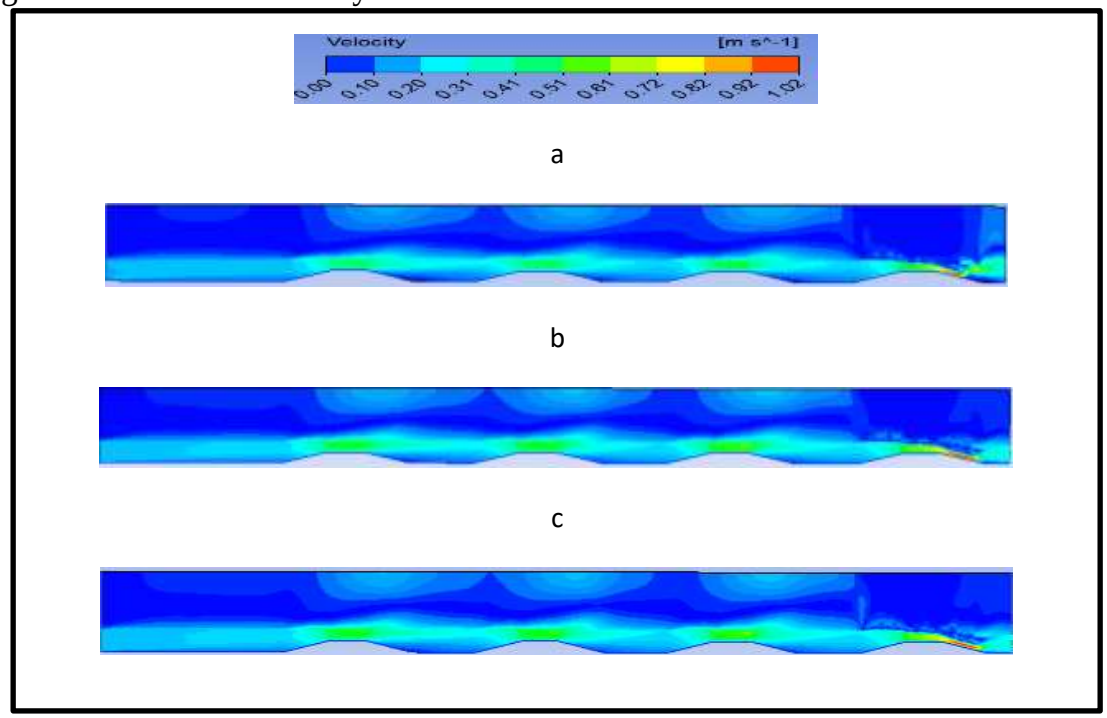

Figure 4.9Velocity distribution along the channel for G2 for (a) 1cm R.H (b) 2cm R.H (c) 4cm R.H

Figure 4.10 shows the velocity contours within the flow in flume for run of G3.

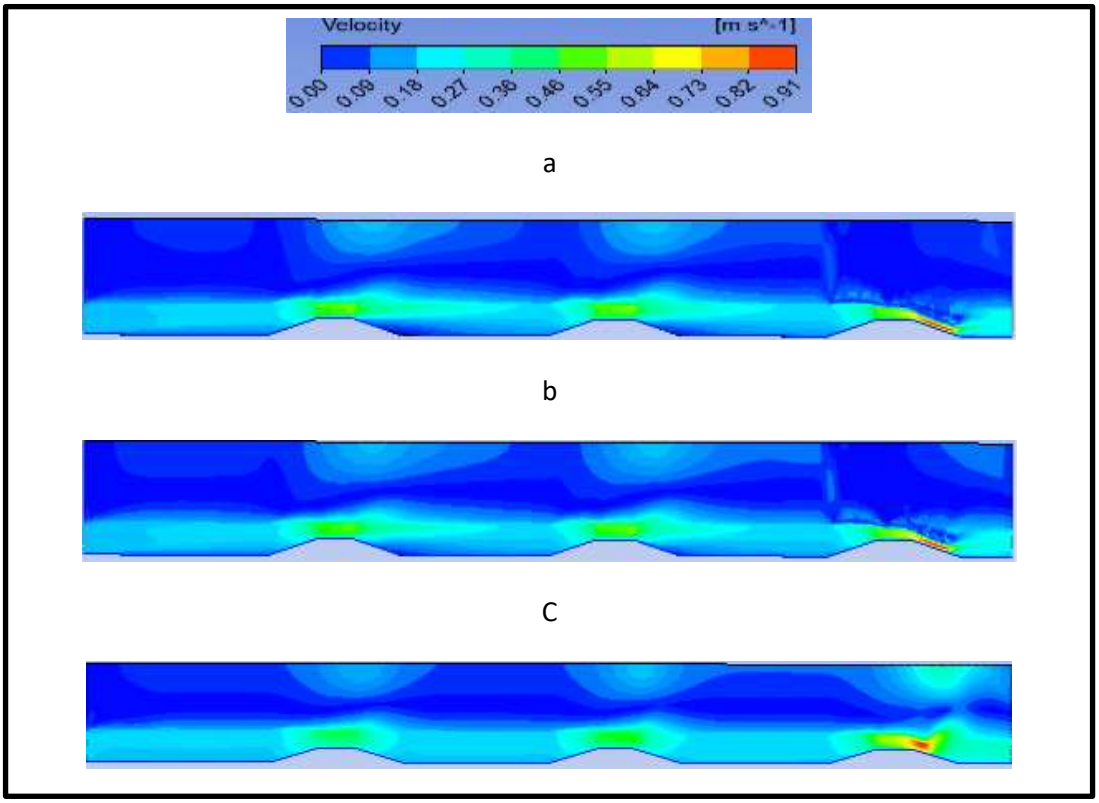

Figure 4.10 Velocity distribution along the channel for G3 for (a) 1cm R.H (b) 2cm R.H (c) 4cm R.H

4.3 Comparison Between Situations

This part presents the variation of velocity with water depth at three different roughness height for three different configurations at location in the center of sections along the flume in cases of 15 L/s and 21 L/s of applied discharges as a comparison between cases.

Results summarized in table (4-4) which show the change in the velocity as a result of the change in the roughness height (R.H), as a percentage of the increase (+) and decrease (-) in the value of the velocity for case of 4cm roughness height compared to the cases of 1cm and 2cm roughness height in each of (Riffle and Pool) regions for each of the three geometries.

Table (4-4):Velocity percentage in center of riffle and pool regions along channel geometries for applied discharges 15L/s and 21L/s

R.H / Geometry	Q=15L/s				Q=21L/s			
	Compared to 1cm		Compared to 2cm		Compared to 1cm		Compared to 2cm	
	Riffle	Pool	Riffle	Pool	Riffle	Pool	Riffle	Pool
G1	-14	-9	-9	-5	-35	-9	-29	-5
G2	-4	-5	+2	-8	-5	-18	-3	-6
G3	-4	-5	-3	-9	-18	-16	-16	-10

Figures 4.11 to 4.19 show the relationship between velocity and relative water depth (y/h) in which y=the distance from the bed and h =flow depth, as a comparison between cases for discharge equal 15 L/s .

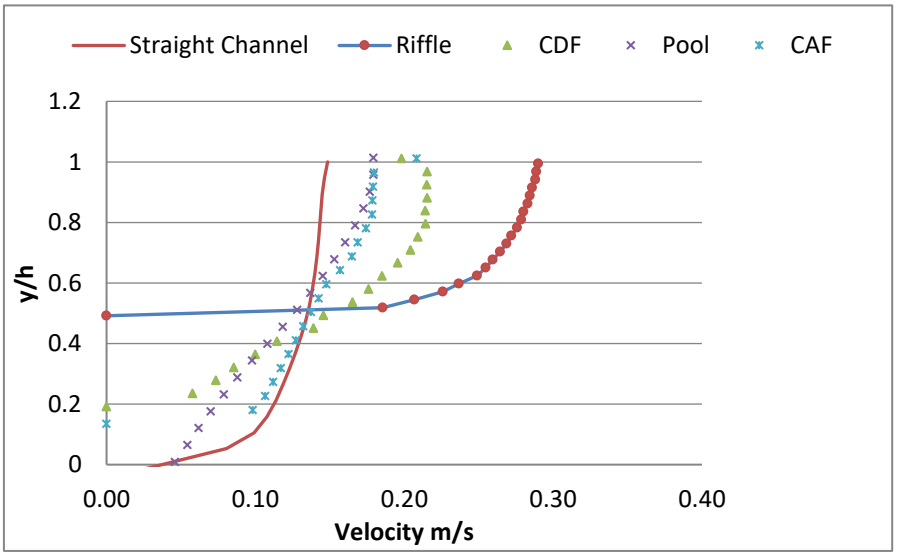

Figure 4.11. Velocity profiles for G1 shown effects of 1cm R.H at center of each location pointed in figure 3.1

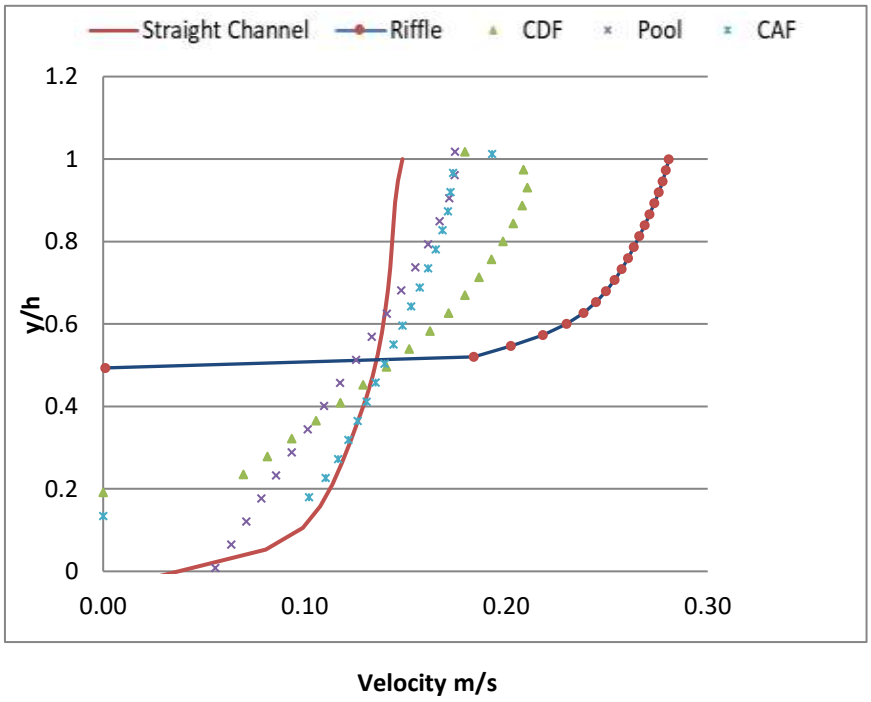

Figure 4.12. Velocity profiles for G1 shows effects of 2cm R.H at center of each location pointed in figure.3.1

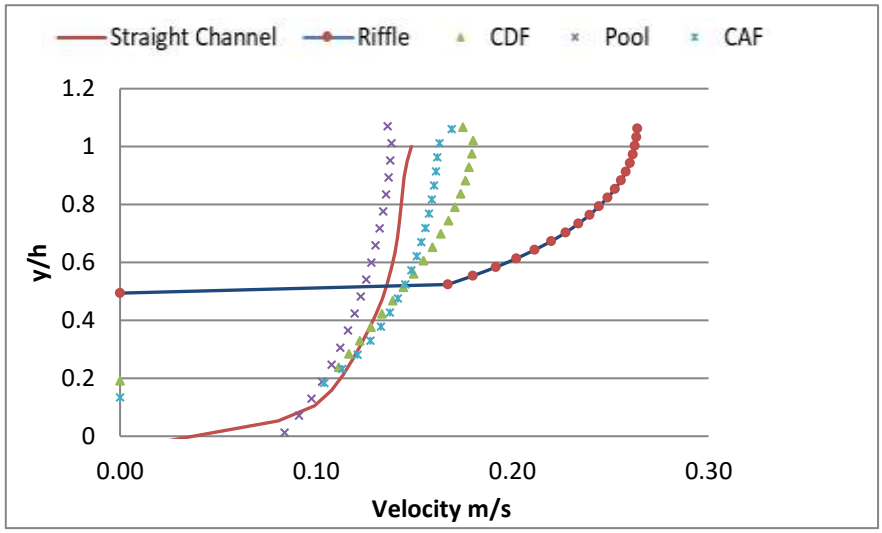

Figure 4.13. Velocity profiles for G1 shows effects of 4cm R.H at center of each location pointed in figure3.1

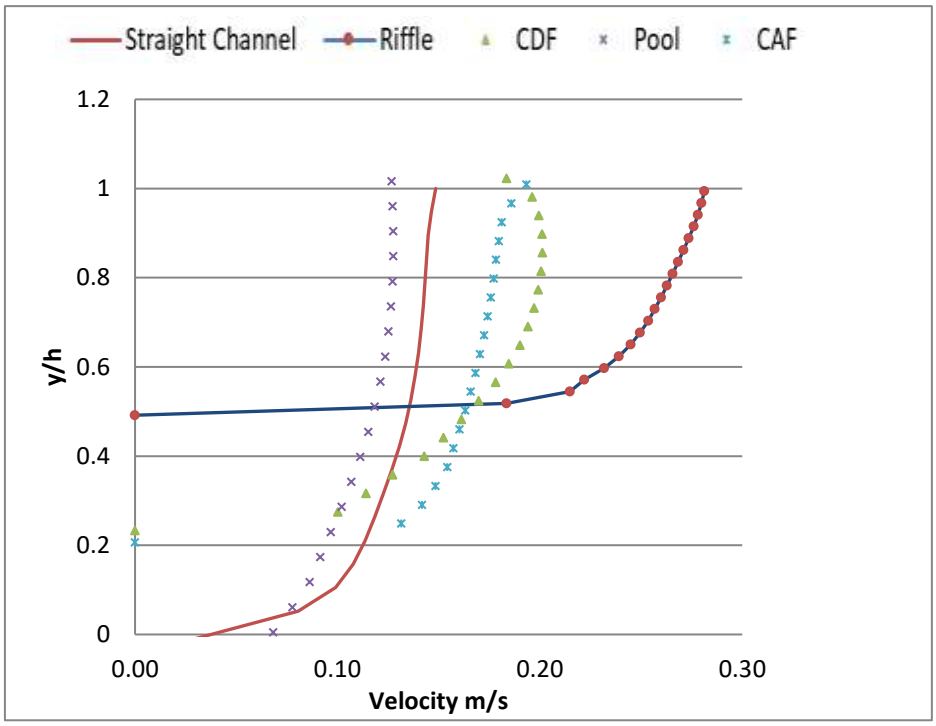

Figure 4.14. Velocity profiles for G2 shows effects of 1cm R.H at center of each location pointed in figure3.1

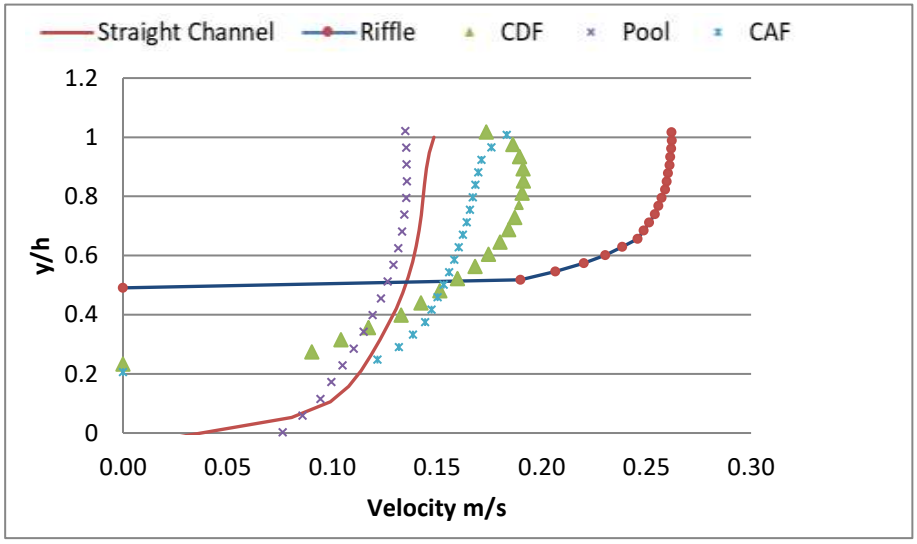

Figure 4.15. Velocity profiles for G2 shows effects of 2cm R.H at center of each location pointed in figure3.1

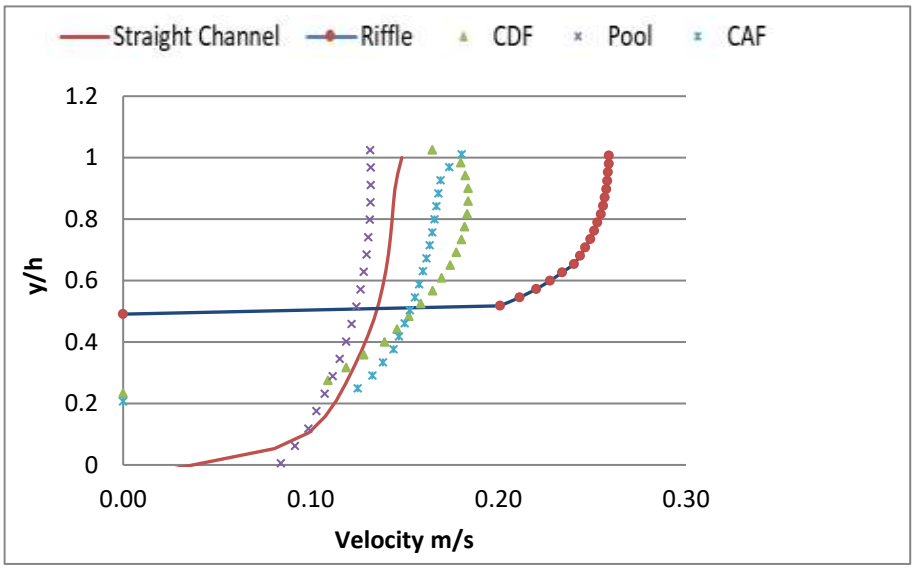

Figure 4.16. Velocity profiles for G2 shows effects of 4cm R.H at center of each location pointed in figure3.1

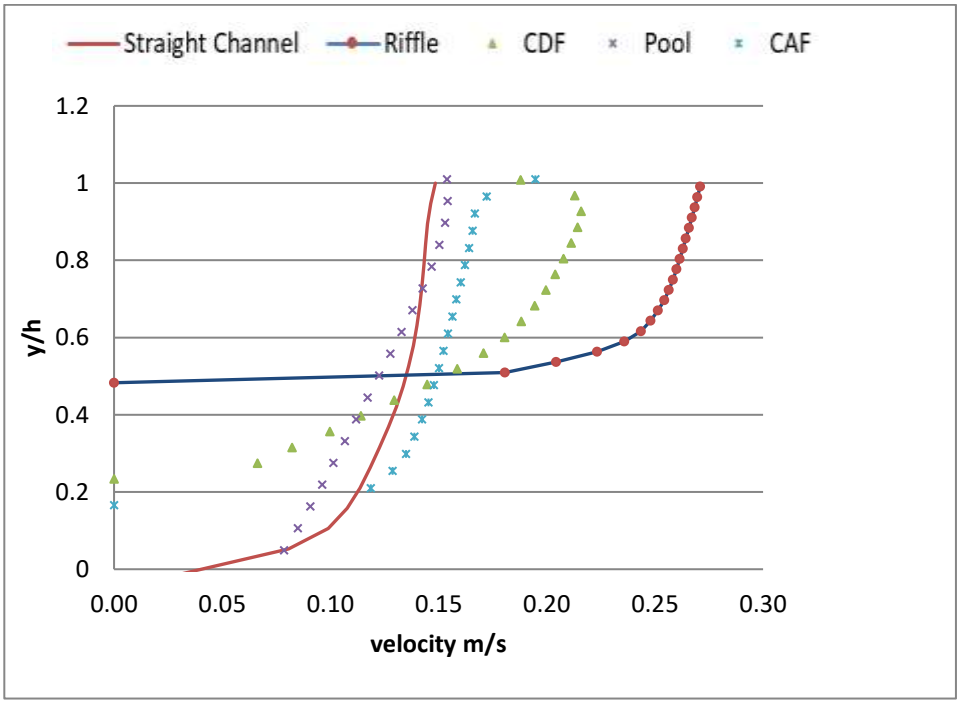

Figure 4.17. Profiles of velocity for G3 shows effects of 1cm R.H at center of each location pointed in figure.3.1

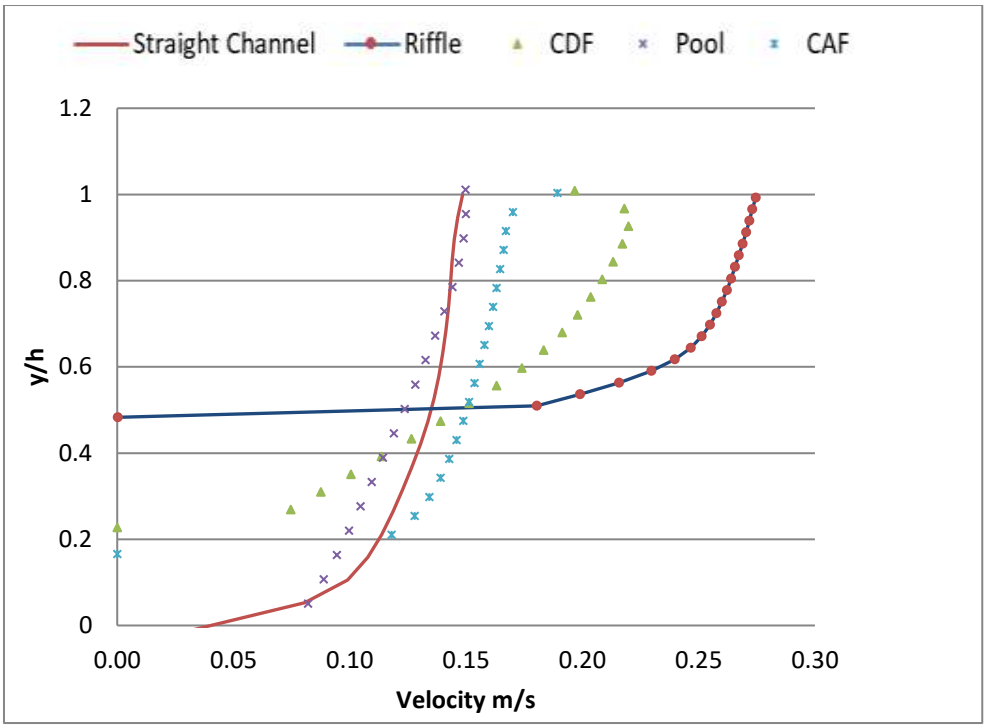

Figure 4.18. Profiles of velocity for G3 shows effects of 2cm R.H at center of each location pointed in figure.3.1

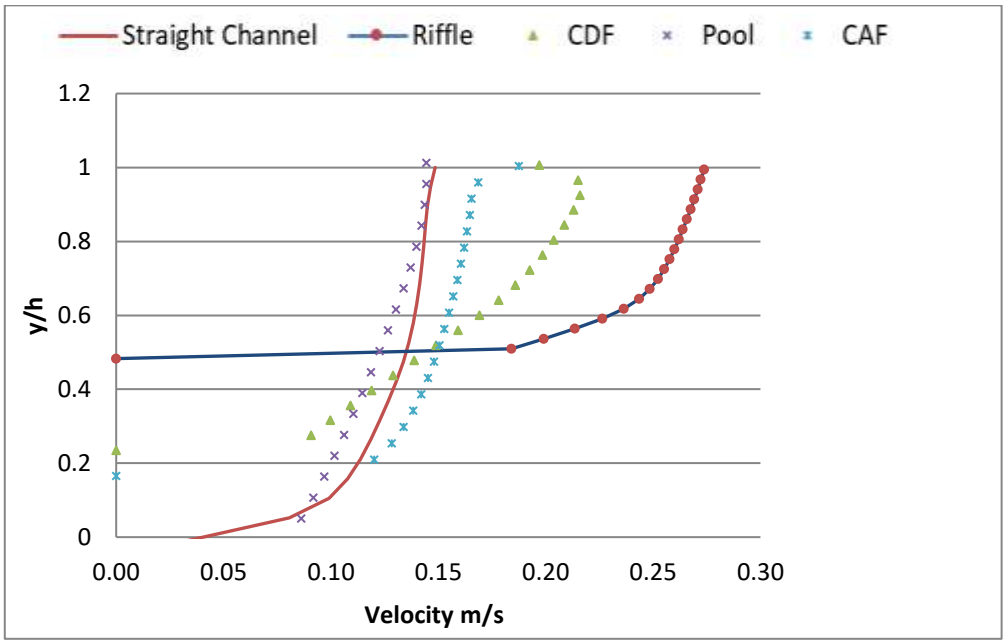

Figure 4.19. Profiles of velocity for G3 shows effects of 4cm R.H at center of each location pointed in figure.3.1

Figures 4.20 to 4.22 show the relationship between velocity and relative water depth as a comparison between cases for discharge equal 21L/s in G1.

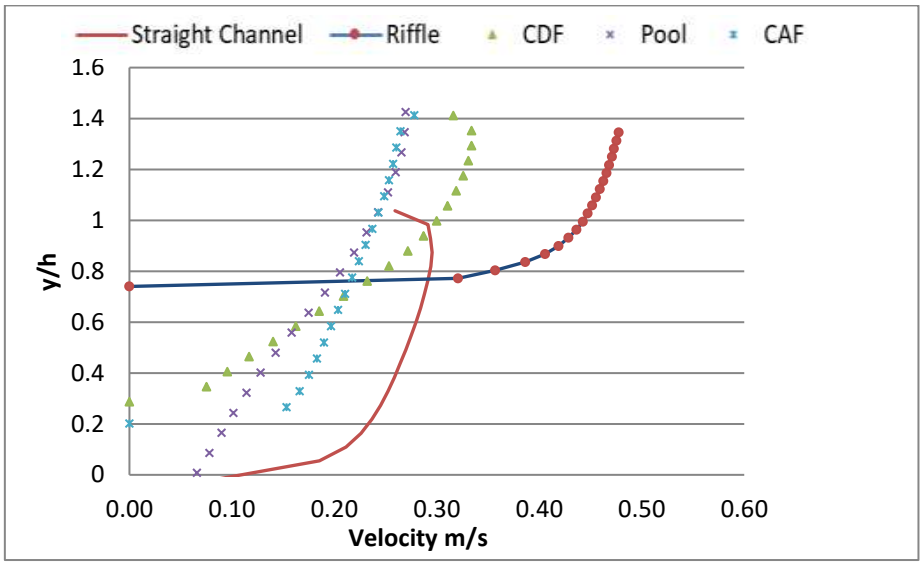

Figure 4.20. Profiles of velocity for G1 shows effects of 1cm R.H at center of each location pointed in figure.3.1

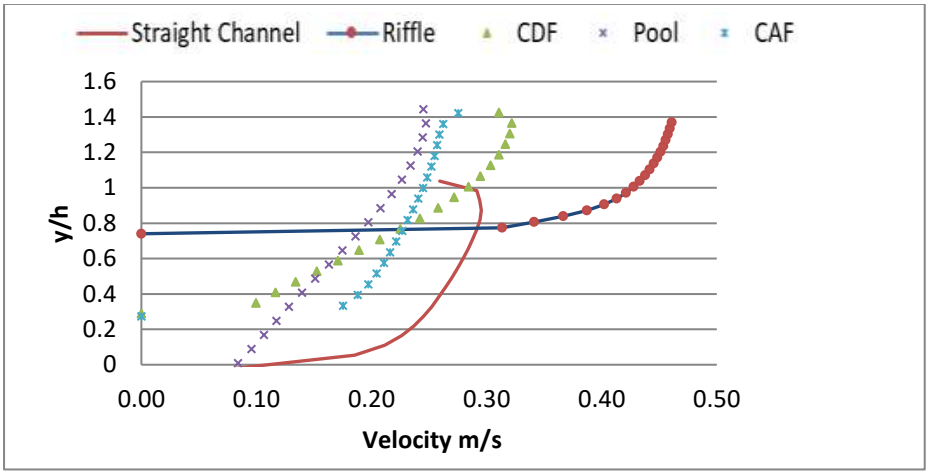

Figure 4.21. Profiles of velocity for G1 shows effects of 2cm R.H at center of each location pointed in figure.3.1

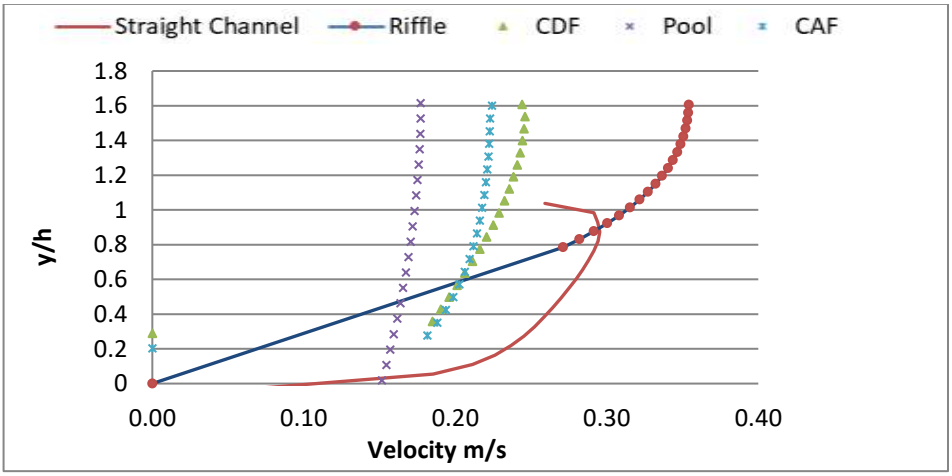

Figure 4.22. Profiles of velocity for G1 shows effects of 4cm R.H at center of each location pointed in figure3.1

Figure 4.23 to 4.25 show the relationship between velocity and relative water depth as a comparison between cases for discharge equal 21L/s in G2.

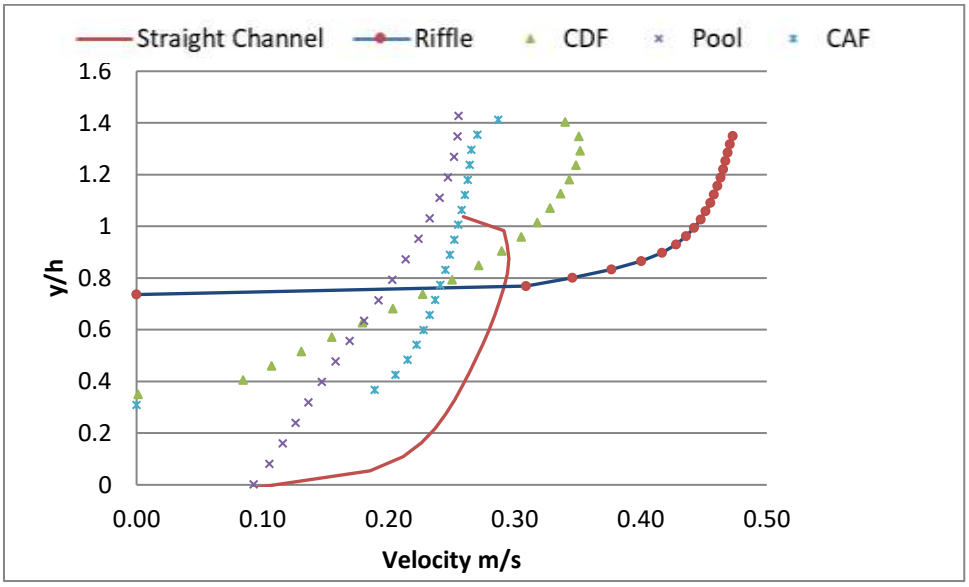

Figure 4.23. Profiles of velocity for G2 shows effects of 1cm R.H at center of each location pointed in figure3.1

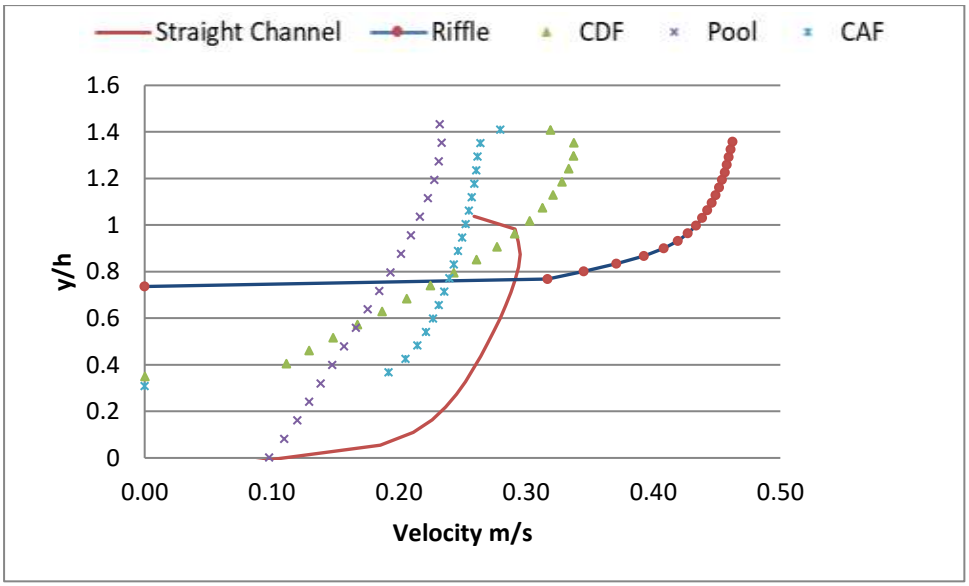

Figure 4.24. Profiles of velocity for G2 shows effects of 2cm R.H at center of each location pointed in figure.3.1

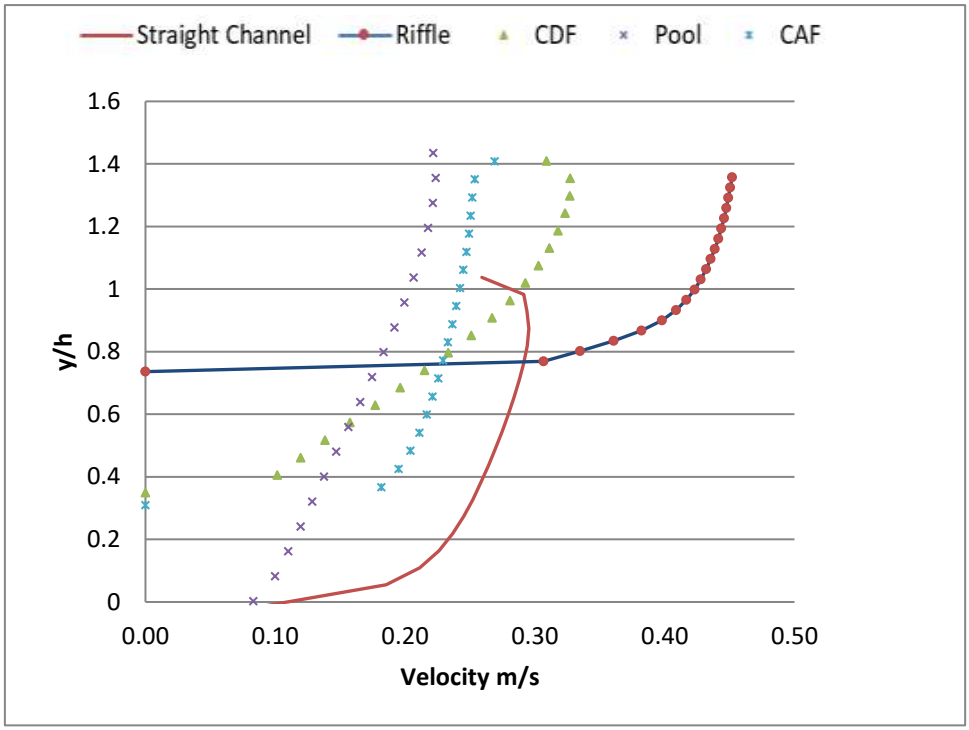

Figure 4.25. Profiles of velocity for G2 shows effects of 4cm R.H at center of each location pointed in figure3.1

Figure 4.26 to 4.28 show the relationship between velocity and relative water depth as a comparison between cases for discharge equal 21 L/s in G3.

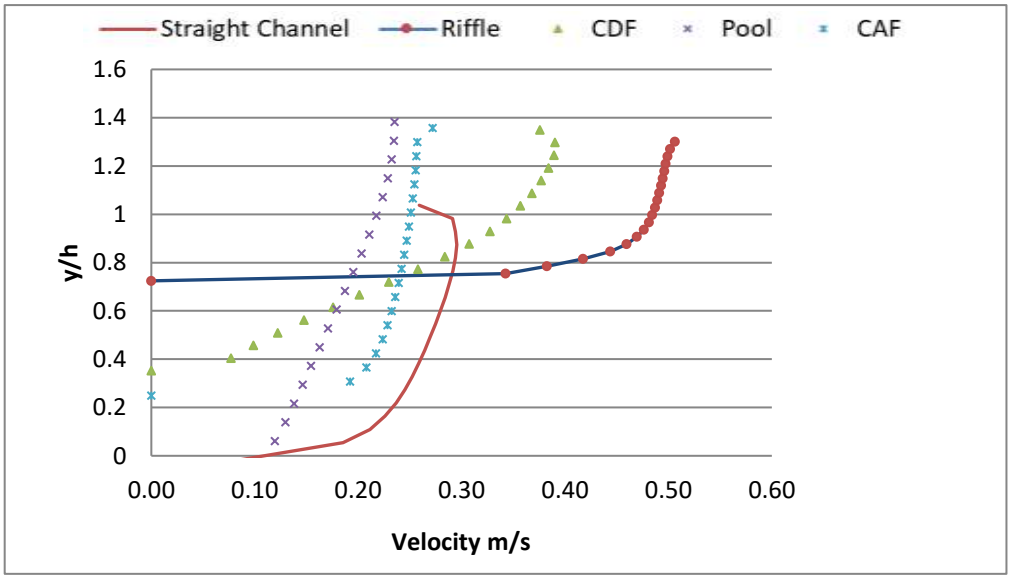

Figure 4.26. Profiles of velocity for G3 shows effects of 1cm R.H at center of each location pointed in figure.3.1

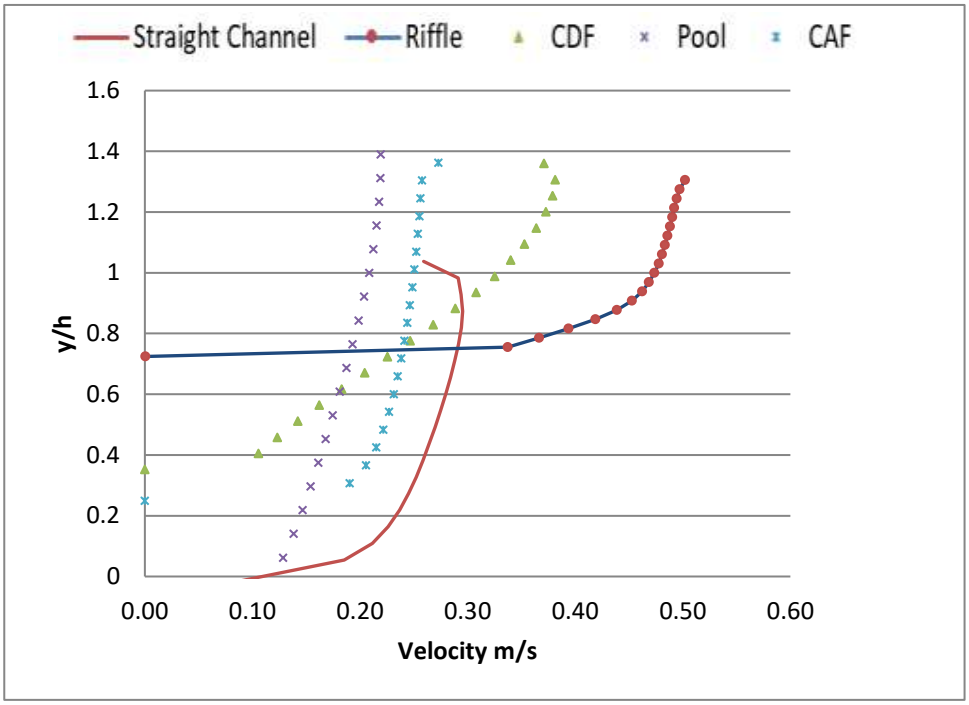

Figure 4.27. Profiles of velocity for G3 shows effects of 2cm R.H at center of each location pointed in figure.3.1

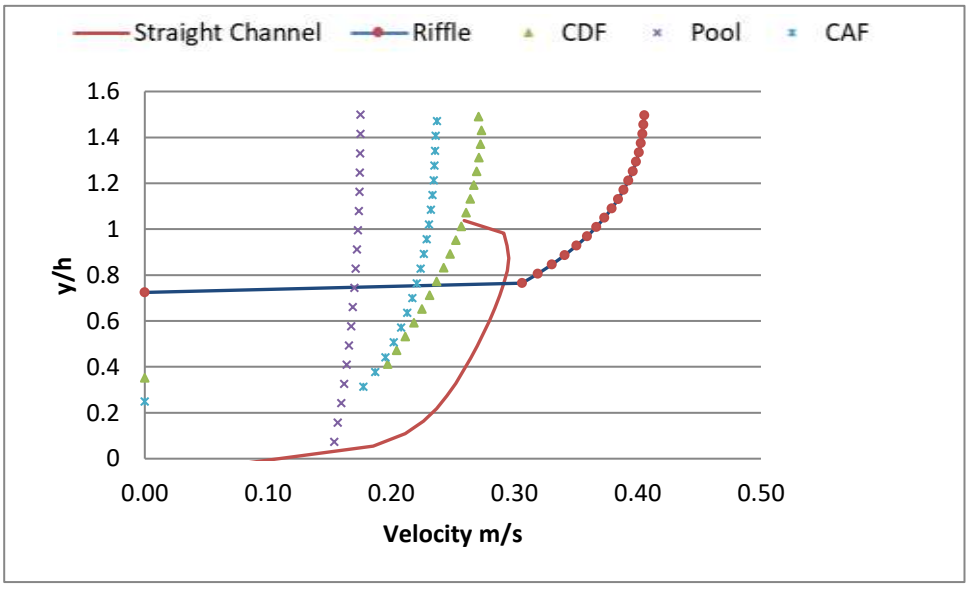

Figure 4.28. Profiles of velocity for G3 shows effects of 4cm R.H at center of each location pointed in figure.3.1

4.4. Impact of Pool Length on Flow Distribution

The data gathered from these runs is included in these results. Figures 4.29 to 4.31 show the streamwise velocity for discharge equal 15 L/s for each run with different configurations and different pool lengths to investigate the effect of changing pool length within the flume.

As the length of the pool elongates, streamwise velocity in the pool zone varies with the change in the roughness. In the case of low roughness of 1 cm, the velocity at the surface is relatively high when the length of the pool is short, while it is slow near the bed, velocity has equal value at y/h ~ 0.45. When roughness increases to 2cm, the velocity at G2 and G3 have approximately the same values nearby bed, while nearby surface, the short pool length has the highest velocity. When the roughness height is increased to 4cm, there is almost no difference in flow distribution between the three cases near the bed, but when reaching y/h = 0.62, velocity begins to vary and increases as the length of the pool rises.

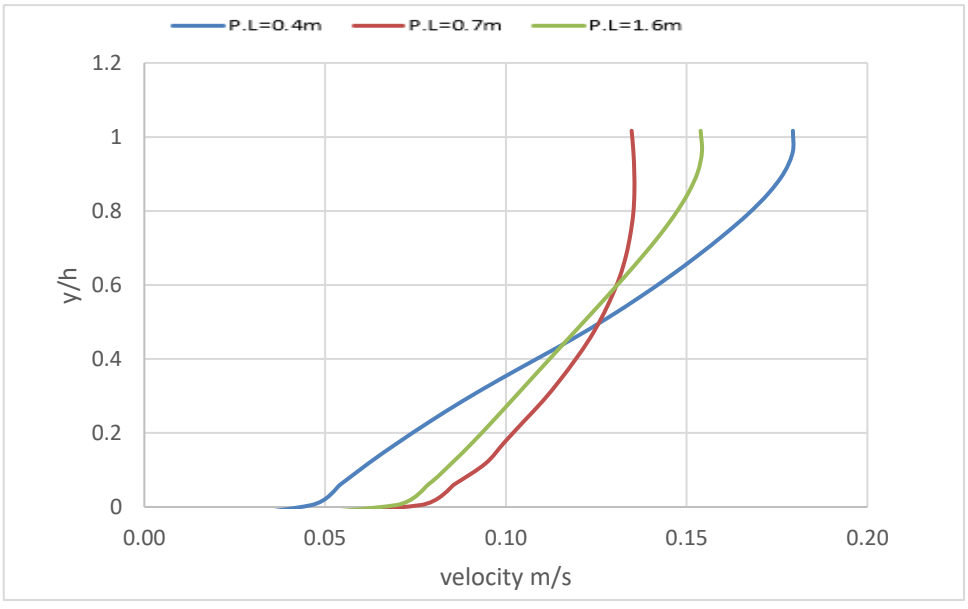

Figure 4.29. Velocity distribution at middle pool's length for runs with roughness height equal 1cm,P.L=Pool Length

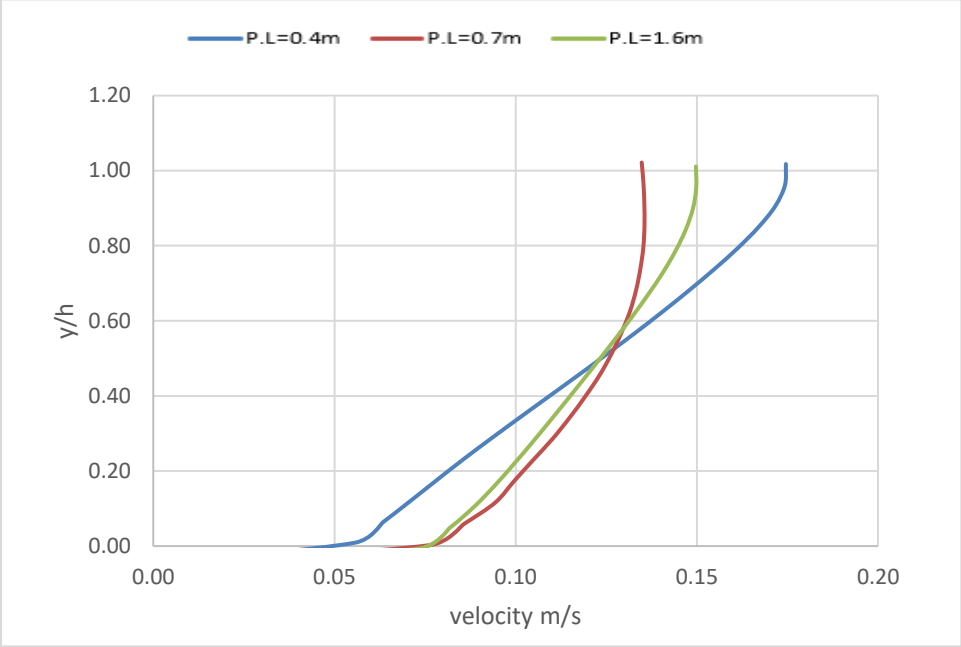

Figure 4.30. Velocity distribution at middle pool's length for runs with roughness height equal 2cm

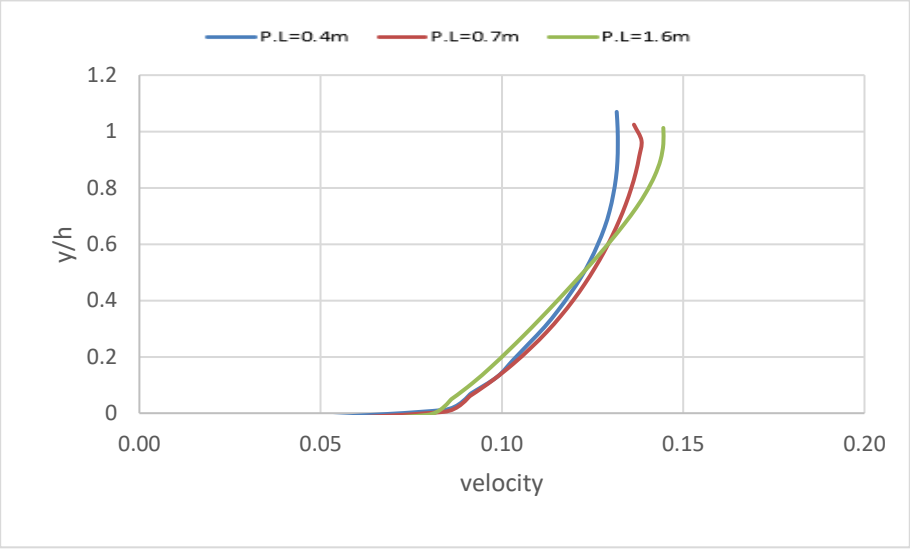

Figure 4.31. Velocity distribution at middle pool's length for runs with roughness height equal 4cm

Figures 4.32 to 4.34 show the streamwise velocity for discharge equal 21L/s. For case of 1cm roughness shorter pool length induces slow velocity near the bed and higher flow distribution at surface. Velocity increases near the bed when the pool length increases and decreases at surface.

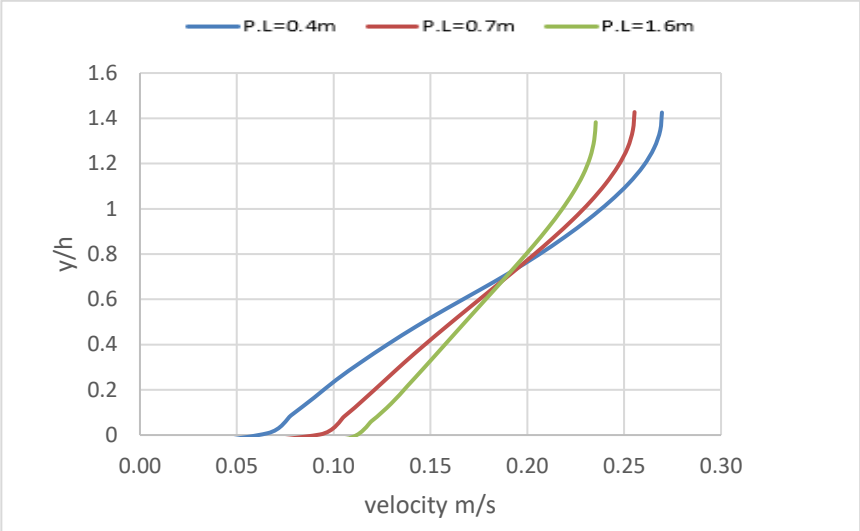

Figure 4.32. Velocity distribution at middle pool's length for runs with roughness height equal 1cm.

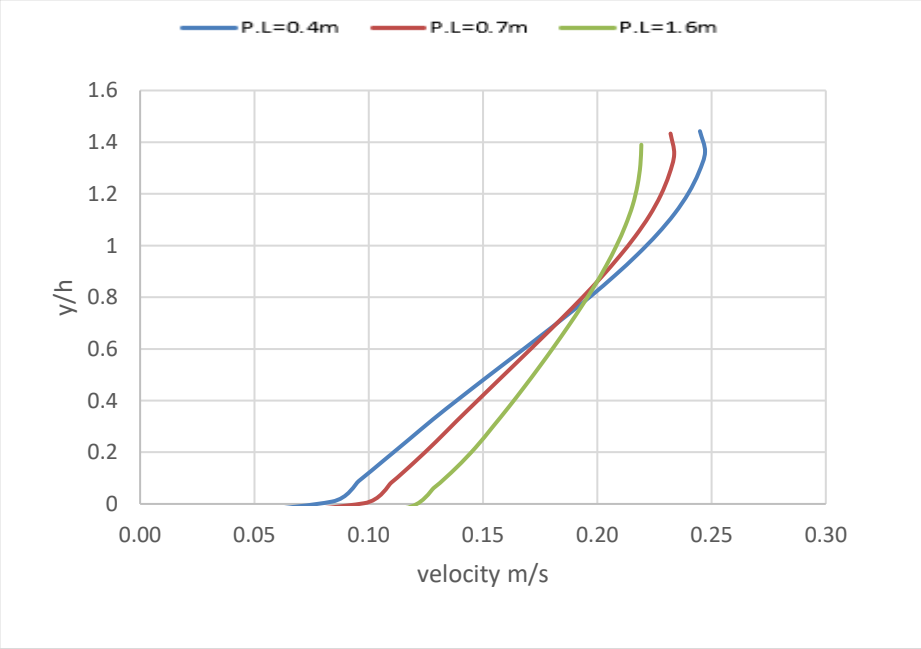

Figure 4.33. Velocity distribution at middle pool's length for runs with roughness height equal 2cm.

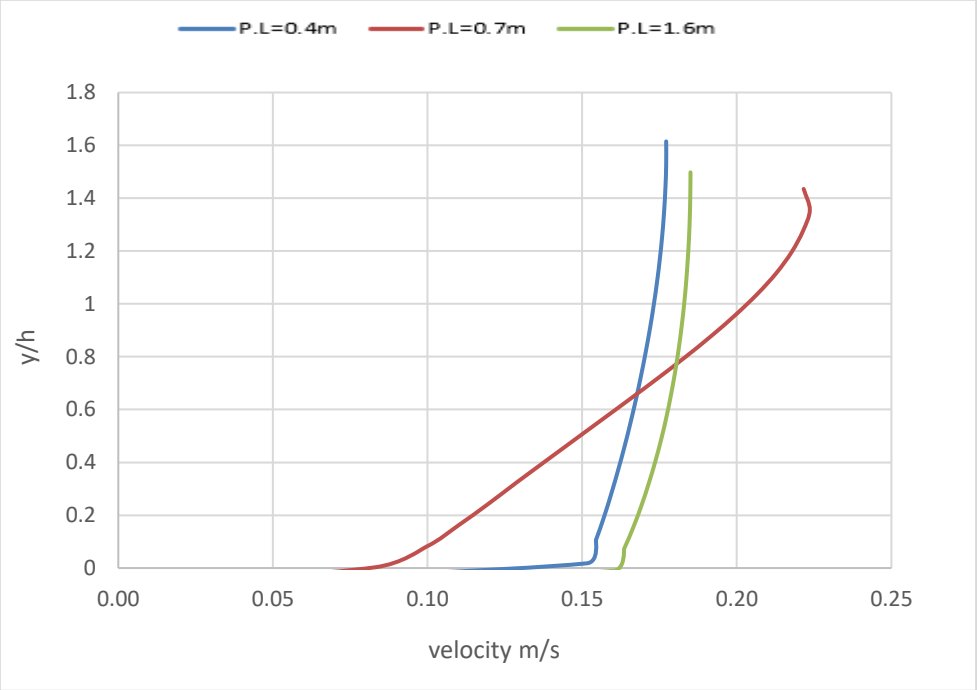

Figure 4.34. Velocity distribution at middle pool's length for runs with roughness height equal 4cm

4.5. Turbulent Intensity

The turbulence intensity, I, is defined as the ratio of the root-mean-square Of the velocity fluctuations, u', to the mean flow velocity ,

$$I = \frac{u'}{u_{\text{avg}}} = 0.16\left(\text{Re}_{D_H}\right)^{-1/8} \qquad (4.1)$$

Where, D_H= Hydraulic Diameter.

Turbulence is a major determinant of the nature and severity of many river processes, including erosion and sediment transport, flow resistance, bed morphology, and natural channel planform.

Results summarized in tables (4-5) and (4-6), which show the change in the turbulence intensity as a result of the change in the roughness height (R.H), as a percentage of the increase (+) and decrease (-) in the value of the turbulence intensity for case of 4cm roughness height compared with the

cases of 1cm and 2cm roughness height in each of (Riffle, CDF, CAF and Pool) regions for each of the three geometries.

Table (4-5): Turbulence intensity percentage % along the channel for Q=15L/s

R.H / Geometry	Compared to1cm				Compared to 2cm			
	Riffle	CDF	Pool	CAF	Riffle	CDF	Pool	CAF
G1	-145	-169	-268	-300	-46	-50	-58	-84
G2	-74	-66	-77	-61	-41	-20	-39	-28
G3	-68	-46	-38	43	-13	+25	-7	-7

Table (4-6): Turbulence intensity percentage % along the channel for Q=21L/s

R.H / Geometry	Compared to1cm				Compared to 2cm			
	Riffle	CDF	Pool	CAF	Riffle	CDF	Pool	CAF
G1	-106	-111	-138	-146	-33	-38	-31	-29
G2	-64	-26	-27	-47	-33	-8	-13	-17
G3	-123	-171	-238	-285	-46	-51	-58	-84

Figures (4.35 to 4.37) show turbulence intensity distribution along the channel bed with respect to depth of flow setups with three roughness components with a discharge of 15 L/s for three geometries. The three configurations have the same performance. Figures (4.38 to 4.40) show a comparison between three different values for roughness height at discharge equal 21 L/s. The observed turbulence intensity generally increases until it reaches a certain distance from the bed and then decreases as approach to the surface.

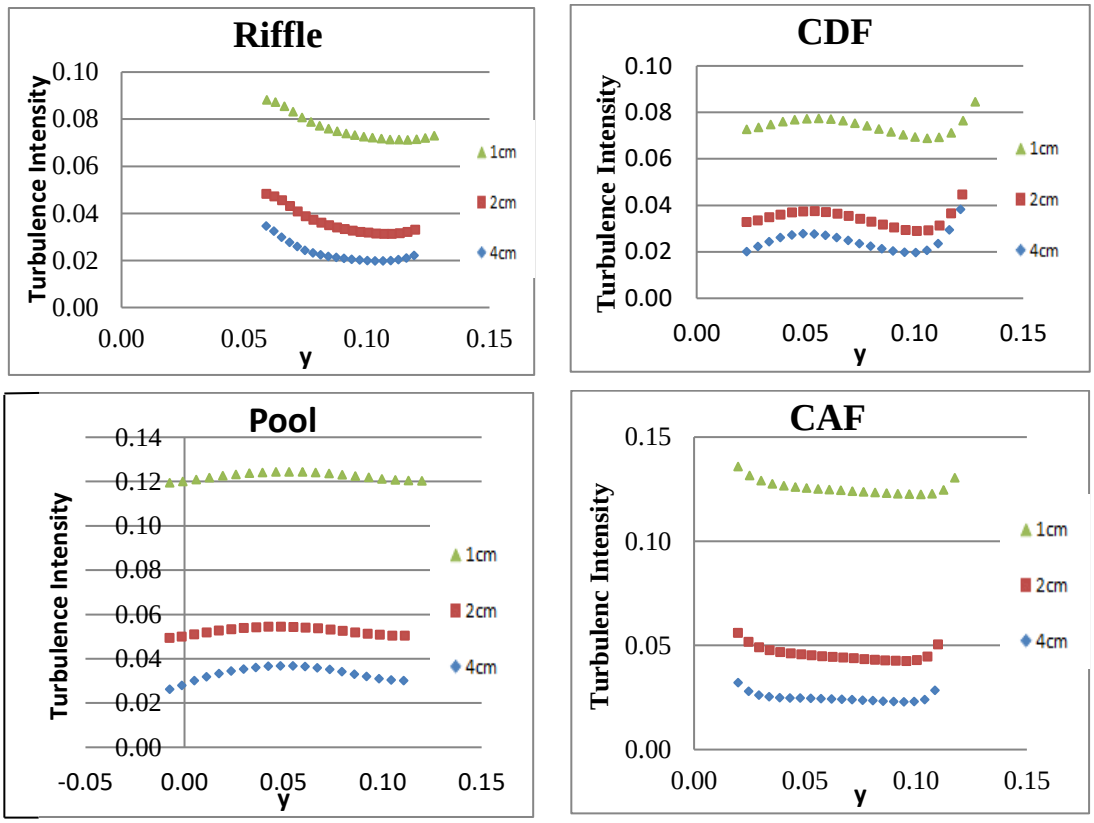

Figure 4.35. Turbulent intensity distribution for G1 for three values of roughness height with Q=15 L/s

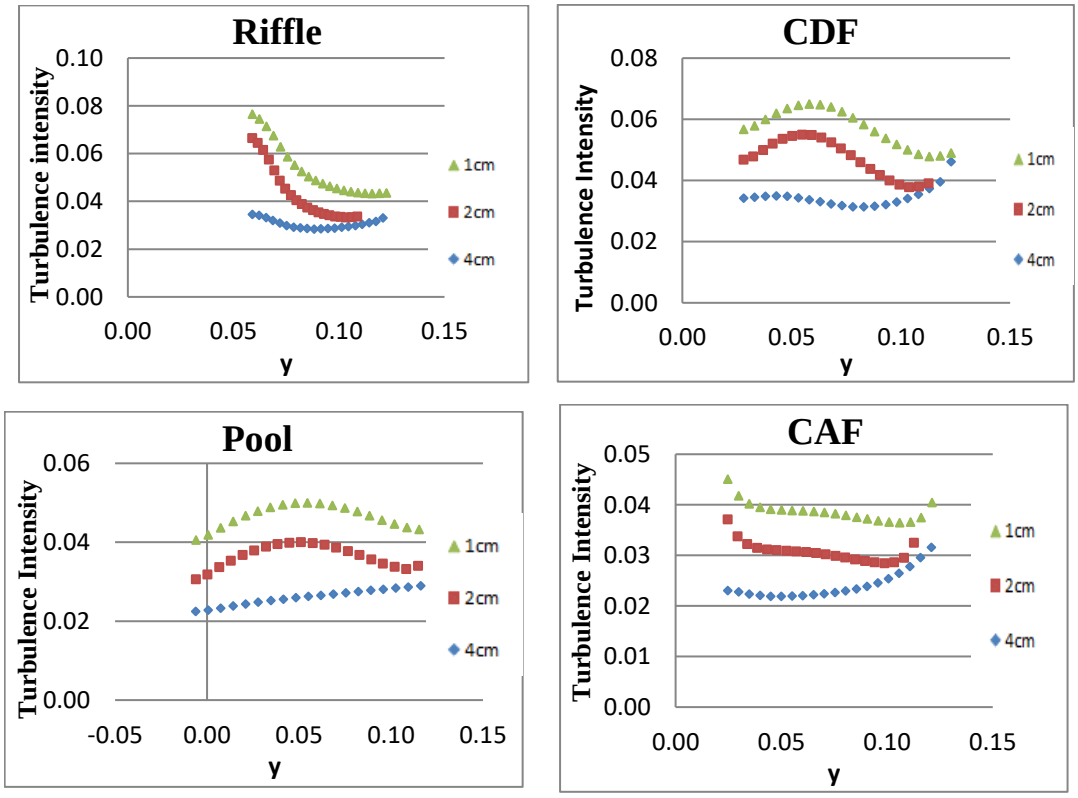

Figure 4.36. Turbulence intensity distribution for G2 for three values of roughness height with Q=15 L/s

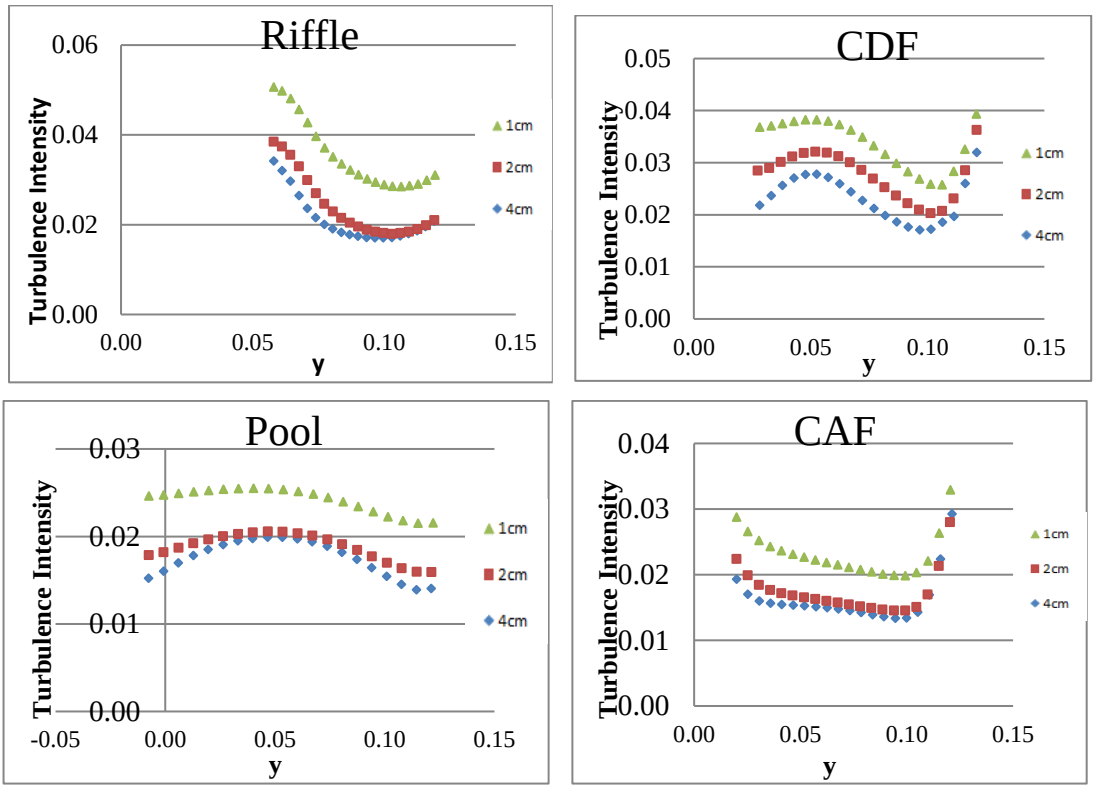

Figure 4.37 Turbulence intensity distribution for G3 for three values of roughness height, Q=15L/s

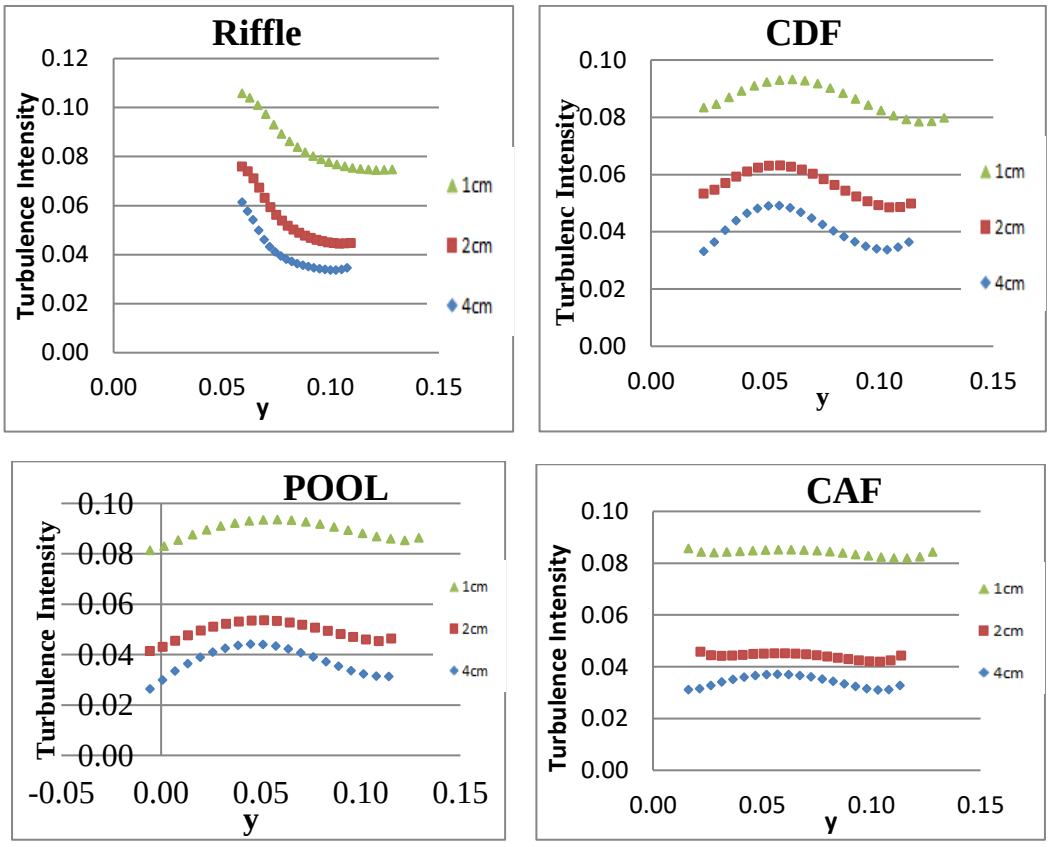

Figure 4.38. Turbulence intensity distribution for G1 for three values of roughness height, discharge =21L/s

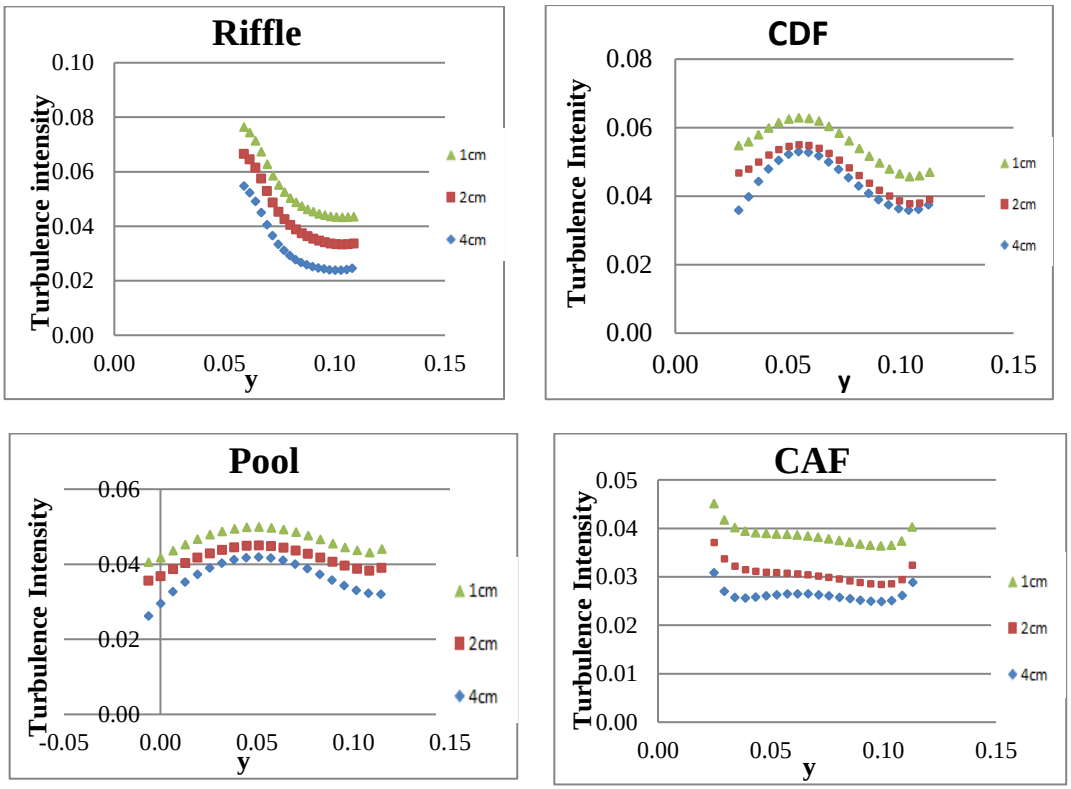

Figure 4.39. Turbulence intensity distribution for G2 for three values of roughness height, Q=21L/s

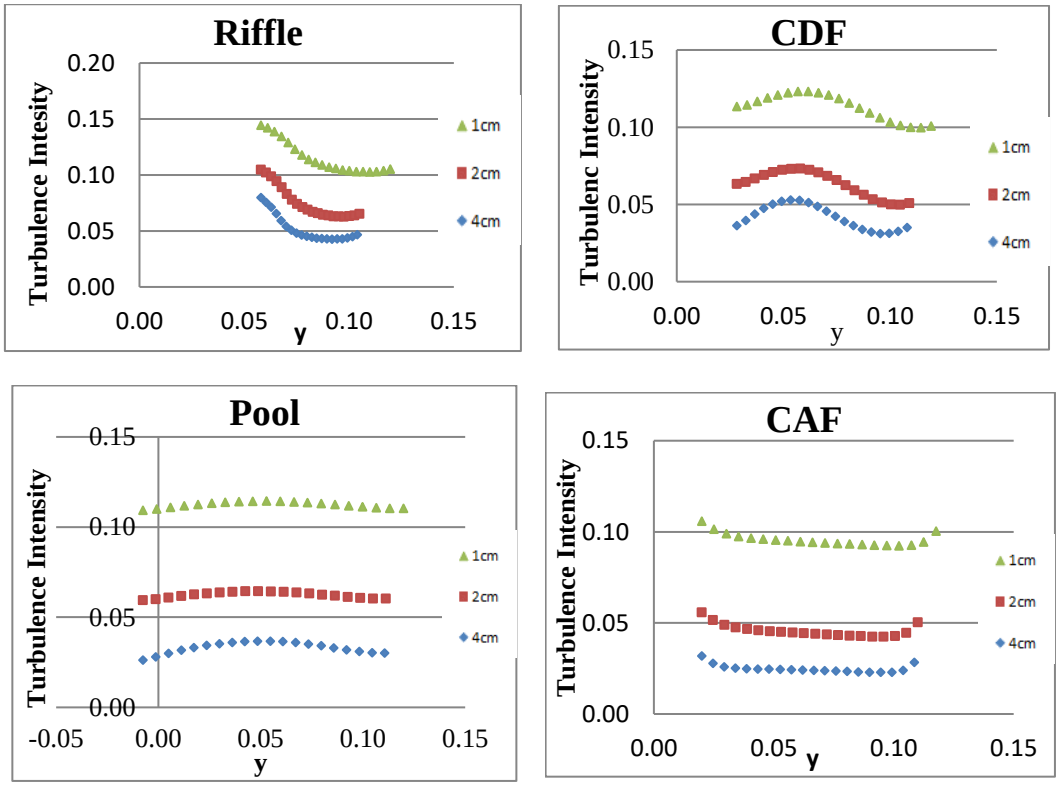

Figure 4.40. Turbulence intensity distribution for G3 for three values of roughness height, Q=21L/s

The results of turbulence intensity distribution indicate that when roughness height rises, the peak value of turbulence intensity reduces. Also, at a flow discharge of 15L/s, when pool length increases, the turbulent intensity decreases, but when discharge increases to 21 L/s, the turbulent intensity decreases at G2 but returns to be increased at G3.

4.6 The Effect of Bed Roughness and Bedform Dimensions on The Velocity of Flow

Figures 4.41and 4.42 display a comparison between G1,G2 and G3 where readings are taken at the center of riffle and pool at two water surface elevations, one at the surface of the water and the other taken at the middle height of the water to show how velocity distribution was affected by roughness height and by changing the length of bedform. For case of 15 L/s discharge at riffle region, the velocity at the water's surface decreased by 4% in G2 and 2% in G3 compared to the first, and decreased by about 1% at the middle height of the water. At the pool, velocity decreased by about 24% in G2 and about 9% in G3 compared to the G1 at the water's surface and by about 3% at mid-height.

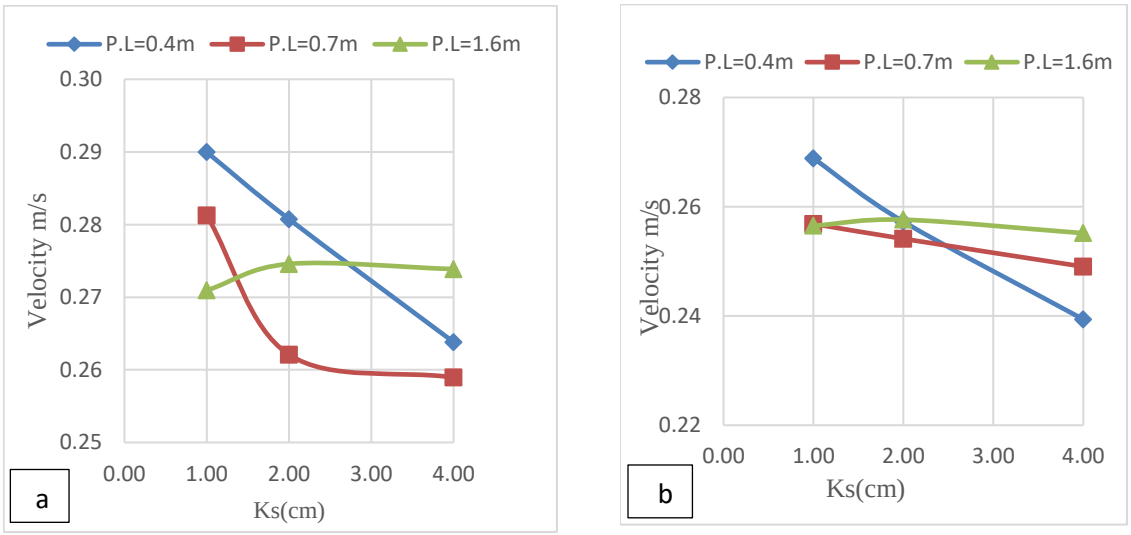

Figure 4.41: Relationship between roughness height and velocity distribution for two water surface elevations in Riffle region (a) at water surface (b) at middle of water height, Q=15L/s

.

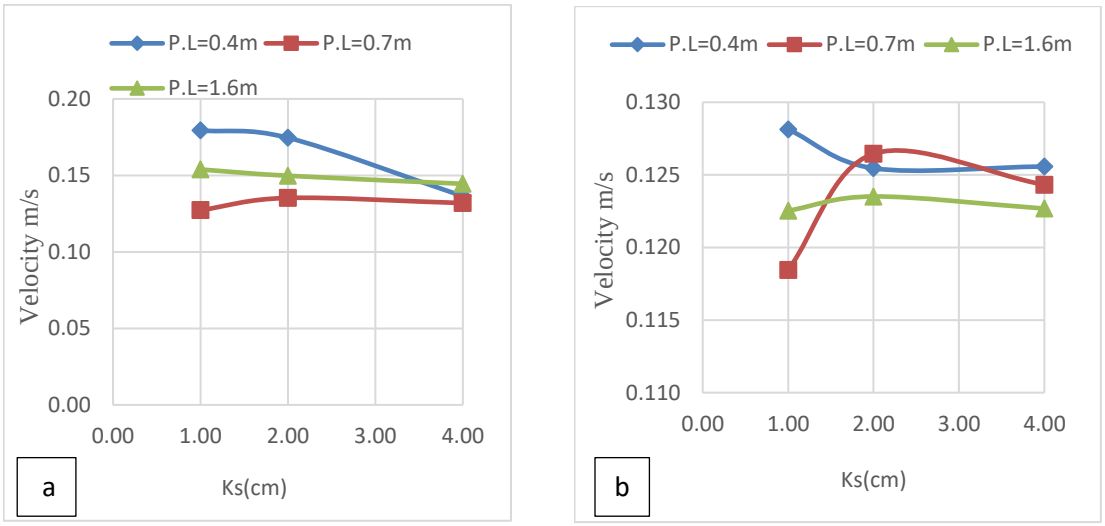

Figure4.42: Relationship between roughness height and velocity distribution for two water surface elevations in pool region (a) at water surface (b) at middle of water height,Q=15L/s

Figures 4.43and 4.44 display a comparison between (G1), (G2) and(G3) where readings are taken at the center of riffle and pool at two sections, one at the surface of the water and the other taken at the middle height of the water to show how velocity distribution was affected by roughness height and by changing the length of bedform. For case of 20L/s discharge we found at riffle region that the velocity at the water's surface increased by 7% in G2 and 9% in G3 compared to G1, and increased by about 8% and 9% in G2 and G3 respectively at the middle height of the water. At the pool, velocity increased by about 2% in G2 and decreased by about 10% in G3 compared to the G1at the water's surface and by about 4% and 3% in G2 and G3 at mid-height.

So, the risk of erosion effect on river sides can be reduced when roughness height increased.

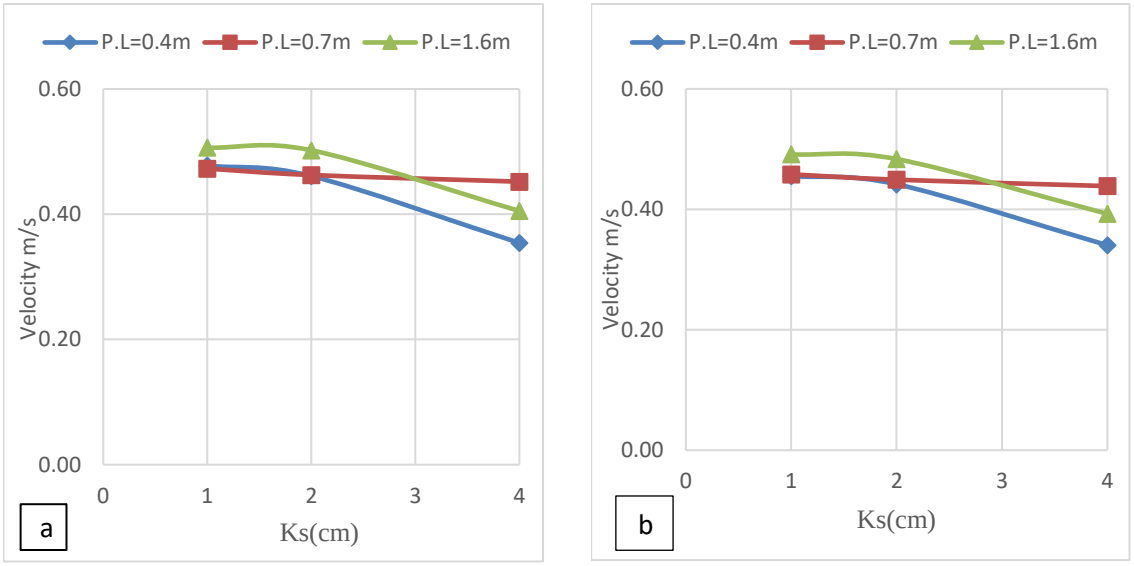

Figure 4.43:Relationship between roughness height and velocity distribution for two water surface elevations in Riffle region (a) at water surface (b) at middle of water height, Q=21L/s

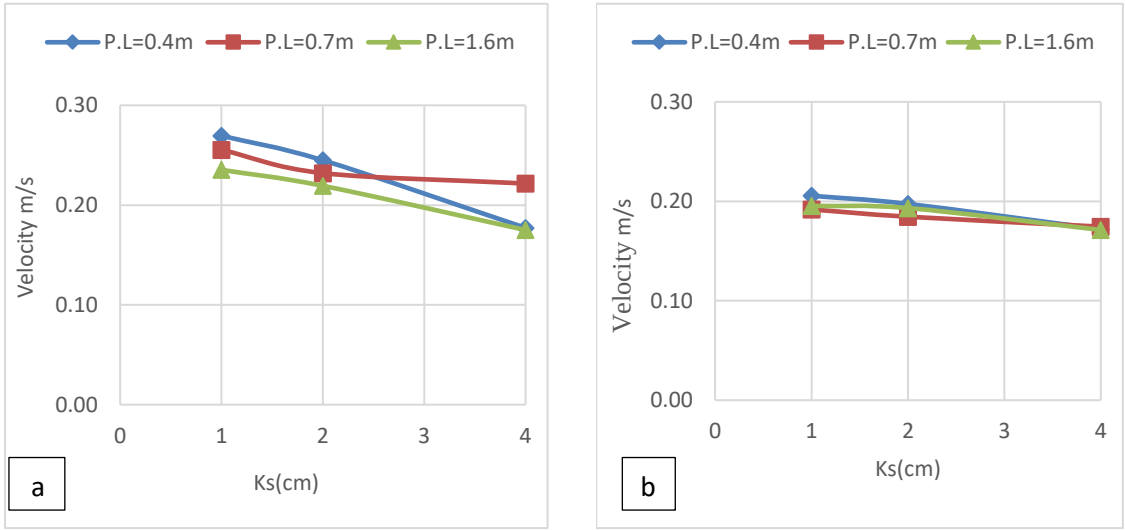

Figure4.44: Relationship between roughness height and velocity distribution for two water surface elevations in pool region (a) at water surface (b) at middle of water height,Q=21L/s

Figures 4.45 to 4.52 show the relation between velocity and bedform dimension with roughness height at sections taken in center of area at riffle ,CDF,Pool,and CAf.

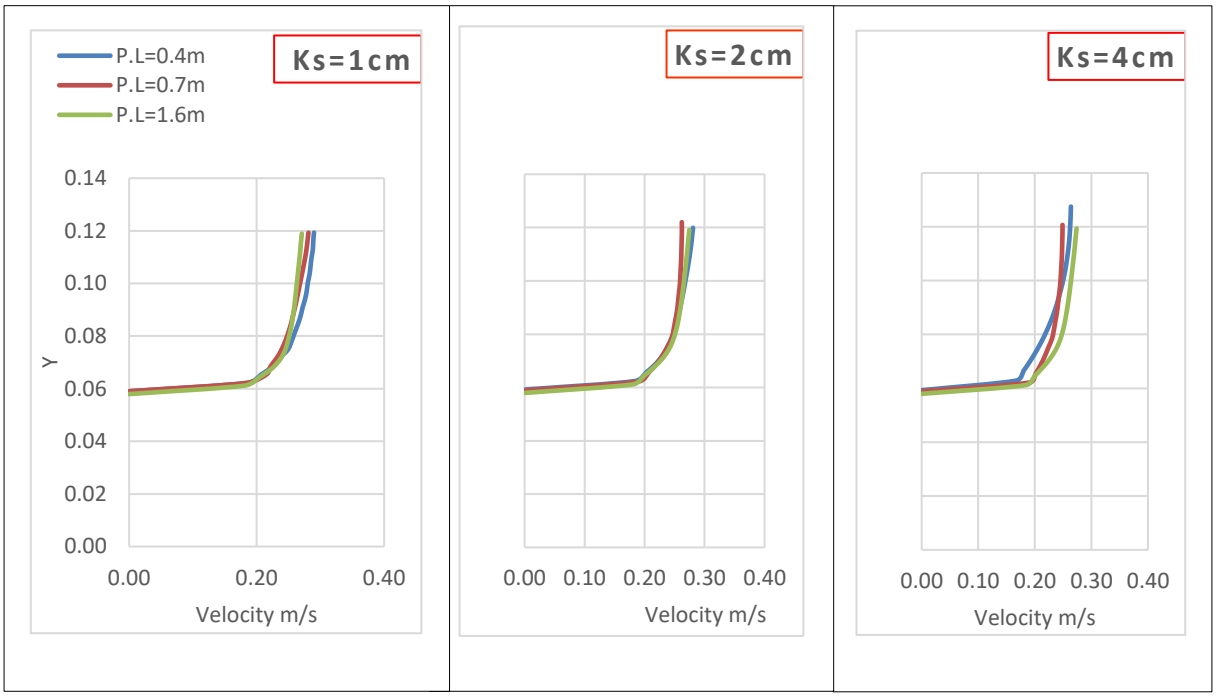

Figure4.45: Effect of change pool length on velocity distribution at riffle section, Q=15L/s ,P.L=Pool Length .

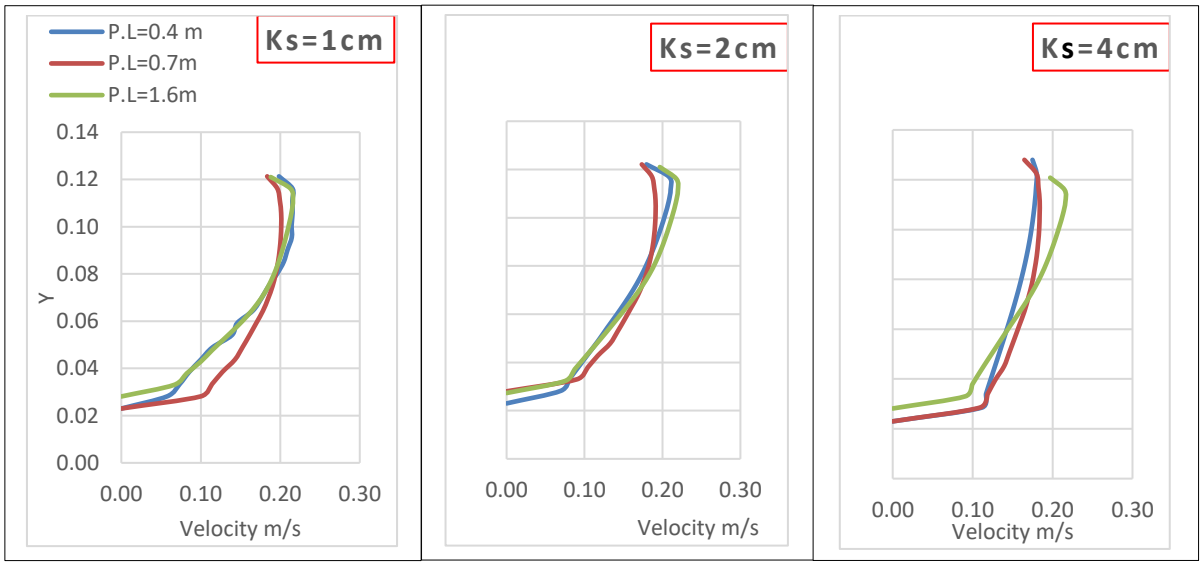

Figure4.46: Effect of change pool length on velocity distribution at CDF section, Q=15L/s.

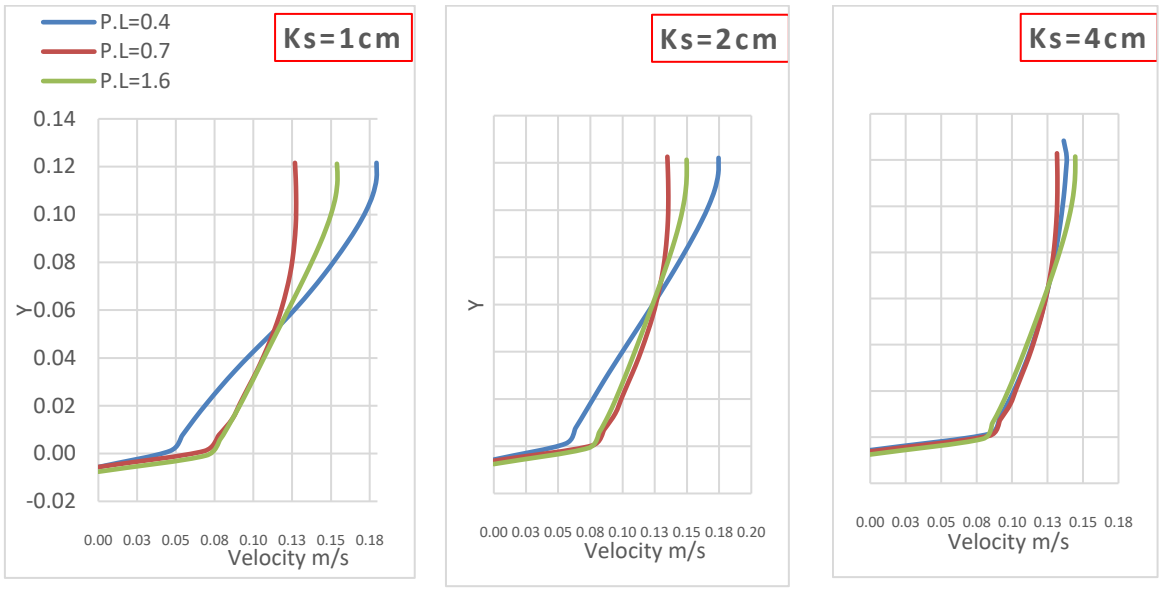

Figure4.47: Effect of change pool length on velocity distribution at pool section, Q=15L/s.

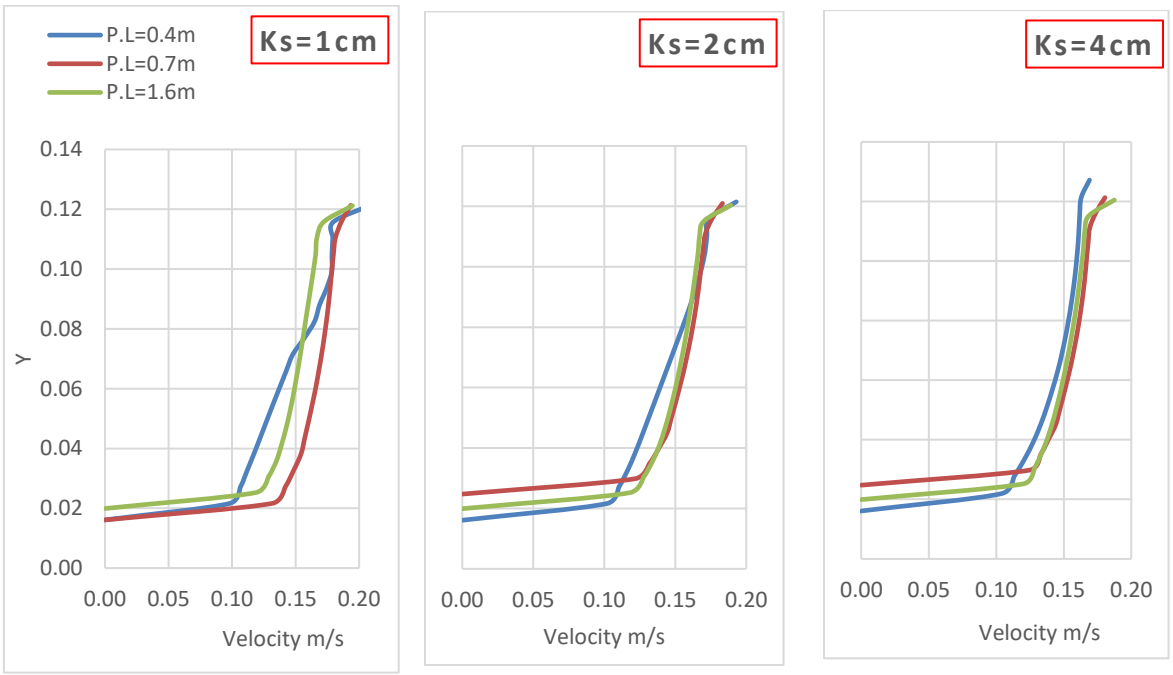

Figure4.48: Effect of change pool length on velocity distribution at CAF section , Q=15L/s.

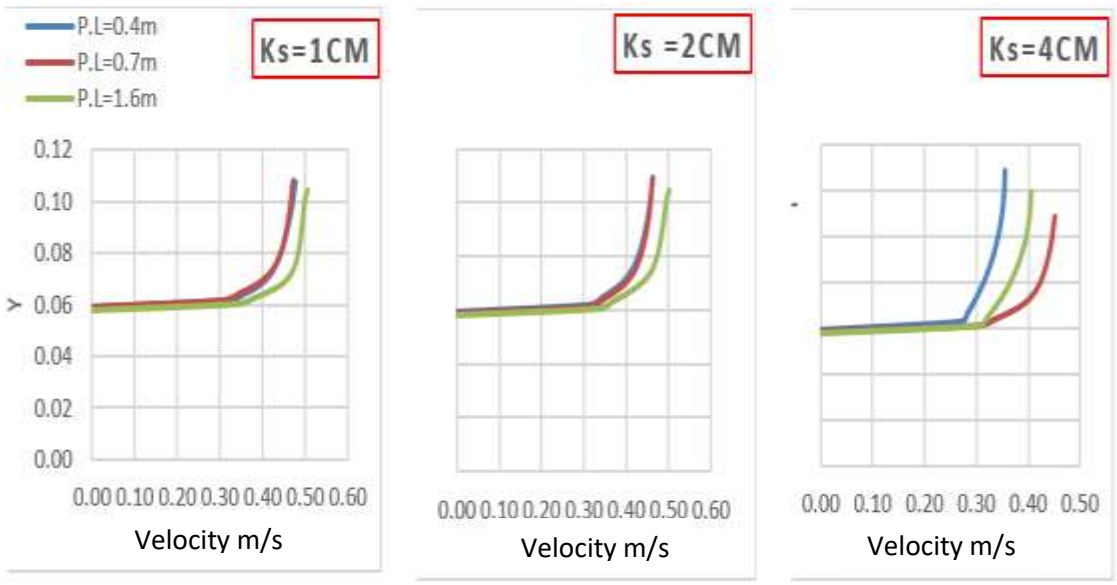

Figure4.49: Effect of change pool length on velocity distribution at riffle section, Q=21L/s .

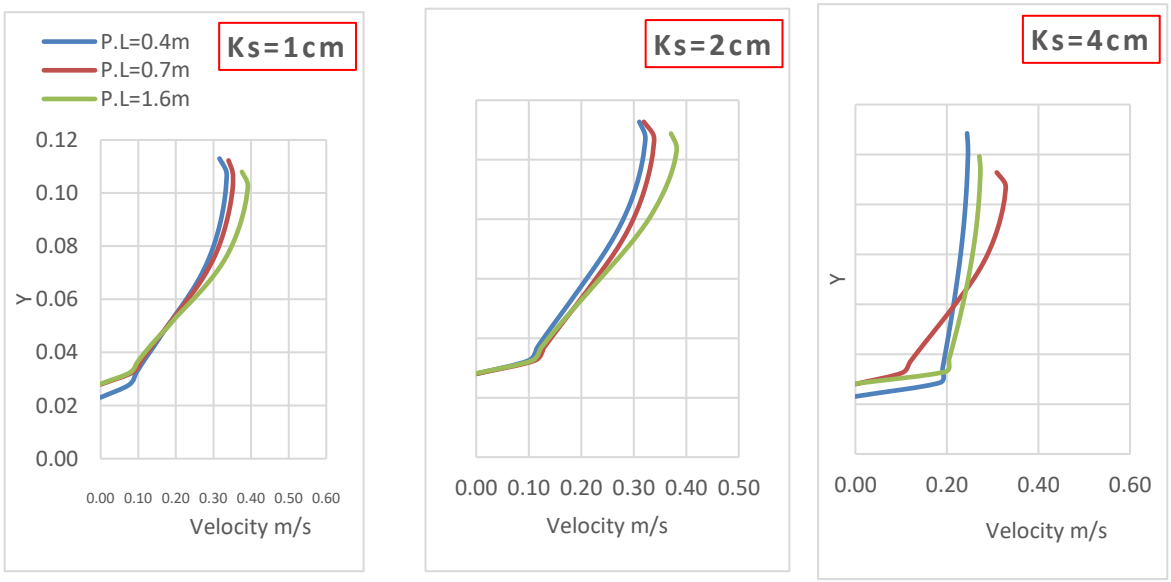

Figure4.50: Effect of change pool length on velocity distribution at CDF section, Q=21L/s.

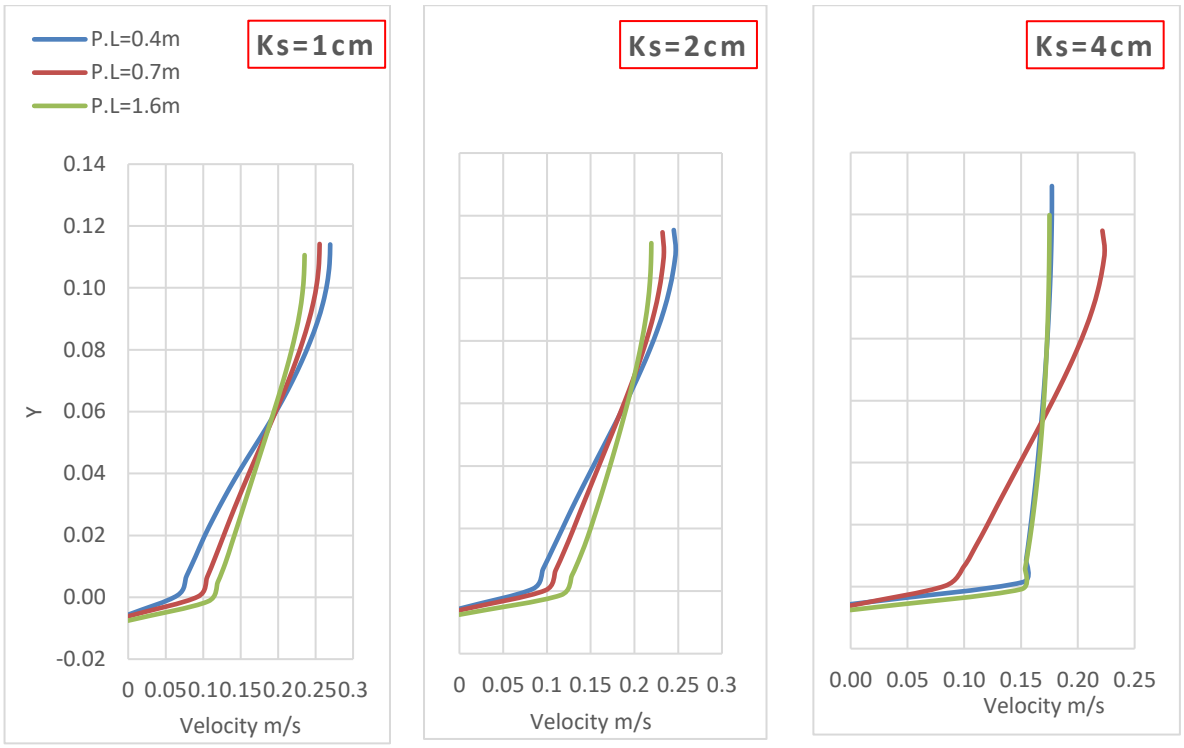

Figure4.51: Effect of change pool length on velocity distribution at pool section , Q=21L/s .

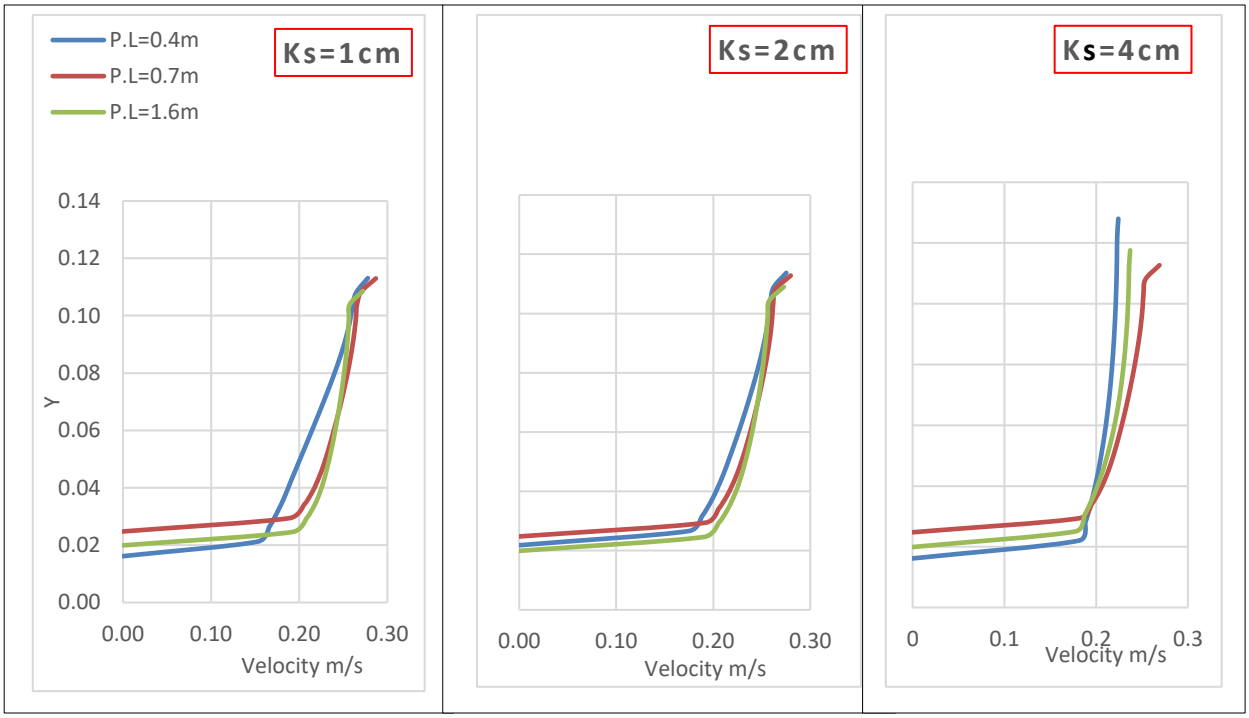

Figure4.52: Effect of change pool length on velocity distribution at CAF section, Q=21L/s

From figures (4.45 to 4.52) concluded that when pool length increased the velocity at surface decreased but at roughness height 4 cm velocity begin to increased, while at discharge 21l/s velocity dropped at surface when pool length increased.

Chapter Five

Conclusion and Recommendation

5.1 Conclusion

The aim of this thesis was to look at the velocity distributions along the flume with varied roughness element, heights, and configurations. These factors are crucial for changing the flow's hydraulic properties. The form, height, and configuration of the roughness components were the considered factors in this thesis. Two discharges were adopted, each with three distinct roughness height, and combinations. To simulate and analyze flowing water through the flume, ANSYS FLUENT are utilized.

The main findings of this study are summarized in the following conclusions:

1. Increasing the water flow discharge enhanced the influence of roughness components.
2. When the pool length increased the velocity at the water surface decreased and at the bottom increased along the channel.
3. The flow velocity decreases in both riffle and pool with increasing roughness height, and this is directly proportional to the discharge.
4. The flow in pools-riffle units got further uniform as pool length rises. This is verified by the fact that the flow in the longer pools recovers to more uniform condition in the direction of end of pool as evidenced by streamwise velocity.
5. Turbulence intensity decreased as bed roughness increased, as does pool length for the same flow rate.
6. Turbulence intensity decreased in both riffle and pool due to increased roughness height, and this is inversely proportional to the discharge.

5.2 Recommendations

To completely comprehend the hydrodynamics of a pool-riffle, further data is required. The following are the recommendations for future research:

1. Investigating three-dimensional pool riffle arrangements.
2. Using another bedforms scale, roughness heights, and different combinations.
3. Investigating sediment transport for these shape.
4. Work on an experimentally studied.

References

Andrews, E. D. (1994). Marginal bed load transport in a gravel bed stream, Sagehen Creek, California. Water Resources Research, 30(7), 2241-2250.

Afzalimehr, H., & Anctil, F. (2000). Accelerating shear velocity in gravel-bed channels. Hydrological sciences journal, 45(1), 113-124

ANSYS Fluent Theory Guide version16.1 (2015), Fluent Inc.

ANSYS Fluent User's Guide version 16.1 (2015), Fluent Inc.

Bayat, E., J. F. Rodrıguez, P. M. Saco,G. A. M. de Almeida, E. Vahidi, & M. H. Garcıa (2017), A tale of two riffles: Using multidimensional, multifractional, time-varying sediment transport to assess self-maintenance in pool-riffle sequences, Water Resour. Res., 53, 2095–2113, doi:10.1002/2016WR019464.

Booker, D. J., Sear, D. A., & Payne, A. J. (2001). Modelling three-dimensional flow structures and patterns of boundary shear stress in a natural pool–riffle sequence. Earth Surface Processes and Landforms: The Journal of the British Geomorphological Research Group, 26(5), 553-576.

Buffington, J. M., Lisle, T. E., Woodsmith, R. D., & Hilton, S. (2002). Controls on the size and occurrence of pools in coarse-grained forest rivers. River Research and Applications, 18(6), 507-531.

Caamaño, D., Goodwin, P., & Buffington, J. M. (2012). Flow structure through pool-riffle sequences and a conceptual model for their sustainability in gravel-bed rivers. River research and applications, 28(3), 377-389.

Caamaño, D., Goodwin, P., Buffington, J. M., Liou, J. C., & Daley-Laursen, S. (2009). Unifying criterion for the velocity reversal hypothesis in gravel-bed rivers. Journal of Hydraulic Engineering. 135 (1): 66-70., 135(1), 66-70.

Carling, P. A., & Orr, H. G. (2000). Morphology of riffle–pool sequences in the River Severn, England. Earth Surface Processes and Landforms: The Journal of the British Geomorphological Research Group, 25(4), 369-384.

Carling, P. A., & Wood, N. (1994). Simulation of flow over pool-riffle topography: A consideration of the velocity reversal hypothesis. Earth Surface Processes and Landforms, 19(4), 319-332

Chanson, H. (2004). Hydraulics of open channel flow. Elsevier

Cherkauer, D. S. (1973). Minimization of power expenditure in a riffle-pool alluvial channel. Water Resources Research, 9(6), 1613-1628

Church, M., & Hassan, M. A. (2002). Mobility of bed material in Harris Creek. Water Resources Research, 38(11), 19-1

Clifford, N. J. (1993). Differential bed sedimentology and the maintenance of riffle-pool sequences. *Catena*, *20*(5), 447-468.

Clifford, N. J., Robert, A., & Richards, K. S. (1992). Estimation of flow resistance in gravel-bedded rivers: A physical explanation of the multiplier of roughness length. Earth Surface Processes and Landforms, 17(2), 111-126.

Dashtpeyma, H., & MacVicar, B. (2018). Vortex-Resistance Hypothesis: Large Eddy Simulation of Turbulent Flow in Isolated Pool-Riffle Units. In E3S Web of Conferences (Vol. 40, p. 05029). EDP Sciences.

Dawson, C. W., Abrahart, R. J., & See, L. M. (2007). HydroTest: a web-

based toolbox of evaluation metrics for the standardised assessment of hydrological forecasts. Environmental Modelling & Software, 22(7), 1034-1052.

De Almeida, G. A. M., & Rodríguez, J. F. (2011). Understanding pool-riffle dynamics through continuous morphological simulations. Water Resources Research, 47(1)

Eaton, B. C., & Lapointe, M. F. (2001). Effects of large floods on sediment transport and reach morphology in the cobble-bed Sainte Marguerite River. Geomorphology, 40(3-4), 291-309.

Fazel Najafabadi, E., Afzalimehr, H., & Sui, J. (2017). A comparison of two-dimensional and three-dimensional flow structures over artificial pool-riffle sequences. Canadian Journal of Civil Engineering, 44(12), 1084-1098.

Fazlollahi, A., Afzalimehr, H., & Sui, J. (2015). Effect of slope angle of an artificial pool on distributions of turbulence. International Journal of Sediment Research, 30(2), 93-99.

Gilbert, G. (1914). The transportation of debris by running water. US Geological Survey, Professional Paper, 86, 263.

Gilbert, R. O. (1987). Statistical methods for environmental pollution monitoring. John Wiley & Sons.

Gregory, K. J., Gurnell, A. M., Hill, C. T., & Tooth, S. (1994). Stability of the pool-riffle sequence in changing river channels. Regulated Rivers: Research & Management, 9(1), 35-43.

Grant, G. E., Swanson, F. J., & Wolman, M. G. (1990). Pattern and origin of stepped-bed morphology in high-gradient streams, Western Cascades, Oregon. Geological Society of America Bulletin, 102(3), 340-352.

Hassan, M. A., & Woodsmith, R. D. (2004). Bed load transport in an obstruction-formed pool in a forest, gravelbed stream. Geomorphology, 58(1-4), 203-221.

Henderson, F. M. (1966). Open channel flow. MacMillan Publishing Co., Inc.New York.

Keeton, W. S., Kraft, C. E., & Warren, D. R. (2007). Mature and old-growth riparian forests: structure, dynamics, and effects on Adirondack stream habitats. Ecological Applications, 17(3), 852-868

Keller, E. A., and Melhorn, W. N. (1978). Rhythmic spacing and origin of pools and riffles. Geological Society of America Bulletin, 89(5), 723-730

Keller, E. A. (1971). Areal sorting of bed-load material: the hypothesis of velocity reversal. Geological Society of America Bulletin, 82(3), 753-756.

Kellerhals, R., & Bray, D. I. (1971). Sampling procedures for coarse fluvial sediments. Journal of the Hydraulics Division, 97(8), 1165-1180.

Komar, P. D. (1996). Entrainment of sediments from deposits of mixed grain sizes and densities. Advances in fluvial dynamics and stratigraphy, 127-181.

Leopold, L. B., Wolman, M. G., & Miller, J. P. (1964). Fluvial processes in geomorphology.

Leopold, L. B., & Wolman, M. G. (1960). River meanders. Geological Society of America Bulletin, 71(6), 769-793.

Lisle, T. E. (1986). Stabilization of a gravel channel by large streamside obstructions and bedrock bends, Jacoby Creek, northwestern California. Geological Society of America Bulletin, 97(8), 999-1011.

Lisle, T. E. (1982). Effects of aggradation and degradation on riffle-pool morphology in natural gravel channels, northwestern California. Water Resources Research, 18(6), 1643-1651.

Lisle, T. E., & Hilton, S. (1992). The volume of fine sediment in pools: an index of sediment supply in gravel-bed streams 1. JAWRA Journal of The American Water Resources Association, 28(2), 371-383

Lisle, T. (1979). A sorting mechanism for a riffle-pool sequence: summary. Geological Society of America Bulletin, 90(7), 616-617.

Lofthouse, C., and Robert, A. (2008). Riffle–pool sequences and meander morphology. Geomorphology, 99(1-4), 214-223.

MacVicar, B. J., and C. D. Rennie (2012), Flow and turbulence redistribution in a straight artificial pool, Water Resour. Res.,48, W02503, doi:10.1029/2010WR009374.

MacVicar, B., and J. Best (2013), A flume experiment on the effect of channel width on the perturbation and recovery of flow in straight pools and riffles with smooth boundaries, J. Geohys. Res. Earth Surf., 118, 1850–1863, doi:10.1002/jgrf.20133.

MacWilliams Jr, M. L., Wheaton, J. M., Pasternack, G. B., Street, R. L., and Kitanidis, P. K. (2006). Flow convergence routing hypothesis for pool-riffle maintenance in alluvial rivers. Water Resources Research, 42(10)

Madej, M. A. (1999). Temporal and spatial variability in thalweg profiles of a gravel-bed river. Earth Surface Processes and Landforms: The Journal of the British Geomorphological Research Group, 24(12), 1153-1169

Milan, D. J. (2013). Virtual velocity of tracers in a gravel-bed river using size-based competence duration. Geomorphology, 198, 107-114.

Milan, D. J., Heritage, G. L., Large, A. R. G., & Charlton, M. E. (2001). Stage dependent variability in tractive force distribution through a riffle–pool sequence. Catena, 44(2), 85-109.

Montgomery, D. R., and Buffington, J. M. (1997). Channel-reach morphology in mountain drainage basins. Geological Society of America Bulletin, 109(5), 596-611.

Montgomery, D. R., Buffington, J. M., Smith, R. D., Schmidt, K. M., & Pess, G. (1995). Pool spacing in forest channels. Water Resources Research, 31(4), 1097-1105.

Morvan, H., Knight, D., Wright, N., Tang, X., & Crossley, A. (2008). The concept of roughness in fluvial hydraulics and its formulation in 1D, 2D

and 3D numerical simulation models. Journal of Hydraulic Research, 46(2), 191-208.

Nash, J.E., & Sutcliffe, J.V. (1970). “River flow forecasting through conceptual models, Part I. A discussion of principles”. J. Hydrol.,10, 282–290.

Nelson, J. M., Shreve, R. L., McLean, S. R., & Drake, T. G. (1995). Role of near-bed turbulence structure in bed load transport and bed form mechanics. Water resources research, 31(8), 2071-2086.

Newbury, R., & Gaboury, M. (1993). Exploration and rehabilitation of hydraulic habitats in streams using principles of fluvial behaviour. Freshwater Biology, 29(2), 195-210.

Obach, L. M. (2011). The hydrodynamics of pool-riffle sequences with changing bedform length (Master's thesis, University of Waterloo).

O'Neill, M. P., & Abrahams, A. D. (1984). Objective identification of pools and riffles. Water resources research, 20(7), 921-92

Richards, K. S. (1978). Simulation of flow geometry in a riffle-pool stream. Earth surface processes, 3(4), 345-354.

Rodrıguez, J. F., C. M. Garcıa, & M. H. Garcıa (2013), Three-dimensional flow in centered pool-riffle sequences, Water Resour. Res., 49, doi:10.1029/2011WR011789.

Rosgen, D. L. (1995). A classification of natural rivers. Catena, 22(3), 169-199.

Sear, D. A. (1996). Sediment transport processes in pool–riffle sequences. Earth Surface Processes and Landforms, 21(3), 241-262.

Simpson, R. O. G. E. R. L. (1989). Turbulent boundary-layer separation. Annual Review of Fluid Mechanics, 21(1), 205-232

Stoesser, T., Kara, S., MacVicar, B., & Best, J. (2010). Turbulent Flow over a mildly sloped pool-riffle sequence. River Flow 2010, 163-168.The Journal of the British Geomorphological Research Group, 26(5), 553-576.

Sumer, B. M., Chua, L. H., Cheng, N. S., & Fredsøe, J. (2003). Influence of turbulence on bed load sediment transport. Journal of Hydraulic Engineering, 129(8), 585-596

Thompson, D. M. (2001). Random controls on semi-rhythmic spacing of pools and riffles in constriction-dominated rivers. Earth Surface Processes and Landforms, 26(11), 1195-1212.

Thompson, D. M. (2004). The influence of pool length on local turbulence production and energy slope: A flume experiment. Earth Surface Processes and Landforms: The Journal of the British Geomorphological Research Group, 29(11), 1341-1358.

Thompson, D. M. (2018). Pool–Riffle Sequences. Reference Module in Earth Systems and Environmental Sciences; Elsevier: Amsterdam, The Netherlands.

Thompson, D. M., & Wohl, E. E. (2009). The linkage between velocity patterns and sediment entrainment in a forced-pool and riffle. 192(June 2008), 177–192.

Thompson, D. M., & McCarrick, C. R. (2010). A flume experiment on the effect of constriction shape on the formation of forced pools. Hydrology and Earth System Sciences, 14(7), 1321-1330.

Thompson, D. M. (2002). Geometric adjustment of pools to changes in slope and discharge: a flume experiment. Geomorphology, 46(3-4), 257-265.

Thompson, D. M., Nelson, M., & Wohl, E. (1998). Interactions between pool geometry and hydraulics. 34(12), 3673–3681.

Thorne, C. R., Hey, R. D., & Newson, M. D. (1997). Applied fluvial geomorphology for river engineering and management.

Walker, D. R., Millar, R. G., & Newbury, R. W. (2004). Energy profiles across constructed riffles. Journal of Hydraulic Engineering, 130(3), 199-207.

Wilkinson, S. N., Keller, R. J., and Rutherfurd, I. D. (2004). Phase-shifts in shear stress as an explanation for the maintenance of pool–riffle sequences. Earth Surface Processes and Landforms, 29(6), 737-753.

Wohl, E. (2007). Channel-unit hydraulics on a pool-riffle channel. Physical Geography, 28(3), 233-248.

Wohl, E. E. (2000). Mountain rivers. American Geophysical Union.

Wohl, E. E., Vincent, K. R., & Merritts, D. J. (1993). Pool and riffle characteristics in relation to channel gradient. Geomorphology, 6(2), 99-110

Wood-Smith, R. D., & Buffington, J. M. (1996). Multivariate geomorphic analysis of forest streams: implications for assessment of land use impacts on channel condition. Earth Surface Processes and Landforms, 21(4), 377-393

Yang, C. T. (1971). Formation of riffles and pools. Water Resources Research, 7(6), 1567-1574.

Yang, C. T. (1987). Energy dissipation rate approach in river mechanics. Sediment Transport

APPENDIX A

INTERFACES AND INPUTS OF ANSYS CFD

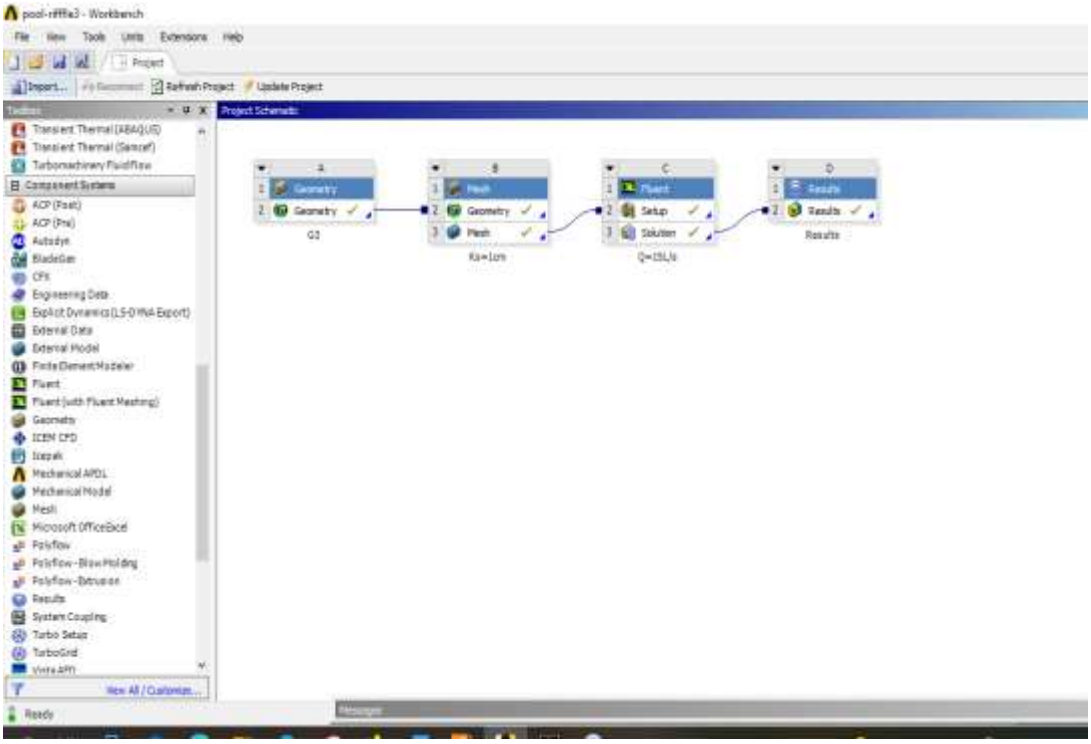

Figure (A-1) Graphical User Interface (GUI)

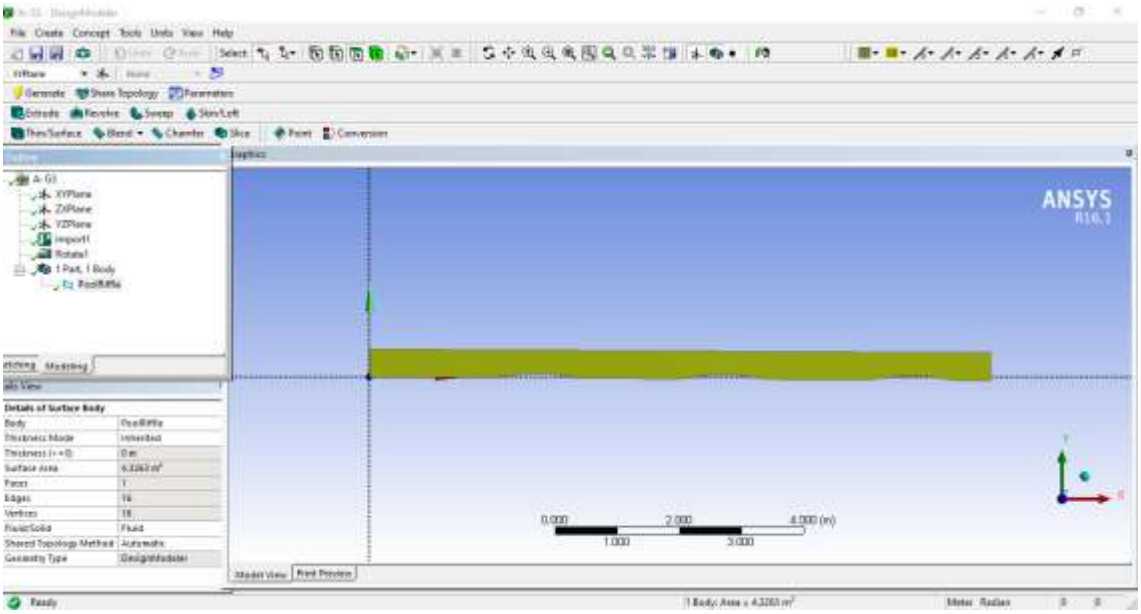

Figure (A-2) The geometry of the case study

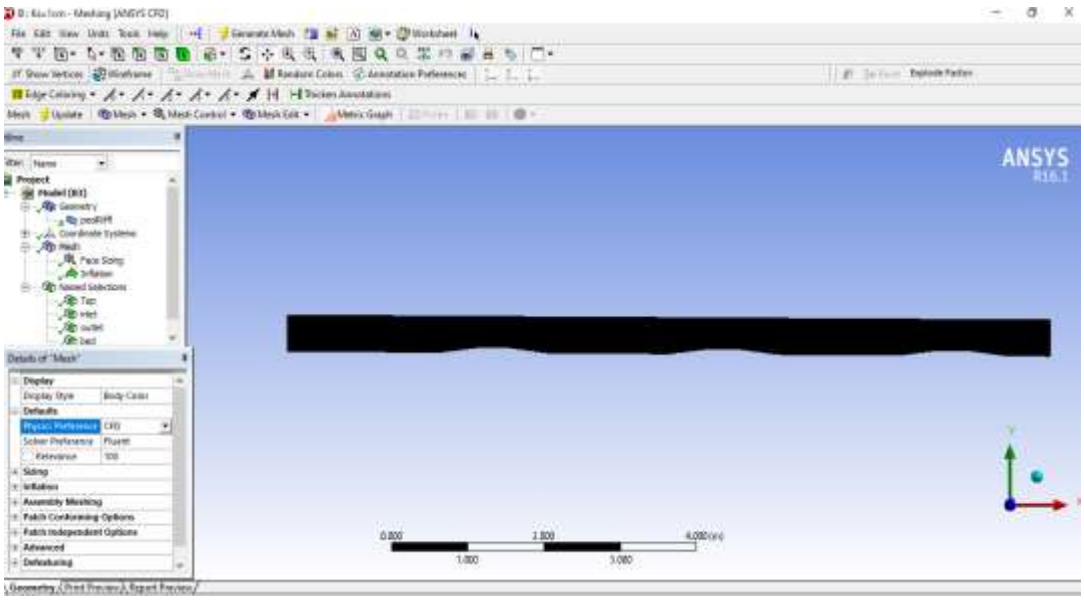

Figure (A-3) The generation mesh

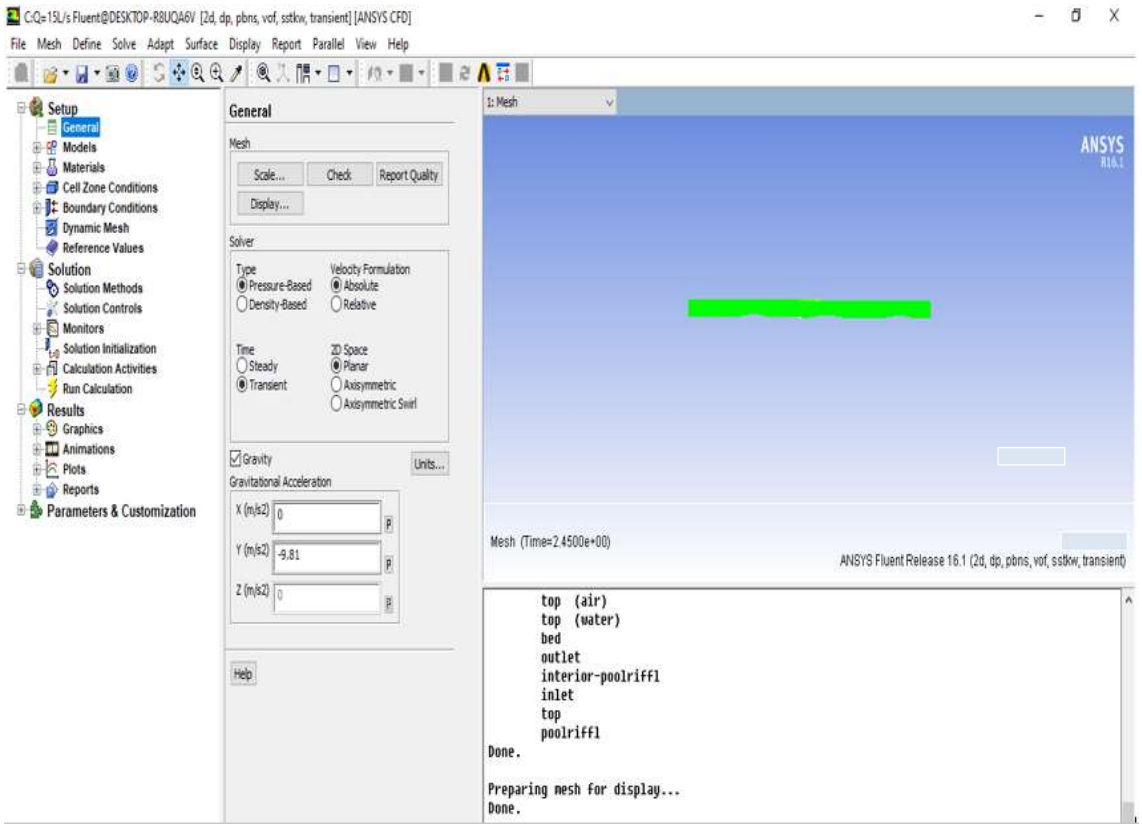

Figure (A-4) The select of solver type.

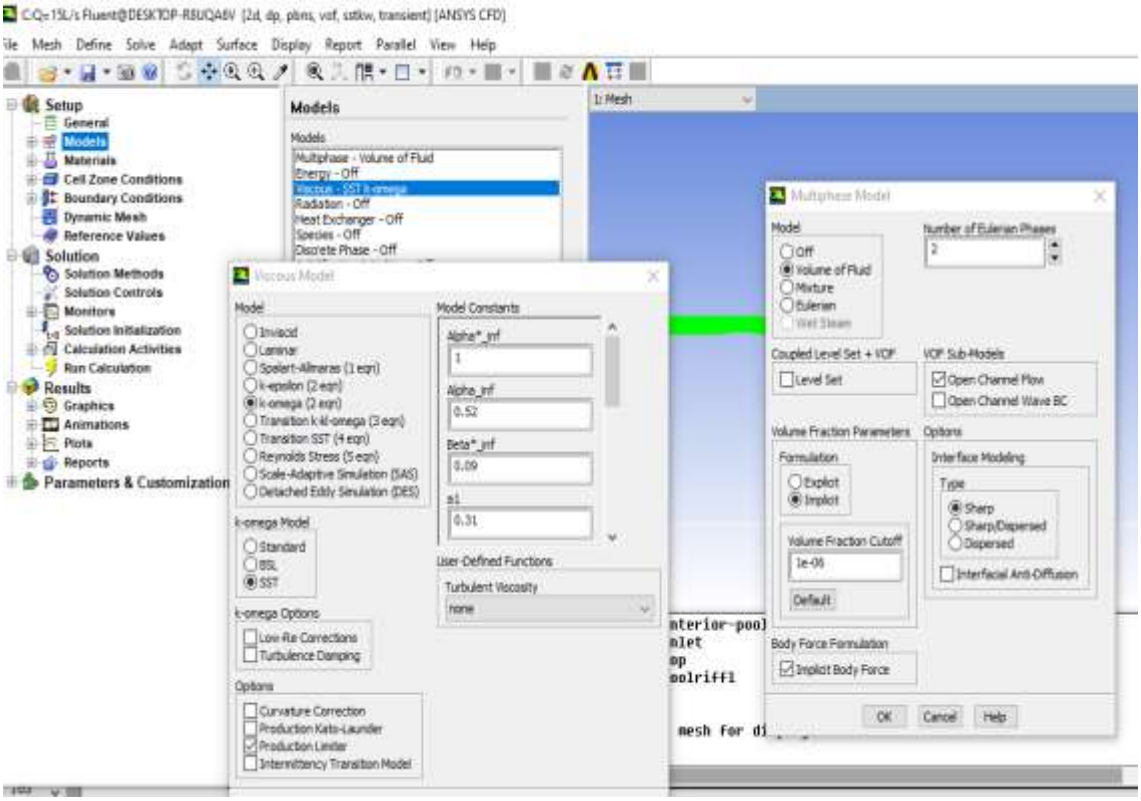

Figure (A-5) Setting of volume of fluid model.

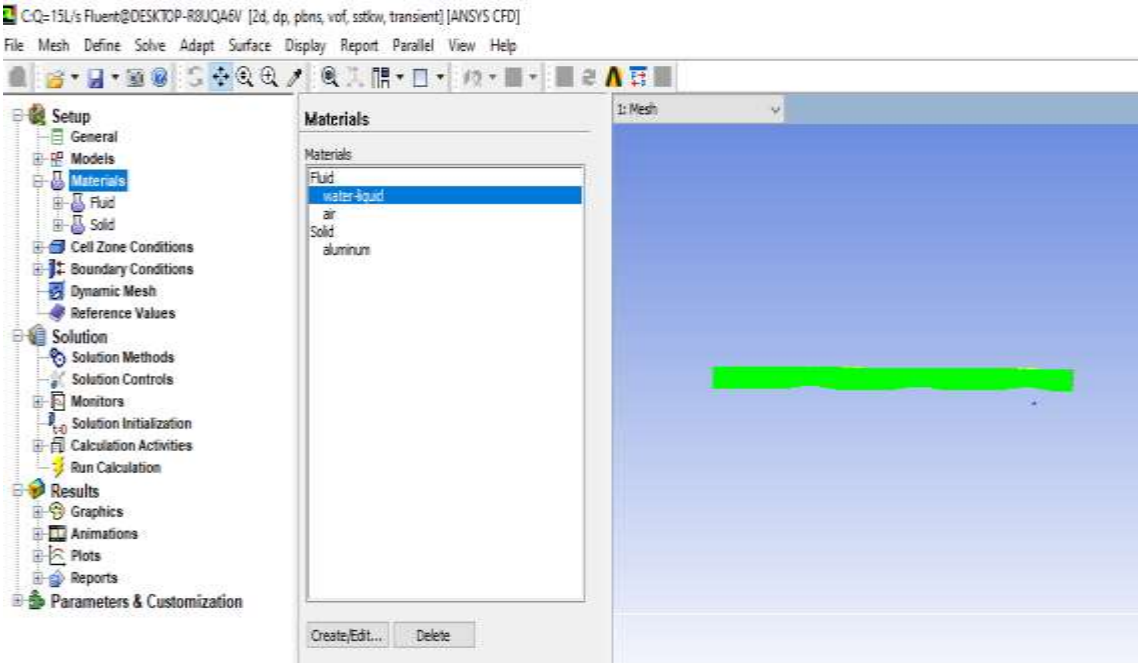

Figure (A-6) Setting of case study materials

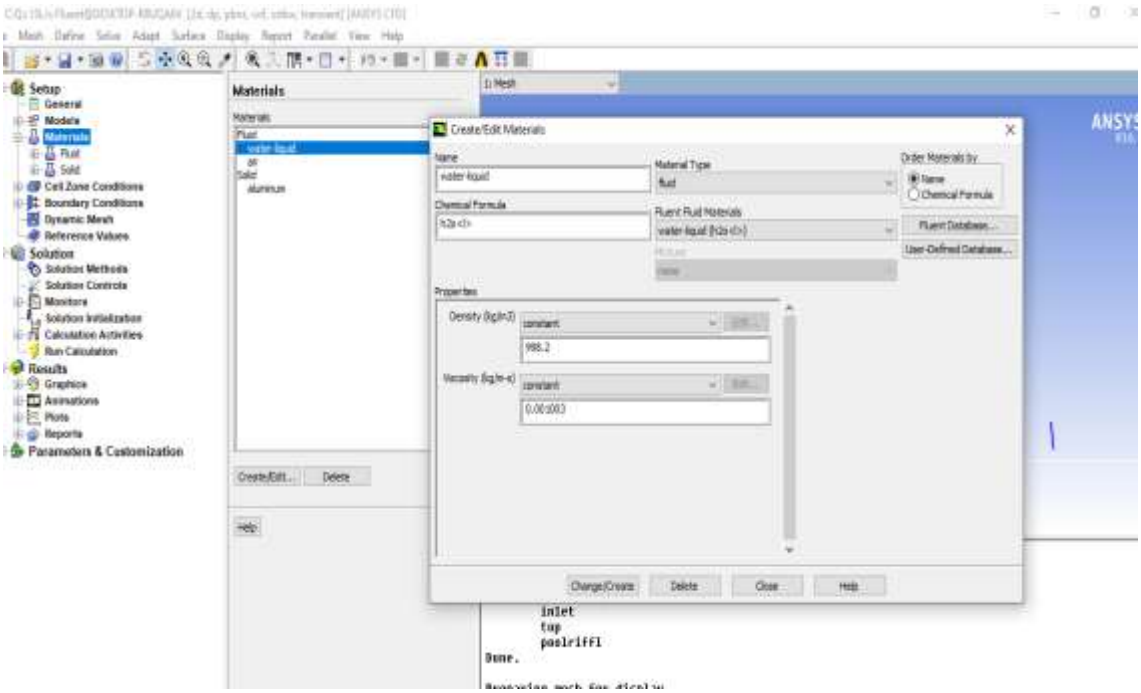

Figure (A-7) Setting of fluids properties

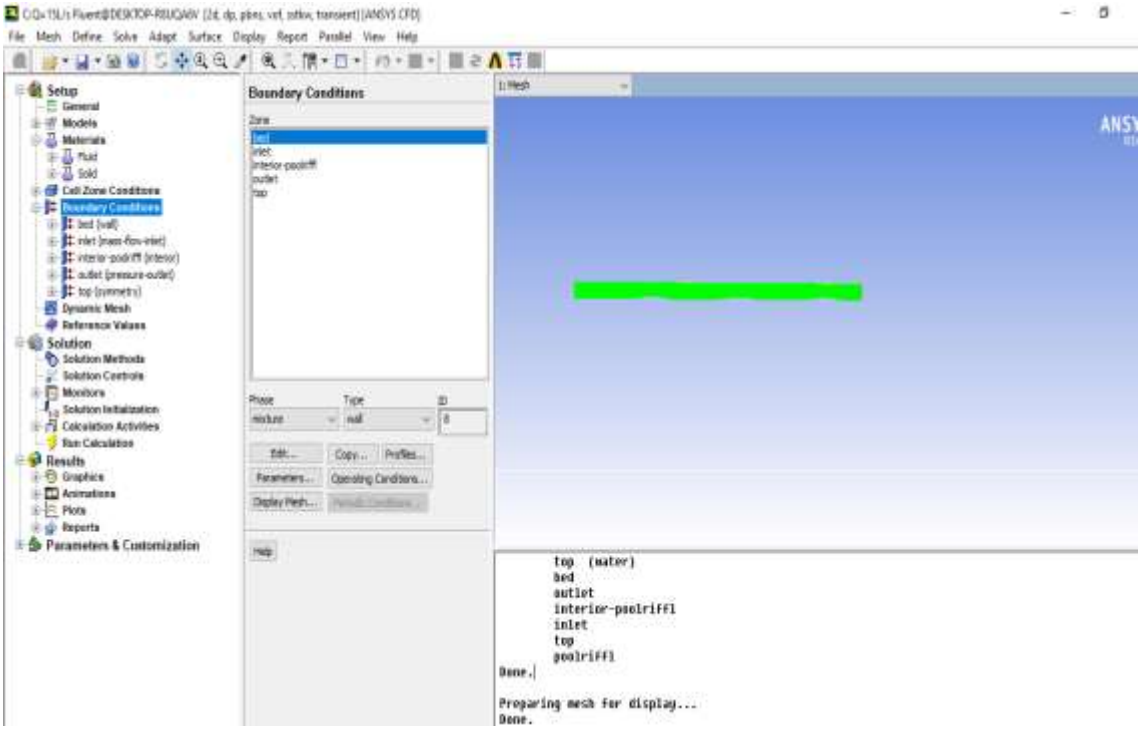

Figure (A-8) Setting of boundary conditions

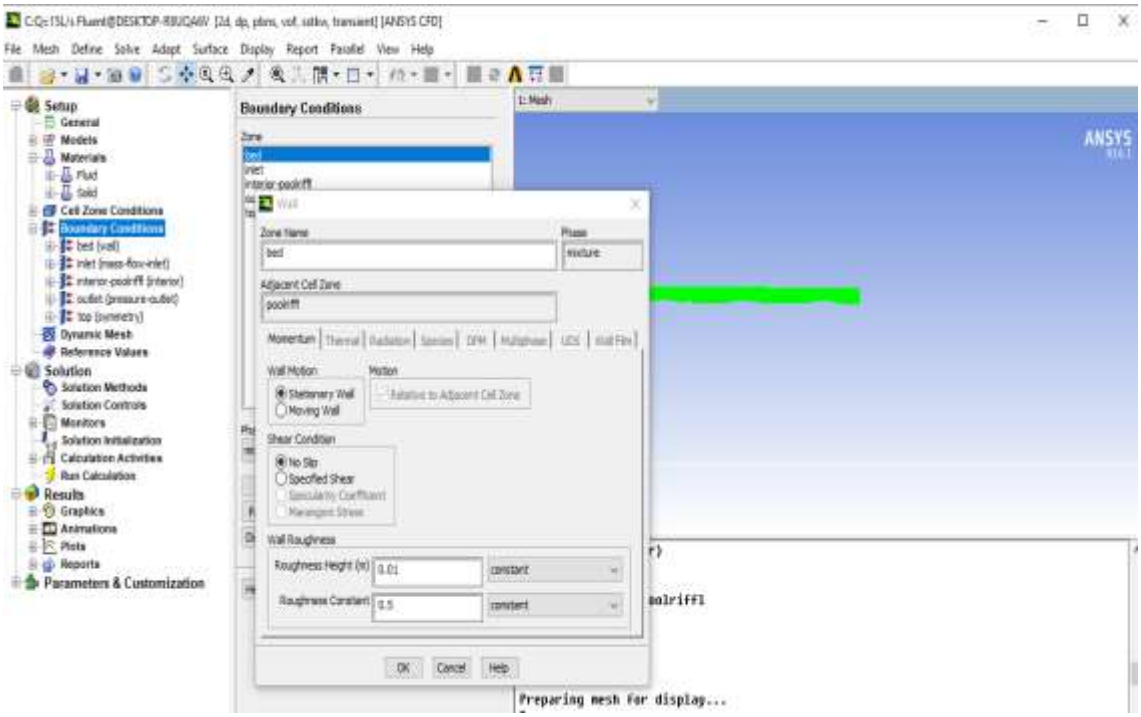

Figure (A-9) Setting of bed boundary conditions.

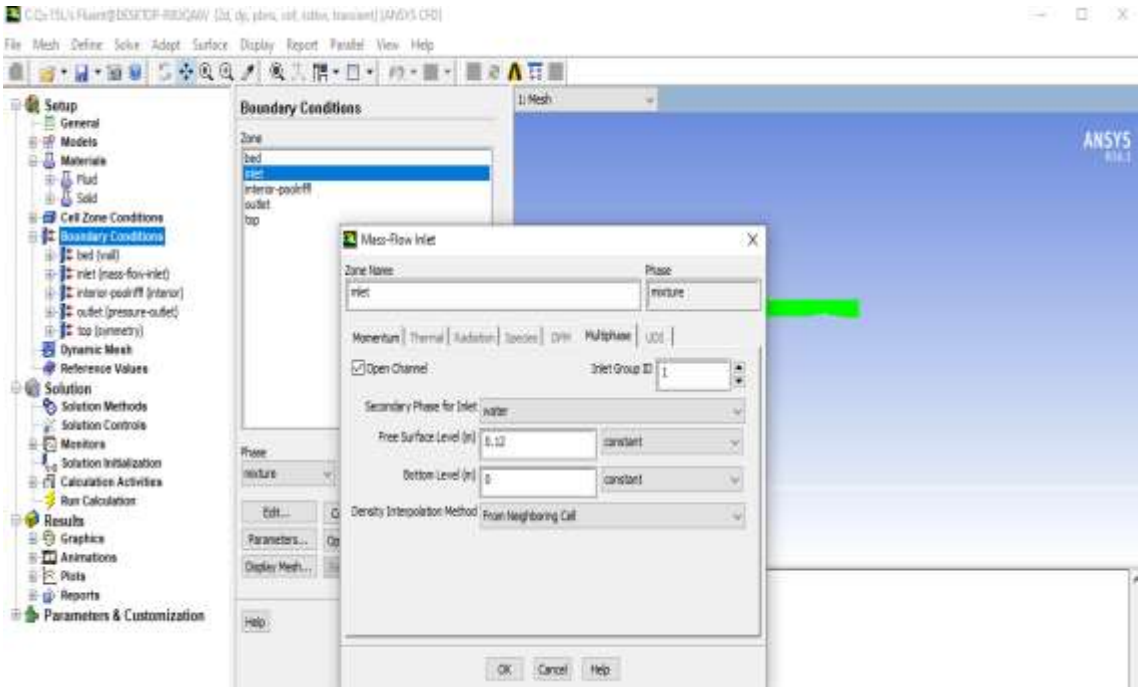

Figure (A-10) Setting of inlet boundary condition

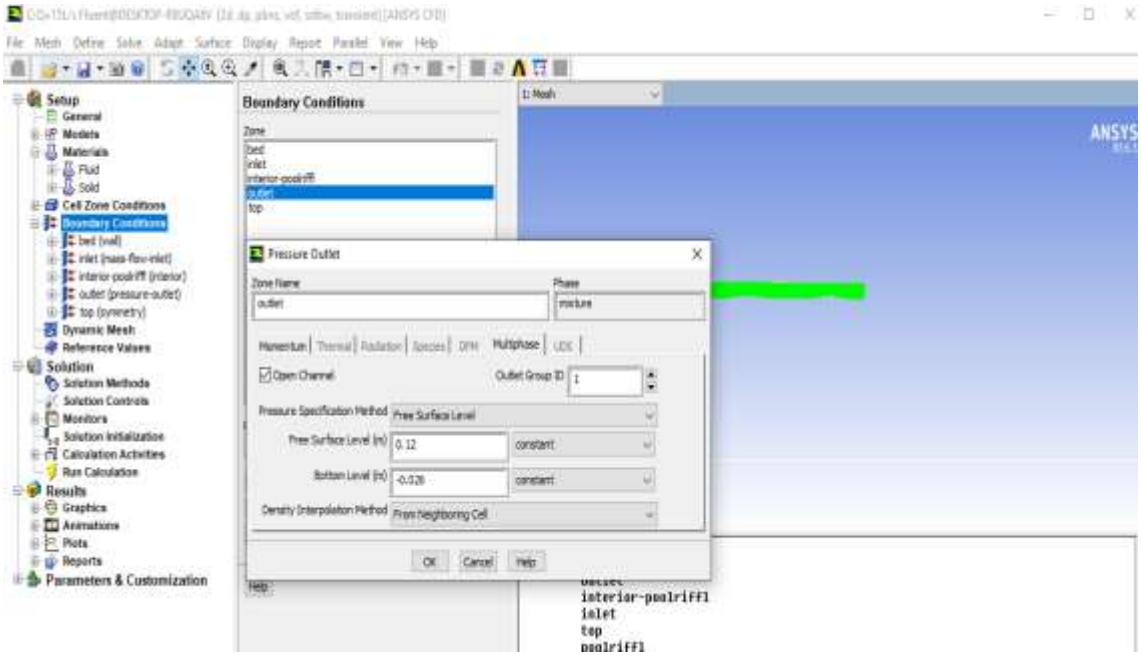

Figure (A-11) Setting of outlet boundary conditions.

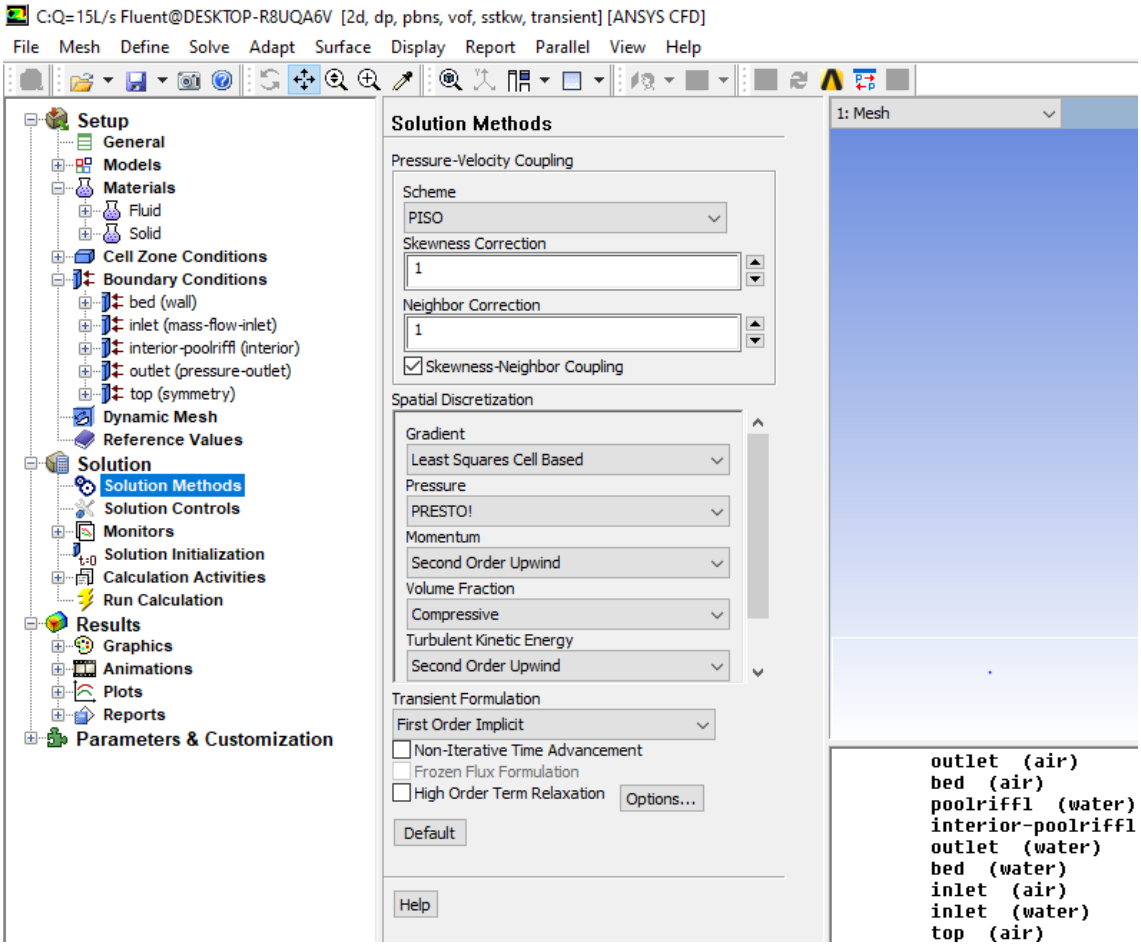

Figure (A-12) Setting of solution methods

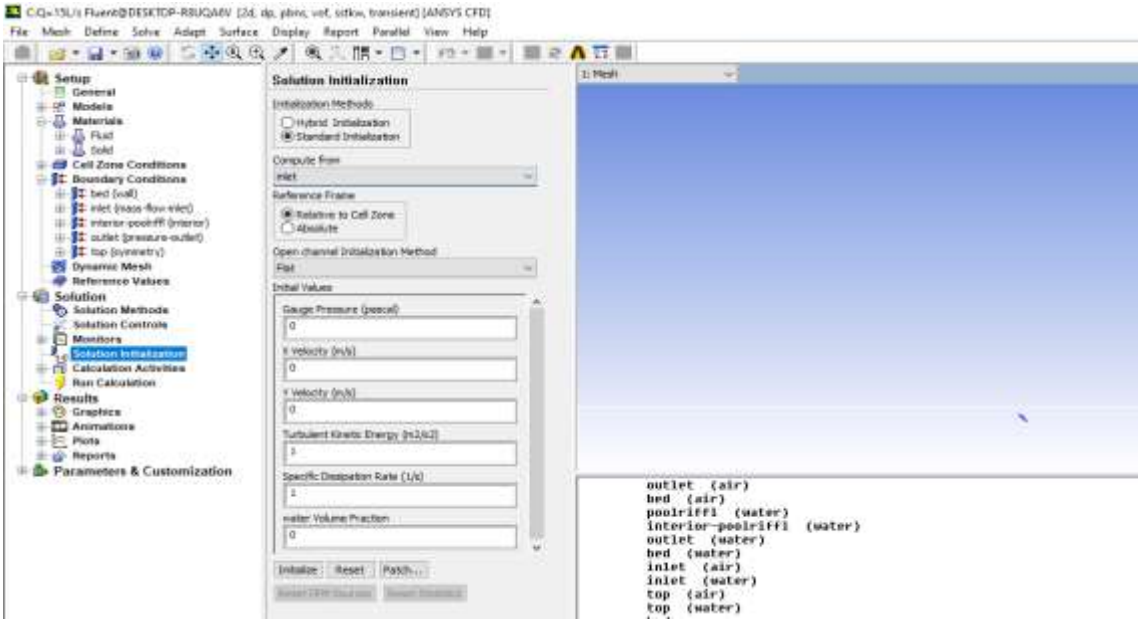

Figure (A-14) Setting of solution initialization

الخلاصة

تعد مشكلة التاكل وانتقال الرسوبيات التي يتعرض لها قعر القنوات المفتوحة وجوانبها من المشكلات التي نالت اهتمام الباحثين في حقل الهيدروليك ،اذ تتعرض تلك القنوات وبخاصة جوانبها الى عوامل التعرية نتيجة السرع العالية للجريان التي تؤدي الى الحاق الضرر الكبير في تلك القنوات ،قام الباحثون في هذا المجال باجراء الدراسات المختبرية والنظرية باستخدام عدة تقنيات لحماية المنشات الهيدروليكية والقنوات المفتوحة من مشكلات التعرية والنحر والحصول على حماية ذات استقرارية عالية ومن تقنيات هذه الحماية ،هي التبطين بالحجارة واستخدام الكتل الكونكريتية والسلال الحصوية.

استخدمت تقنية جديدة في هذه الدراسة تدعى تقنية مناطق الارتفاع -الانخفاض المتتابع ،تعد هذه التقنية وحدات رئيسية لكثير من الانهار ذات القاع الحصوية الخشنة وهذه الظاهرة تعتبر مهمة لصحة النظام البيئي واستقرار القناة.

بزيادة خشونة قاع الانهر سوف تقل سرعة الجريان وبالتالي سوف تقل التاكل . حيث تم اعتماد هذا المبدأ في هذه الدراسة من أجل الوصول إلى أفضل حل التآكل و بأقل تكلفة.

أجريت العديد من الدراسات لمحاكاة خصائص جريان المياه عبر تقنية الارتفاع -الانخفاض المتتابع ذات الميول المعتدلة والتي تحدث قي الارضيات الخشنة للانهار تمت دراسة توزيع السرع وشدة الاضطراب على طول القناة لارتفاعات خشونة مختلفة. تمت محاكاة الجريان في قناة مفتوحة ذات سطح قاع خشن باستخدام Fluent Ansys تقنية ديناميك المائع الحسابي (CFD). تم تحديد تصميم الاختبارات من خلال مجموعة متنوعة من العوامل ، بما في ذلك التصريف وعمق المياه في اتجاه مقدم ومؤخر القناة ، مع ثلاث ارتفاعات لخشونة القاع تبلغ 1 و 2 و 4 سم.

بشكل عام ، يكون لطول مناطق الانخفاض -الارتفاع تأثير كبير على توزيع الجريان والاضطراب داخل القناة. يؤدي الاضطراب وإعادة توزيع الجريان إلى حالة جريان منتظم إلى فقدان الطاقة في منطقة الانخفاض و مع ارتفاع سرعة الجريان في منطقة الارتفاع تزداد الطاقة الحركية ومع زيادة الطول يميل الجريان نحو حالة جريان منتظم جديدة.

أشارت النتائج إلى أن زيادة تصريف جريان المياه زاد من تأثير خشونة القاع على توزيع السرعة. علاوة على ذلك ، فإن زيادة ارتفاع الخشونة لقاع القناة يؤثر على قيم السرعة.

خلصت هذه الرسالة ان تقليل سرعة جريان الماء باستخدام هذه الطريقة كانت ناجحة وكفؤة وان هذه الطريقة ذات فائدة في السيطرة على بيئة الانهار والحفاظ على مناسيب ومقاطع مستقرة لها.كذلك ان استخدام تقنية CFD كانت ناجحة بمحاكاة هذه الضاهرة وتحقيق الاهداف المطلوبة . كذلك تم دراسة تأثير خشونة قاع القناة على شدة الاضطراب ووجد أن له دورًا مهمًا في تقليل شدة اضطراب الجريان.

جمهورية العراق
وزارة التعليم العالي والبحث العلمي
جامعة بابل كلية الهندسة
قسم الهندسة المدنية

تمثيل الجريان المعتمد على ديناميك الموائع الحسابي لسلسلة ارتفاع – انخفاض ذات ميل معتدل

الرسالة

مقدمة الى كلية الهندسة في جامعة بابل وهي جزء من متطلبات الحصول على درجة الماجستير في الهندسة/ الهندسة المدنية / الموارد المائية

من قبل

سجى علي عبيد واوي

إشراف

أ.د.ثائر جبار مزهر الفتلاوي

م.د.فائز حسين المرعب

1444هـ

2022م